EXPLORATIONS IN YANG-MILLS MATRIX GAUGE THEORIES WITH MASSIVE DEFORMATIONS

A THESIS SUBMITTED TO
THE GRADUATE SCHOOL OF NATURAL AND APPLIED SCIENCES
OF
MIDDLE EAST TECHNICAL UNIVERSITY

BY

ONUR OKTAY

IN PARTIAL FULFILLMENT OF THE REQUIREMENTS
FOR
THE DEGREE OF DOCTOR OF PHILOSOPHY
IN
PHYSICS

DECEMBER 2019

Approval of the thesis:

EXPLORATIONS IN YANG-MILLS MATRIX GAUGE THEORIES WITH MASSIVE DEFORMATIONS

submitted by **ONUR OKTAY** in partial fulfillment of the requirements for the degree of **Doctor of Philosophy in Physics Department, Middle East Technical University** by,

Prof. Dr. Halil Kalıpçılar
Dean, Graduate School of **Natural and Applied Sciences** _____

Prof. Dr. Altuğ Özpineci
Head of Department, **Physics** _____

Prof. Dr. Seçkin Kürkcüoğlu
Supervisor, **Physics, METU** _____

Examining Committee Members:

Prof. Dr. Ali Ulvi Yılmazer
Physics Engineering, Ankara University _____

Prof. Dr. Seçkin Kürkcüoğlu
Physics, METU _____

Prof. Dr. Altuğ Özpineci
Physics, METU _____

Prof. Dr. İsmail Turan
Physics, METU _____

Assoc. Prof. Dr. İsmet Yurduşen
Mathematics, Hacettepe University _____

Date:

I hereby declare that all information in this document has been obtained and presented in accordance with academic rules and ethical conduct. I also declare that, as required by these rules and conduct, I have fully cited and referenced all material and results that are not original to this work.

Name, Surname: Onur Oktay

Signature :

ABSTRACT

EXPLORATIONS IN YANG-MILLS MATRIX GAUGE THEORIES WITH MASSIVE DEFORMATIONS

Oktay, Onur
Ph.D., Department of Physics
Supervisor: Prof. Dr. Seçkin Kürkcüoğlu

December 2019, 149 pages

We focus on two research projects on Yang-Mills (YM) matrix models with massive deformation terms, where fuzzy four-spheres, as well as fuzzy two-spheres appear as matrix configurations which are of interest. We first concentrate on an $SU(N)$ YM gauge theory in $0+1$-dimensions with five Hermitian matrices, a YM 5-matrix model, with a massive deformation term and search for matrix configurations of fuzzy four-spheres, which are formed by taking tensor products of certain irreducible and reducible representations of the isometry group SO(5) of the fuzzy four-spheres, which may be understood as new static configurations satisfying the classical equations of motion of this matrix model. The reducible representation of $SO(5)$ that we employ is formed by following a Schwinger type construction which utilizes four pairs of fermionic annihilation-creation operators and their SO(5) irreducible representation (IRR) content is determined. It is shown that in addition to standard fuzzy four-spheres, the generalized fuzzy four-spheres, S^4_Λ, that recently appeared in the literature [1], also emerge as solutions to the YM 5–matrix model. We examine the quantization of the coset space $O_2 \equiv SU(4)/(SU(2) \times U(1) \times U(1))$ via the coad-

joint orbit method to provide a perspective on the structure of S^4_Λ and employ the generalized coherent states associated to $SO(6) \approx SU(4)$ to discuss some aspects of both the basic and generalized fuzzy four-spheres. In the second part of the thesis, we examine a YM matrix model that can be contemplated as a massive deformation of the bosonic part of the Banks-Fischler-Shenker-Susskind (BFSS) model. An ansatz configuration involving fuzzy two- and four-spheres with collective time dependence is proposed to arrive at a set of reduced actions whose chaotic dynamics are revealed by calculating their Lyapunov spectrum, Poincaré sections and in particular largest Lyapunov exponents by using numerical solutions to their Hamiltonian equations of motion. We also analyze how the largest Lyapunov exponents change as a function of the energy.

Keywords: Fuzzy Spheres, Matrix Gauge Theories, Coadjoint Orbits, BFSS Matrix Model, Chaotic Dynamics, Lyapunov Exponents, Poincaré sections

ÖZ

KÜTLE DEFORMASYONLU YANG-MİLLS MATRİS AYAR TEORİLERİ ÜZERİNE ARAŞTIRMALAR

Oktay, Onur
Doktora, Fizik Bölümü
Tez Yöneticisi: Prof. Dr. Seçkin Kürkcüoğlu

Aralık 2019 , 149 sayfa

Bu tezde, kütle deformasyon terimleri taşıyan Yang-Mills (YM) matris modellerine odaklanılmıştır. Fuzzy 2-küre ve fuzzy 4-küre konfigürasyonları bu modellerin potansiyellerinin ekstremumları olarak ortaya çıkmaktadır. Öncelikle, beş Hermityen matris içeren, $0+1$ boyutta bir $SU(N)$ ayar teorisi olan kütle deformasyonlu YM 5-matris modeli ele alınmıştır. Bu bağlamda, fuzzy 4-kürelerin izometri grubu olan $SO(5)$ grubunun birtakım indirgenebilir ve indirgenemez gösterimlerinin tensör çarpımlarını hesaplamak suretiyle, YM 5-matris modelinin klasik hareket denklemlerini sağlayan yeni fuzzy 4-küre konfigürasyonları araştırılmıştır. Bu araştırma esnasında kullanılan indirgenebilir $SO(5)$ gösterimleri, dört çift fermiyonik yaratma ve yok etme operatörü vasıtasıyla tanımlanan Schwinger tipi bir yapıyla oluşturulmuş ve bu sayede $SO(5)$'in indirgenemez gösterimleri cinsinden içeriği belirlenmiştir. Standart fuzzy 4-kürelerin yanında, literatüre kısa bir süre önce girmiş olan [1] genelleştirilmiş fuzzy 4-kürelerin $\left(S^4_\Lambda\right)$ de YM 5-matris modelinin çözümleri olduğu gösterilmiştir. S^4_Λ yapılarının daha iyi anlaşılması maksadıyla, coadjoint yörünge metodundan yararlanılarak $O_2 \equiv SU(4)/(SU(2)\times U(1)\times U(1))$ koset uzayının kuantizasyonu incelen-

miştir. Bunun yanında, $SO(6) \approx SU(4)$ gruplarının eş uyumlu durumları kullanılarak hem standart hem de genelleştirilmiş fuzzy 4-kürelerin özellikleri irdelenmiştir. Tezin ikinci bölümünde, Banks-Fischler-Shenker-Susskind (BFSS) modelinin bozonik sektörünün kütleli deformasyonu şeklinde açıklanabilecek yeni bir YM matris modeli incelenmiştir. Eş zamanlı dinamik yapılara sahip fuzzy 2- ve 4-kürelerden oluşan bir konfigürasyon ansatz olarak alınmış ve bu sayede indirgenmiş bir eylem kümesi elde edilmiştir. İndirgenmiş eylemlerin kaotik dinamiklerini ortaya koymak amacıyla Hamilton denklemleri nümerik yöntemlerle çözülerek ilgili Lyapunov spektrumları, Poincaré kesitleri ve en büyük Lyapunov üstleri hesaplanmıştır. Ayrıca, en büyük Lyapunov üstlerinin enerjiye bağlı değişimleri analiz edilmiştir.

Anahtar Kelimeler: Fuzzy Küreler, Matris Ayar Teorileri, Coadjoint Yörüngeler, BFSS Matris Modeli, Kaotik Dinamik, Lyapunov Üsleri, Poincaré Kesitleri

To the memory of

Sakibe Gürkan (1960 - 2016)

ACKNOWLEDGMENTS

Several people have helped and taught me at our research group over the years, I thank them all. I would like to express my gratitude to my supervisor Prof. Dr. Seçkin Kürkçüoğlu for his guidance. Also, I wish to thank Mr. Orhan Akalp for his constant support.

TABLE OF CONTENTS

ABSTRACT v

ÖZ vii

ACKNOWLEDGMENTS x

TABLE OF CONTENTS xi

LIST OF TABLES xiv

LIST OF FIGURES xv

LIST OF ABBREVIATIONS xvii

CHAPTERS

1 INTRODUCTION 1

2 FUZZY SPHERES AND YANG-MILLS MATRIX MODELS 5

2.1 Geometry of Two-Sphere 6

2.2 Hopf Fibration 10

2.3 Fuzzy Spheres 12

2.3.1 Construction of Fuzzy 2-Sphere 12

2.3.2 Construction of Fuzzy 4-Sphere 19

2.3.2.1 Symmetric Tensor Product of Matrices 23

2.3.2.2 Geometry of S_F^4 25

2.4 BFSS Matrix Model 27

2.5 Review of Yang-Mills Matrix Models 32

3 YANG-MILLS 5-MATRIX MODEL AND GENERALIZED FUZZY FOUR-SPHERE 35

3.1 Overview 35

3.2 New Solutions of the Mass Deformed YM Model 37

3.2.1 Reducible Representation of SO(5) and Schwinger Construction 38

3.2.2 SO(5) and SO(6) Irreducible Representation Content of Y_a . . 40

3.3 Coadjoint Orbit Method and Fuzzy Spaces 44

3.3.1 Warmup 45

3.4 Quantization of O_2 48

3.5 Fuzzy Spheres and Coherent States 55

3.5.1 CP^3 Coherent States and S_F^4 55

3.5.2 O_2 Coherent States and S_Λ^4 61

4 BFSS MODEL WITH MASS DEFORMATIONS 63

4.1 Yang-Mills Matrix Models with Double Mass Deformation 64

4.2 Ansatz *I* and the Effective Action 65

4.2.1 Linear Stability Analysis in the Phase Space 69

4.2.2 Chaotic Dynamics 71

4.2.2.1 Lyapunov Spectrum 71

4.2.2.2 Poincaré Sections 75

4.2.3 Other Mass Values 75

4.3 Ansatz *II* 77

4.4 Effective Action with Single Time-Dependence 79

5 CONCLUSIONS 97

APPENDICES

A IDENTITIES AND DERIVATIONS RELATED TO S_F^4 101

A.1 Gamma Matrices, SO(6) Spinor Generators and Fermionic Basis . . . 101

A.2 Evaluation of $(Y_a)^2$ 102

A.3 Evaluation of $(Z_{ab})^2$ 103

A.4 Evaluation of $(Z_{gh})^2$ 105

B COADJOINT ORBITS OF SU(3) 109

C THE WESS-ZUMINO TERM AND COADJOINT ORBITS 113

D QUANTIZATION OF O_4 117

E CANONICAL COHERENT STATES 121

F DERIVATION OF CP^3 EMBEDDING FUNCTIONS 125

G MATLAB CODES 127

H JACOBI ELLIPTIC FUNCTIONS 131

I POINCARÉ SECTIONS 135

J LYAPUNOV EXPONENTS 139

REFERENCES 141

CURRICULUM VITAE 149

LIST OF TABLES

TABLES

Table 4.1 $c_\mu(n)$ values for Ansatz 1 and $n = 1, \ldots, 7$ 67

Table 4.2 h_1 and h_2 values for $n = 2, \ldots, 7$ 68

Table 4.3 Fixed point energies for $n = 2, \ldots, 7$ 69

Table 4.4 Eigenvalues of the fixed points for Ansatz 1 70

Table 4.5 α_n and β_n values for the fitting curve (4.2.20) 73

Table 4.6 $\tilde{\alpha}_n$ and $\tilde{\beta}_n$ values for the fitting curve (4.2.24) 77

Table 4.7 $c_\mu(n)$ values for Ansatz 2 and $n = 2, 3, 5$ 78

LIST OF FIGURES

FIGURES

Figure 4.1 $T(\kappa)$ vs. κ and $r_2(t)$ vs. time 79

Figure 4.2 Lyapunov exponents vs. time for Ansatz 1 at $\mu_1^2 = -16$ and $\mu_2^2 = -2$ 82

Figure 4.2 Lyapunov exponents vs. time for Ansatz 1 at $\mu_1^2 = -16$ and $\mu_2^2 = -2$ 83

Figure 4.3 Poincaré Sections for Ansatz 1 at $\mu_1^2 = -16$ and $\mu_2^2 = -2$ 83

Figure 4.3 Poincaré Sections for Ansatz 1 at $\mu_1^2 = -16$ and $\mu_2^2 = -2$ 84

Figure 4.3 Poincaré Sections for Ansatz 1 at $\mu_1^2 = -16$ and $\mu_2^2 = -2$ 85

Figure 4.3 Poincaré Sections for Ansatz 1 at $\mu_1^2 = -16$ and $\mu_2^2 = -2$ 86

Figure 4.4 MLLE vs. Energy for Ansatz 1 at $\mu_1^2 = -16$ and $\mu_2^2 = -2$ 87

Figure 4.4 MLLE vs. Energy for Ansatz 1 at $\mu_1^2 = -16$ and $\mu_2^2 = -2$ 88

Figure 4.5 Lyapunov exponents vs. time for Ansatz 1 at $\mu_1^2 = -8$ and $\mu_2^2 = 1$ 89

Figure 4.5 Lyapunov exponents vs. time for Ansatz 1 at $\mu_1^2 = -8$ and $\mu_2^2 = 1$ 90

Figure 4.6 Poincaré Sections for Ansatz 1 at $\mu_1^2 = -8$ and $\mu_2^2 = 1$ 91

Figure 4.6 Poincaré Sections for Ansatz 1 at $\mu_1^2 = -8$ and $\mu_2^2 = 1$ 92

Figure 4.7 MLLE vs. Energy for Ansatz 1 at $\mu_1^2 = -8$ and $\mu_2^2 = 1$ 93

Figure 4.8 Lyapunov exponents vs. time for Ansatz 2 94

Figure 4.9 Poincarè sections for Ansatz 2 95

Figure 4.9 Poincarè sections for Ansatz 2 96

Figure I.1 Poincarè sections for E = $\frac{1}{120}, \frac{1}{15}, \frac{1}{8}, \frac{1}{6}$ 136

LIST OF ABBREVIATIONS

YM	Yang-Mills
IRR	Irreducible Representation
DLCQ	Discrete Light-Cone Quantization
LLE	Largest Lyapunov Exponent
MLLE	Mean Largest Lyapunov Exponent
BFSS	Banks-Fischler-Shenker-Susskind
BMN	Berenstein-Maldacena-Nastase
pp-wave	pure plane wave
SUSY	Supersymmetry

CHAPTER 1

INTRODUCTION

Over the past few decades, there has been an immense and determined effort in theoretical physics community to enhance our understanding of matrix gauge theories [2, 3, 4, 5, 6]. Among these theories, the models proposed by Banks-Fischler-Shenker-Susskind (BFSS) [2] and Berenstein-Maldacena-Nastase(BMN) [5] have been densely studied and hold prominent places in the literature. These models appear as supersymmetric $SU(N)$ gauge theories in $0+1$-dimensions and commonly called as matrix quantum mechanics in the literature. This name may be attributed to the fact that they are build up from $N \times N$ matrices whose entries only depend on time. For instance, the bosonic part of these models contain nine $N \times N$ Hermitian matrices, has $SU(N)$ gauge and $SO(9)$ global symmetries and contains a quartic interaction term among the matrices. BFSS model is associated to the type II-A string theory and appears as the discrete light-cone quantization (DLCQ) of the M-theory in the flat background [7, 8]. The BMN model is a deformation of the BFSS, which contains quadratic and qubic terms in addition to the quartic term and preserves the maximal amount of supersymmetry, and can be obtained as the DLCQ of M-theory on pp-wave background [5, 9]. BFSS theory with $SU(N)$ gauge symmetry may be understood as describing the dynamics of N-coincident $D0$-branes, i.e. point-like Dirichlet branes in string theory, in flat background [10, 11], where the diagonal entries of the nine $N \times N$ matrices give the positions of these $D0$-branes in 9-dimensions, and the off-diagonal elements describe the interactions among them. The BMN model aims to describe the $D0$-brane dynamics in spherical backgrounds. This is due to the fact that fuzzy 2-spheres are stable vacuum configurations in the BMN model [12]. Thus, the diagonal entries of the matrices may now be interpreted in part as the coordinates of $D0$-branes on the fuzzy sphere. These models have gravity duals, which are obtained

in the large N, and strong coupling/low temperature limit [13, 10]. It has been shown that $D0$-branes then form a black brane phase, which is essentially a string theoretical black hole in $9+1$-dimensions [7, 8, 14]. Due to large number of degrees of freedom interacting through a quartic Yang-Mills (YM) potential, it does not appear quite possible that general solutions of the BFSS/BMN models can be determined. Even the smallest Yang-Mills matrix model with two 2×2 matrices and with $SU(2)$ gauge symmetry has not been completely solved until this date [15]. Nevertheless, there are both analytic and recently increasingly more numerical techniques being applied to these models to explore their structure and dynamics [16, 17, 18]. In this context, there are two major research topics within matrix models to which the findings presented in this thesis are connected: massive deformations of Yang-Mills matrix models [5, 19, 20] and chaotic dynamics emerging from the BFSS and related matrix models [21, 17, 22, 18, 20]. We study two problems in this thesis and in the rest of this introduction we outline the basic features of these problems and briefly state the results that we have obtained.

In this thesis, we focus on different of aspects of Yang-Mills matrix gauge theories with massive deformations. The first problem we examine is finding new static solutions for the Yang-Mills matrix model with five matrices and a massive deformation term. This model can also be seen as a particular massive deformation of a subsector of the BFSS model which is distinct from the BMN theory. It is already known that fuzzy four-spheres constitute static solutions to the equations of motion in this model [19, 23]. To search for new solutions, we adapt the approach applied in a series of papers [24, 25] in $SU(N)$ gauge theories coupled to adjoint scalar fields and massive deformations of $\mathscr{N} = 4$ supersymmetric (SUSY) YM, where fuzzy two-spheres in various direct sum forms are obtained as new vacuum configurations. This is performed by augmenting an additive new part using a Schwinger type realization of $SU(2)$ generators with fermionic annihilation-creation operators to matrices which are already satisfying the equations of motion. For the model we study the situation is rather more complicated due to the geometrically elaborate structure of fuzzy four spheres. By using Schwinger type realization of $SO(5)$ generators with "fermionic" oscillators we find matrix configurations serving as new static solutions to the YM 5-matrix model. These configurations contain not only direct sums of fuzzy four-

spheres, but also matrices whose structure describe genealized fuzzy four-spheres recently introduced in [1]. Using the representation theory of $SO(5)$ and $SO(6)$, we discuss in detail how the new static solutions are obtained and subsequently turn our attention to discuss essential features of generalized fuzzy four-spheres appearing in our solutions. As an alternative to the approach given in [1], we use quantization of coadjoint orbit methods [26, 27] and handle the quantization of a particular 10-dimensional coadjoint orbit of $SO(6)$, namely O_2, to discuss the formulation and properties of generalized fuzzy four-spheres. Coherent states associated to the Lie group $SO(6) \approx SU(4)$ are also used in this context to compare the structure and properties of the ordinary and generalized fuzzy four-spheres as certain squashed limits of the fuzzy $\mathbb{CP}^3$ and fuzzy $O_2 = \frac{SU(4)}{SU(2)\times U(1)\times U(1)}$. Using these techniques we also solve a related problem, namely the Landau problem on O_2 and briefly state its connection to the fuzzy O_2.

In chapter 4, we focus our attention to a YM matrix model with two massive deformation terms to study the emerging chaotic motions as we shall explain shortly. Recently, there has been intense interest in exploring, modelling and understanding the emergence of chaos from matrix models of Yang-Mills theories [17, 18, 22]. Attention has been focused on examining many aspects and features of chaos in the BFSS and BMN models. A strong motivation in studying possible chaotic dynamics possessed by these matrix models comes from possibilities in acquiring an in depth perspective and perhaps even discovering novel physical phenomena relating to the dual black-brane phases, such as their thermalization, evaporation processes. For this purpose, authors of [22] considered simple ansätze for the BMN model at the matrix levels $N = 2, 3$ satisfying the Gauss law constraint to probe the chaotic dynamics. The model we study in chapter 4, has the same matrix content as the bosonic part of the BFSS matrix model, but contains mass deformation terms breaking the global $SO(9)$ symmetry of the latter to $SO(5) \times SO(3) \times \mathbb{Z}_2$. Introducing an ansatz configuration involving fuzzy four and two spheres with collective time dependence, we examine the chaotic dynamics in a family of effective Lagrangians obtained by tracing over the aforementioned ansatz configurations at the matrix levels $N = \frac{1}{6}(n+1)(n+2)(n+3)$, for $n = 1, 2, \cdots 7$. Before presenting a full numerical analysis of the chaotic dynamics, we first identify the fixed points of the phase space for the model at each matrix

level and perform a linear stability analysis of these points. The latter allows us to identify both the stable and unstable fixed points, and it also suggests that the possible chaotic motion in these models could start at energies around and above the lowest unstable fixed point energy within a given model. This expectation is corroborated through the numerical work we perform, in which we obtain the Lyapunov spectrum and analyze how the largest Lyapunov exponents change as a function of the energy. We also give the Poincaré sections of these effective models at selected energies that best describes the dynamics prior to, at and after, the onset of chaos.

Chapter 2 start out with introducing the first and second Hopf fibrations which are later employed in the general discussion of the construction of fuzzy spaces. This introductory part is followed by the construction of the simplest example of the fuzzy spaces, i.e. the fuzzy two-sphere S_F^2 [28, 29, 30, 31]. After providing a detailed description of the construction of S_F^2, we move on to the discussion of the fuzzy four-sphere, S_F^4 [32, 33, 34]. Although there is an apparent resemblance between the constructions of S_F^2 and S_F^4, as it is shown from both geometric and algebraic sides, the fuzzy four-sphere is indeed a quite distinct object. This fact is thoroughly demonstrated in the extensive review we present regarding the construction of S_F^4. In concluding chapter 2, we give a self-contained review of the bosonic part of the BFSS matrix model and introduce the Yang-Mills 5-matrix model. Chapter 5 summarizes the results obtained and states the conclusions we have reached in this thesis.

CHAPTER 2

FUZZY SPHERES AND YANG-MILLS MATRIX MODELS

This chapter provides an introduction on the general aspects of fuzzy spheres and their connection to the Yang-Mills matrix models. The approach we take on here is mainly one of review and aims to explain concepts that relate to the ensuing chapters. In order to gain familiarity with the problem of construction of fuzzy spaces, it is appropriate to initiate the developments with a consideration of the well-known example of the fuzzy two-sphere. In order to do so, we first start with a description of the basic features of commutative manifolds C^2, S^2, S^3 and show the realization of S^2 from S^3 via the first Hopf fibration. This is followed by the quantization of these manifolds using the canonical procedures and leads us to the construction of the fuzzy two-sphere, S_F^2, which is comprehensively presented in subsection 2.3.1. This discussion is based on the references [28, 29, 30, 31].

There is also a four-dimensional version of the fuzzy sphere, the basic fuzzy four-sphere, S_F^4 [32, 33, 34]. In order to provide a detailed account of the construction of S_F^4, the descent chain of manifolds $\mathbb{C}^4 \to S^7 \to S^4$, i.e. the second Hopf map, is identified in section 2.2. In subsection 2.3.2, we perform the quantization of this descent chain and give an extensive review of the construction of S_F^4. In this review, we explicitly show that S_F^4 cannot be obtained in a canonical way by quantizing the second Hopf map. Rather, it should be thought of as emerging from the quantization of the fibration $S^2 \to \mathbb{CP}^3 \to S^4$.

In section 2.4, we give a self-contained review of the bosonic part of the Banks-Fischler-Shenker-Susskind (BFSS) matrix model including its derivation from the Yang-Mills theory in $9+1$ dimensions with $\mathscr{N}=1$ supersymmetry. In the final section of this chapter, we introduce the Yang-Mills 5-matrix model whose new vacuum

solutions will be explored in chapter 3.

2.1 Geometry of Two-Sphere

For any natural number n, the n-sphere S^n can be defined in terms of its embedding in the $(n+1)$-dimensional Euclidean space, $\mathbb{R}^{n+1}$, as the set of points that are equidistant from a fixed central point [35]. In particular, the two-sphere, S^2, can be defined as the two-dimensional, real, compact manifold via its embedding in $\mathbb{R}^3$ by the constraint

$$\rho_1{}^2 + \rho_2{}^2 + \rho_3{}^2 = \rho^2, \qquad (\rho_1, \rho_2, \rho_3) \in \mathbb{R}^3, \tag{2.1.1}$$

where ρ is the radius of S^2. It is sufficient to introduce two parameters to describe S^2. For instance, we may use the spherical angles θ and φ where the polar angle ranges from the values $0 \leq \theta \leq \pi$ and the azimuthal angle is in the range $0 \leq \varphi \leq 2\pi$. The Euclidean coordinates can be expressed in terms of these angles by

$$\rho_1 = \rho \sin\theta \cos\varphi, \quad \rho_2 = \rho \sin\theta \sin\varphi, \quad \rho_3 = \rho \cos\theta. \tag{2.1.2}$$

The coordinates $\rho_\mu (\mu = 1, 2, 3)$ together with (2.1.1) generate an infinite-dimensional commutative algebra of smooth bounded functions on S^2 denoted as $C^\infty(S^2)$. Any element $\Omega \in C^\infty(S^2)$ can be expanded in terms of polynomials of ρ_μ as

$$\Omega(\vec{\boldsymbol{\rho}}) = \sum_{\mu_1,\ldots,\mu_m} \Omega_{\mu_1 \ldots \mu_m} \rho_{\mu_1} \cdots \rho_{\mu_m}. \tag{2.1.3}$$

An equivalent expansion of Ω can also be provided in terms of the spherical harmonics $Y_{lm}(\theta, \varphi)$ as follows

$$\Omega(\theta, \varphi) = \sum_{l=0}^{\infty} \sum_{m=-l}^{l} c_{lm} Y_{lm}(\theta, \varphi). \tag{2.1.4}$$

The spherical harmonics satisfy the normalization and orthogonality conditions given by [36]

$$\int_0^{2\pi} \int_0^{\pi} Y_{lm}(\theta, \varphi) Y^*_{l'm'}(\theta, \varphi) \sin\theta \, \mathrm{d}\theta \, \mathrm{d}\varphi = \delta_{ll'} \delta_{mm'} \,. \tag{2.1.5}$$

Isometry group of S^2 is the group of rotations $SO(3)$. We may therefore, use the generators of $SO(3)$ as the derivations on the algebra of functions $C^\infty(S^2)$. Explicitly, we have

$$L_\mu = -i(\vec{\boldsymbol{\rho}} \times \vec{\boldsymbol{\nabla}})_\mu = -i\epsilon_{\mu\nu\eta} \rho_\nu \partial_\eta. \tag{2.1.6}$$

acting on $C^\infty(S^2)$. They fulfill the $SO(3)$ commutation relations

$$[L_\mu, L_\nu] = i\epsilon_{\mu\nu\eta}L_\eta. \tag{2.1.7}$$

A glance at equation (2.1.6) reveals that $\vec{\boldsymbol{L}}$ is perpendicular to the position vector $\vec{\boldsymbol{\rho}}$ which is parallel to the radial direction on S^2. Therefore, we immediately see that this vector differential operator is tangential to the two-sphere. Indeed L_μ are derivations on $C^\infty(S^2)$, because they provide a map from $C^\infty(S^2)$ onto itself fulfilling the Leibniz rule

$$L_\mu(\Omega_1\Omega_2) = (L_\mu\Omega_1)\Omega_2 + \Omega_1(L_\mu\Omega_2). \tag{2.1.8}$$

The Laplacian operator on S^2 can be written as

$$\boldsymbol{L^2} = L_\nu L_\nu = {L_1}^2 + {L_2}^2 + {L_3}^2. \tag{2.1.9}$$

As the simultaneous eigenfunctions of $\boldsymbol{L^2}$ and L_3 operators, spherical harmonics satisfy the following eigenvalue equations:

$$\boldsymbol{L^2}Y_{lm}(\vec{\boldsymbol{\rho}}) = l(l+1)Y_{lm}(\vec{\boldsymbol{\rho}}), \tag{2.1.10}$$

$$L_3Y_{lm}(\vec{\boldsymbol{\rho}}) = mY_{lm}(\vec{\boldsymbol{\rho}}), \tag{2.1.11}$$

where the index l takes the integer values $0, 1, 2, ...$ and the index m runs through values $-l, ..., l$.

Having now presented the basic features of the two-sphere, we move on to discuss its geometrical properties. To proceed further, it is convenient to review two necessary group theoretical concepts: cosets of a Lie group and adjoint action of a Lie group on its Lie algebra and also as a manifold for which it is the group of isometries. Given a Lie group G with a subgroup H, an equivalence relation can be constructed in G using H. For any two elements $g_1, g_2 \in G$, if there exist an element $h \in H$ such that

$$g_1 = g_2h, \tag{2.1.12}$$

we shall say that g_1 and g_2 are in the same equivalence class and express this relation as $g_1 \sim g_2$. Since equation (2.1.12) constitutes an equivalence relation, G can be partitioned into a disjoint union of these equivalence classes, each of which is a coset. The set of cosets, which are denoted by G/H, are called right cosets of G. The right coset space can be defined as [37]

$$G/H = \left\{ g \sim gh \,\middle|\, g \in G\,,\, h \in H \right\}. \tag{2.1.13}$$

If $\mathfrak{g}$ denotes the Lie algebra of G then we may define the adjoint action of G on $\mathfrak{g}$ as

$$Ad(g)Y = gYg^{-1}, \qquad g \in G\,,\, Y \in \mathfrak{g}\,. \tag{2.1.14}$$

Let us use these definitions for the isometry group $SO(3) \simeq SU(2)$ of S^2. Since $SU(2)$ is the group of 2×2 unitary matrices with unit determinant, we may introduce a generic element in the form

$$g = \begin{pmatrix} z_1 & -{z_2}^* \\ z_2 & {z_1}^* \end{pmatrix}, \quad g^\dagger = g^{-1}\,, \qquad z_1, z_2 \in \mathbb{C}\,, \tag{2.1.15}$$

with $|z_1|^2 + |z_2|^2 = 1$. Then, the adjoint action of $SU(2)$ on σ_3 is found to be equal to

$$Ad(g)\sigma_3 = g\sigma_3 g^\dagger = \widehat{q}\cdot\vec{\sigma}\,. \tag{2.1.16}$$

Explicitly, $\widehat{q}\cdot\vec{\sigma}$ is

$$\widehat{q}\cdot\vec{\sigma} = \begin{pmatrix} |z_1|^2 - |z_2|^2 & 2z_1{z_2}^* \\ 2(z_1{z_2}^*)^* & -|z_1|^2 + |z_2|^2 \end{pmatrix}, \tag{2.1.17}$$

where $\vec{\sigma} = (\sigma_1, \sigma_2, \sigma_3)$ is the vector of Pauli matrices and the components of the unit vector $\widehat{q}$ are given by

$$q_1 = 2Re(z_1{z_2}^*), \quad q_2 = -2Im(z_1{z_2}^*), \quad q_3 = |z_1|^2 - |z_2|^2. \tag{2.1.18}$$

In order to check that $\widehat{q}$ is actually a unit vector, squaring both sides of equation (2.1.16) we find

$$\begin{aligned} g\sigma_3 g^{-1} g\sigma_3 g^{-1} &= q_\mu\sigma_\mu q_\nu\sigma_\nu\,, \\ g{\sigma_3}^2 g^{-1} &= q_\mu q_\nu(\delta_{\mu\nu}\mathbb{1}_2 + i\epsilon_{\mu\nu\eta}\sigma_\eta)\,, \\ \mathbb{1}_2 &= q_\mu q_\mu \mathbb{1}_2\,, \end{aligned}$$

thus

$$\widehat{q}\cdot\widehat{q} = q_\mu q_\mu = 1\,, \tag{2.1.19}$$

which leads us to realize that q_μ correspond to the coordinates of a unit 2-sphere. Therefore, we may interpret equation (2.1.16) as a projection map from $SU(2)$ to S^2 as follows [38, 39]

$$\mathscr{M}_1 : \quad SU(2) \mapsto S^2$$

$$g \mapsto Ad(g)(\widehat{q}_0 \cdot \vec{\sigma}) = \widehat{q} \cdot \vec{\sigma}, \tag{2.1.20}$$

where $\widehat{q_0} = (0, 0, 1)$ is the unit vector pointing along the third axis. Now consider two elements $g_1, g_2 \in G$ in the same equivalence class given by

$$g_1 = g_2 h, \qquad h = e^{\frac{i}{2}\theta\sigma_3} \in U(1) \subset SU(2). \tag{2.1.21}$$

We can verify that g_1 and g_2 are projected onto the same point $\widehat{q}$ as follows

$$g_1 \sigma_3 g_1^{-1} = \widehat{q} \cdot \vec{\sigma} \tag{2.1.22a}$$

$$\begin{aligned} g_2 h \sigma_3 (g_2 h)^{-1} &= g_2 h \sigma_3 h^{-1} g_2^{-1} \\ &= g_2 e^{(i/2)\theta\sigma_3} \sigma_3 e^{(-i/2)\theta\sigma_3} g_2^{-1} \\ &= g_2 \sigma_3 g_2^{-1} \\ &= \widehat{q} \cdot \vec{\sigma}, \end{aligned} \tag{2.1.22b}$$

which implies that $\widehat{q}$ can be identified with the equivalence class $\left[g e^{(i/2)\theta\sigma_3}\right] \in SU(2)/U(1)$. Therefore, we deduce that unlike S^1 and S^3, the two-sphere is not a group manifold but an example of a coset manifold [40], and we may express this as

$$S^2 \equiv \frac{SU(2)}{U(1)}. \tag{2.1.23}$$

Another way to see two-sphere as a coset manifold is by considering the linear action of $SU(2)$ on $\mathbb{C}^2$. Let us take two complex numbers which correspond to the coordinates of $\mathbb{C}^2$ with its origin removed, i.e.

$$z = (z_1, z_2), \qquad z \in \mathbb{C}^2 \setminus \{(0, 0)\}. \tag{2.1.24}$$

The complex projective line, $\mathbb{CP}^1$, is the set of complex lines going through the origin of $\mathbb{C}^2$ that are grouped through an equivalence relation given by

$$\mathbb{CP}^1 = \{(z_1, z_2) \sim \lambda(z_1, z_2) |\, \lambda \in \mathbb{C}\}. \tag{2.1.25}$$

$SU(2)$ maps a complex line to another complex line. Hence, its action on $\mathbb{CP}^1$ is transitive. The isotropy group of $SU(2)$, which leaves the complex line of $\mathbb{CP}^1$ invariant is $U(1)$ which is generated by the phase of $\lambda \in \mathbb{C}$ in (2.1.25). Therefore, $\mathbb{CP}^1$ is also diffeomorphic to $SU(2)/U(1)$. To summarize, the topological equivalence of S^2 and $\mathbb{CP}^1$ to the adjoint orbit of $SU(2)$ can be expressed as

$$S^2 \equiv \mathbb{CP}^1 \equiv \frac{SU(2)}{U(1)}. \tag{2.1.26}$$

2.2 Hopf Fibration

A Hopf fibration is a many-to-one continuous function from a higher dimensional sphere to a lower dimensional one. Generally, there are four Hopf fibrations, on S^1, S^3, S^7, and S^{15} [41]. In this section, we review the fibrations on the three-sphere and the seven-sphere.

The first and best known example of a Hopf fibration is a map from the three-sphere into the two-sphere known as the first Hopf map whose bundle structure is denoted by $S^1 \hookrightarrow S^3 \xrightarrow{\mathscr{H}_1} S^2$ meaning that the total space S^3 is a $S^1 \cong U(1)$ bundle over the base space S^2 [42]. In this mapping, the inverse image of a point on S^2 is a circle on S^3. Given the unit three-sphere as a submanifold of $\mathbb{R}^4$ by

$$x_1^2 + x_2^2 + x_3^2 + x_4^2 = 1, \qquad (x_1, x_2, x_3, x_4) \in \mathbb{R}^4, \tag{2.2.1}$$

and the unit two-sphere by equation (2.1.19), the first Hopf map $\mathscr{H}_1 : S^3 \to S^2$ is defined by

$$q_1 = 2(x_1 x_3 + x_2 x_4), \tag{2.2.2a}$$

$$q_2 = 2(x_2 x_3 - x_1 x_4), \tag{2.2.2b}$$

$$q_3 = x_1^2 + x_2^2 - x_3^2 - x_4^2. \tag{2.2.2c}$$

An equivalent description of $\mathscr{H}_1$ can be formulated by regarding the three-sphere as embedded in $\mathbb{C}^2 \setminus \{0, 0\}$. Since the coordinates given by equation (2.1.24) are never all zero, they can be normalized as

$$\kappa_\alpha := \frac{z_\alpha}{\sqrt{|z_1|^2 + |z_2|^2}} \quad ; \qquad \alpha = 1, 2\,, \tag{2.2.3}$$

such that they describe a three-sphere embedded in $\mathbb{C}^2 \setminus \{0, 0\}$

$$S^3 = \left\{ \kappa^\dagger \kappa = 1\,,\, \kappa = (\kappa_1, \kappa_2)^T \right\}. \tag{2.2.4}$$

The coordinate functions on S^2 can be defined in terms of the complex argument κ as

$$y_\mu(\kappa) := \kappa^\dagger \sigma_\mu \kappa, \tag{2.2.5}$$

where σ_μ are the Pauli matrices. The Hopf map between κ_α and y_μ is equivalent to the projection map from S^3 to S^2 which may be introduced as

$$\mathscr{M}_2 : S^3 \mapsto S^2, \qquad \kappa_\alpha \mapsto y_\mu(\kappa). \tag{2.2.6}$$

It is obvious that $y_\mu(\kappa)$ are left invariant under the $U(1)$ transformations $\kappa \to e^{i\theta}\kappa$. Furthermore, a closer inspection of equation (2.2.5) reveals that they are indeed real functions

$$y_\mu{}^* = \left(\kappa^\dagger \sigma_\mu{}^\dagger (\kappa^\dagger)^\dagger\right)^* = y_\mu. \tag{2.2.7}$$

y_μ can be written out explicitly as follows

$$y_1 = \kappa_1{}^*\kappa_2 + \kappa_2{}^*\kappa_1, \tag{2.2.8a}$$

$$y_2 = i(\kappa_2{}^*\kappa_1 - \kappa_1{}^*\kappa_2), \tag{2.2.8b}$$

$$y_3 = \kappa_1{}^*\kappa_1 - \kappa_2{}^*\kappa_2\,. \tag{2.2.8c}$$

The Fierz identity for Pauli matrices is given by

$$(\sigma_\mu)_{\alpha\beta}(\sigma_\mu)_{\delta\gamma} = 2\delta_{\alpha\gamma}\delta_{\beta\delta} - \delta_{\alpha\beta}\delta_{\delta\gamma}\,. \tag{2.2.9}$$

The sum of the squares of y_μ can be determined by invoking equation (2.2.9)

$$\begin{aligned} y_\mu y_\mu &= (\kappa^\dagger)_\alpha(\sigma_\mu)_{\alpha\beta}(\kappa)_\beta(\kappa^\dagger)_\delta(\sigma_\mu)_{\delta\gamma}(\kappa)_\gamma \\ &= (\kappa^\dagger)_\alpha(\kappa)_\beta(\kappa^\dagger)_\delta(\kappa)_\gamma(2\delta_{\alpha\gamma}\delta_{\beta\delta} - \delta_{\alpha\beta}\delta_{\delta\gamma}) \\ &= 2\,\kappa^\dagger\kappa\kappa^\dagger\kappa - \kappa^\dagger\kappa\kappa^\dagger\kappa \\ &= 1, \end{aligned} \tag{2.2.10}$$

which proves that y_μ are the Euclidean coordinates on the unit two-sphere.

There also exists a second Hopf bundle $S^3 \hookrightarrow S^7 \xrightarrow{\mathscr{H}_2} S^4$, consisting of the four-sphere as the base space, and the seven-sphere as the bundle space with the fibers being S^3. In order to explain the second Hopf map, $\mathscr{H}_2$, we should first note that S^7 can be represented in $\mathbb{C}^4$ by utilizing the complex coordinates $\zeta_\tau (\tau = 1, 2, 3, 4)$ as described below

$$S^7 = \left\{ \zeta^\dagger\zeta = 1\,, \zeta_\tau = \frac{\mathscr{E}_\tau}{|\mathscr{E}|}\,, \zeta = (\zeta_1, \zeta_2, \zeta_3, \zeta_4)^T \,|\, \mathscr{E}_\tau \in \mathbb{C}^4 \setminus \{\bar{0}\} \right\}, \tag{2.2.11}$$

where $|\mathscr{E}|^2 = \sum_\tau |\mathscr{E}_\tau|^2$ and $\bar{0} \equiv (0, 0, 0, 0)$. The Euclidean coordinates on the four-sphere base of the fibration is defined by [43, 44]

$$\Psi_a(\zeta) = \zeta^\dagger\gamma_a\zeta\,, \qquad a = 1, ..., 5, \tag{2.2.12}$$

where γ_a are the gamma-matrices in five dimensions that are associated to the $SO(5)$ group. They are 4×4 matrices satisfying the anticommutation relations

$$\{\gamma_a, \gamma_b\} = 2\delta_{ab}\mathbb{1}_4\,. \tag{2.2.13}$$

A possible representation of these matrices is given in A.1. The map $\mathscr{H}_2$ may then be written out explicitly in this basis as

$$\Psi_1 = \zeta_1{}^*\zeta_4 + \zeta_2{}^*\zeta_3 + \zeta_3{}^*\zeta_2 + \zeta_4{}^*\zeta_1, \tag{2.2.14a}$$

$$\Psi_2 = -i(\zeta_1{}^*\zeta_4 - \zeta_2{}^*\zeta_3 + \zeta_3{}^*\zeta_2 - \zeta_4{}^*\zeta_1), \tag{2.2.14b}$$

$$\Psi_3 = -\zeta_1{}^*\zeta_3 + \zeta_2{}^*\zeta_4 - \zeta_1\zeta_3^* + \zeta_2\zeta_4^*, \tag{2.2.14c}$$

$$\Psi_4 = i(\zeta_1{}^*\zeta_3 + \zeta_2{}^*\zeta_4 - \zeta_3{}^*\zeta_1 - \zeta_4{}^*\zeta_2), \tag{2.2.14d}$$

$$\Psi_5 = -\zeta_1{}^*\zeta_1 - \zeta_2{}^*\zeta_2 + \zeta_3{}^*\zeta_3 + \zeta_4{}^*\zeta_4. \tag{2.2.14e}$$

Using (2.2.14) we directly evaluate $\Psi_a\Psi_a$

$$\begin{aligned}
\Psi_a\Psi_a &= 4[(\zeta_1{}^*\zeta_4 + \zeta_3{}^*\zeta_2)(\zeta_2{}^*\zeta_3 + \zeta_4{}^*\zeta_1) - (\zeta_1{}^*\zeta_3 - \zeta_2\zeta_4{}^*)(\zeta_2{}^*\zeta_4 - \zeta_1\zeta_3{}^*)] \\
&\qquad + \left(|\zeta_1|^2 + |\zeta_2|^2 - |\zeta_3|^2 - |\zeta_4|^2\right)^2 \\
&= \left(|\zeta_1|^2 + |\zeta_2|^2\right)^2 + \left(|\zeta_3|^2 + |\zeta_4|^2\right)^2 + 2(|\zeta_1|^2 + |\zeta_2|^2)(|\zeta_3|^2 + |\zeta_4|^2) \\
&= (\zeta^\dagger\zeta)^2 \\
&= 1,
\end{aligned} \tag{2.2.15}$$

hence we have verified that Ψ_a correspond to the Euclidean coordinates on the unit S^4 and completed the constructions of the descent chains of manifolds $\mathbb{C}^2 \to S^3 \to S^2$ and $\mathbb{C}^4 \to S^7 \to S^4$.

2.3 Fuzzy Spheres

2.3.1 Construction of Fuzzy 2-Sphere

In section 2.1, we have collected several essential facts about the geometry of the two-sphere and demonstrated that S^2 is an adjoint orbit of $SU(2)$. For compact and semi-simple groups like $SU(2)$, the adjoint orbits are isomorphic to the coadjoint[1]

[1] Coadjoint action of a Lie group can be defined as its action on the dual vector space underlying the Lie algebra [45]. We give a detailed discussion of coadjoint orbits for $SU(2)$, $SU(3)$ and $SU(4)$ groups in chapter 3 and in appendix B.

orbits which are symplectic manifolds. Therefore, they are equipped with a symplectic structure. Thus, the two-sphere can be quantized by employing the quantization procedure detailed in [31]. We may note that S^4 is not a symplectic manifold and can not be quantized in the same manner.

In order to achieve the quantization of S^2, we should explore the descent chain of manifolds $\mathbb{C}^2 \to S^3 \to S^2$ and construct a noncommutative version of the first Hopf map to obtain the fuzzy two-sphere S_F^2. To start with, the Poisson bracket of two functions Ω_1 and Ω_2 on $\mathbb{C}^2$ is given by [46]

$$\{\Omega_1, \Omega_2\} = \sum_{\alpha=1}^{2} \left(\frac{\partial \Omega_1}{\partial z_\alpha} \frac{\partial \Omega_2}{\partial z_\alpha^*} - \frac{\partial \Omega_1}{\partial z_\alpha^*} \frac{\partial \Omega_2}{\partial z_\alpha} \right), \tag{2.3.1}$$

where the complex variables z_α and their conjugates z_α^* satisfy

$$\left\{ z_\alpha, z_\beta^* \right\} = \delta_{\alpha\beta}, \quad \left\{ z_\alpha, z_\beta \right\} = 0, \quad \left\{ z_\alpha^*, z_\beta^* \right\} = 0. \tag{2.3.2}$$

The next step in the quantization of $\mathbb{C}^2$ is to change all of the complex variables into linear operators acting on a Hilbert space. To achieve this, we can now proceed by replacing the Poisson bracket algebra of equation (2.3.2) by an analogous quantum mechanical commutation algebra of the form

$$\left[\hat{a}_\alpha, \hat{a}_\beta{}^\dagger \right] = \theta_{nc} \delta_{\alpha\beta}, \quad \left[\hat{a}_\alpha, \hat{a}_\beta \right] = 0, \quad \left[\hat{a}_\alpha^\dagger, \hat{a}_\beta{}^\dagger \right] = 0, \tag{2.3.3}$$

where $\hat{a}_\alpha{}^\dagger (\hat{a}_\alpha)$ are the harmonic oscillator creation (annihilation) operators that act on the two-particle Fock space and θ_{nc} is the noncommutative parameter with dimension length squared. It is possible to rewrite the commutation relations of equation (2.3.3) in the more familiar form of

$$\left[\hat{a}_\alpha, \hat{a}_\beta{}^\dagger \right] = \delta_{\alpha\beta}, \quad \left[\hat{a}_\alpha, \hat{a}_\beta \right] = 0, \quad \left[\hat{a}_\alpha^\dagger, \hat{a}_\beta{}^\dagger \right] = 0, \tag{2.3.4}$$

with the scaling $\hat{a}_\alpha \to \left(\hat{a}_\alpha / \sqrt{\theta_{nc}} \right)$.

The quantization of the three-sphere can be performed in a similar fashion by replacing the complex coordinates of equation (2.2.3) with the annihilation and creation operators:

$$\hat{\kappa}_\alpha = \hat{a}_\alpha \frac{1}{\sqrt{\widehat{N}}} = \frac{1}{\sqrt{1 + \widehat{N}}} \hat{a}_\alpha \,, \tag{2.3.5a}$$

$$\hat{\kappa}_\alpha{}^* = \frac{1}{\sqrt{\widehat{N}}}\hat{a}_\alpha{}^\dagger = \hat{a}_\alpha{}^\dagger\frac{1}{\sqrt{1+\widehat{N}}}\,, \tag{2.3.5b}$$

where $\widehat{N}$ is the number operator defined by

$$\widehat{N} = \sum_\alpha \hat{a}_\alpha{}^\dagger \hat{a}_\alpha, \qquad \widehat{N} \neq 0. \tag{2.3.6}$$

Although the presence of $\widehat{N} \neq 0$ condition might be interpreted as the exclusion of vacuum state from the Fock space, this conclusion would be misleading as successive application of the $\hat{\kappa}_\alpha$ operator on any state in Fock space will eventually result in the creation of the vacuum state. Thus, the construction of noncommutative S^3 may be taken only as an auxilary step toward the construction of fuzzy S^2.

Before completing the generalization of the first Hopf map to the noncommutative spaces, we should inspect another commutation relation which is

$$\begin{aligned}
\left[\widehat{N}, a^\dagger\sigma_\mu a\right] &= \left[\hat{a}^\dagger_\alpha\hat{a}_\alpha, \hat{a}^\dagger_\beta\left(\sigma_\mu\right)_{\beta\gamma}\hat{a}_\gamma\right] \\
&= (\sigma_\mu)_{\beta\gamma}\left(\left[\hat{a}^\dagger_\alpha\hat{a}_\alpha, \hat{a}^\dagger_\beta\right]\hat{a}_\gamma + \hat{a}^\dagger_\beta\left[\hat{a}^\dagger_\alpha\hat{a}_\alpha, \hat{a}^\dagger_\gamma\right]\right) \\
&= (\sigma_\mu)_{\beta\gamma}\left(\delta_{\alpha\beta}\hat{a}^\dagger_\alpha\hat{a}_\gamma + \hat{a}^\dagger_\beta\left(-\delta_{\gamma\alpha}\hat{a}_\alpha\right)\right) \\
&= (\sigma_\mu)_{\beta\gamma}\left(\hat{a}^\dagger_\beta\hat{a}_\gamma - \hat{a}^\dagger_\beta\hat{a}_\gamma\right) \\
&= 0,
\end{aligned} \tag{2.3.7}$$

where $a = (\hat{a}_1, \hat{a}_2)^T$ is a column vector consisting of the annihilation operators. Intuitively, it should be clear that the commutator in the left hand side of (2.3.7) vanishes since, $a^\dagger\sigma_\mu a$ term contains equal number of annihilation and creation operators in each component. As a result of combining (2.3.7) with the quantized version of equation (2.2.5), we arrive at the set of operators $\hat{x}_\mu$ that corresponds to the noncommutative coordinates of S^2_F as follows

$$\hat{x}_\mu = \frac{1}{\sqrt{\widehat{N}}}a^\dagger\sigma_\mu a\frac{1}{\sqrt{\widehat{N}}} = \frac{1}{\widehat{N}}a^\dagger\sigma_\mu a\,, \tag{2.3.8}$$

where we have used (2.3.7) for the last equality in (2.3.8), as (2.3.7) is valid for any function of $\widehat{N}$. We can immediately observe that the number operator commutes with these coordinates:

$$\left[\widehat{N}, \hat{x}_\mu\right] = 0, \tag{2.3.9}$$

which suggests that it is possible to restrict $\hat{x}_\mu$ to the $(N+1)$-dimensional subspace $\mathscr{H}_N$ of the Fock space in which the eigenvalue of the number operator is never zero, i.e., $\widehat{N} \equiv N \neq 0$ on any of the vectors of $\mathscr{H}_N$. The set of orthogonal vectors $|N_1, N-N_1\rangle$ that are defined by

$$|N_1, N-N_1\rangle = \frac{\left(\hat{a}_1{}^\dagger\right)^{N_1}\left(\hat{a}_2{}^\dagger\right)^{N-N_1}}{\left(N_1!\,(N-N_1)!\right)^{1/2}}\,|0,0\rangle\,, \tag{2.3.10}$$

constitute a convenient basis for spanning $\mathscr{H}_N$. In this basis, $\hat{x}_\mu$ are $(N+1)\times(N+1)$ Hermitian matrices whose polynomials generate the matrix algebra $\mathit{Mat}(N+1)$. Here, it is essential to note that, as a consequence of the quantization of the first Hopf map, the algebra of functions on S^2, $C^\infty(S^2)$, is converted into the noncommutative algebra of matrices $\mathit{Mat}(N+1)$ on S_F^2.

These foregoing considerations about the noncommutative coordinates of (2.3.8) can be enriched by focusing on the relationship between the algebraic theory of angular momentum and quantum oscillators. The Jordan-Schwinger map, which may be thought of as an operator analogue of the Hopf maps, is a mapping from a set of matrices into the annihilation (creation) operators of either bosonic or fermionic type [47, 48]. As a specific example, consider the map $\mathscr{M}_3$ given over the bosonic operators:

$$\mathscr{M}_3 : \frac{1}{2}\sigma_\mu \mapsto J_\mu = \frac{1}{2}a^\dagger\sigma_\mu a, \tag{2.3.11}$$

where σ_μ are the Pauli matrices. The operators J_μ correspond to the generators of $SU(2)$ group on the Fock space spanned by

$$|n_1, n_2\rangle = \frac{\left(\hat{a}_1{}^\dagger\right)^{n_1}\left(\hat{a}_2{}^\dagger\right)^{n_2}}{\left(n_1!\,n_2!\right)^{1/2}}\,|0,0\rangle\,, \tag{2.3.12}$$

and Jordan-Schwinger map assures that they satisfy the commutation relations

$$[J_\mu, J_\nu] = i\epsilon_{\mu\nu\eta}J_\eta. \tag{2.3.13}$$

The operators J_μ may be expressed in an explicit form as

$$J_1 = \frac{1}{2}\left(\hat{a}_1{}^\dagger\hat{a}_2 + \hat{a}_2{}^\dagger\hat{a}_1\right), \tag{2.3.14a}$$

$$J_2 = \frac{i}{2}\left(\hat{a}_2{}^\dagger\hat{a}_1 - \hat{a}_1{}^\dagger\hat{a}_2\right), \tag{2.3.14b}$$

$$J_3 = \frac{1}{2}\left(\hat{a}_1{}^\dagger\hat{a}_1 - \hat{a}_2{}^\dagger\hat{a}_2\right), \tag{2.3.14c}$$

from which we easily find that

$$J_\mu \left|0,0\right\rangle = 0, \tag{2.3.15}$$

hence the ground state is an $SU(2)$ singlet. Furthermore, the adjoint action of J_μ on the annihilation operators is

$$\begin{aligned}\left[J_\mu, \hat{a}_\alpha\right] &= \frac{1}{2}\left[\hat{a}_\beta{}^\dagger \left(\sigma_\mu\right)_{\beta\gamma} \hat{a}_\gamma, \hat{a}_\alpha\right] \\ &= \frac{1}{2}(\sigma_\mu)_{\beta\gamma}\left(\hat{a}^\dagger_\beta\left[\hat{a}_\gamma, \hat{a}_\alpha\right] + \left[\hat{a}^\dagger_\beta, \hat{a}_\alpha\right]\hat{a}_\gamma\right) \\ &= \frac{1}{2}(\sigma_\mu)_{\beta\gamma}\left(-\delta_{\alpha\beta}\hat{a}_\gamma\right) \\ &= -\frac{1}{2}(\sigma_\mu)_{\alpha\gamma}\hat{a}_\gamma,\end{aligned} \tag{2.3.16}$$

and similarly we have

$$\left[J_\mu, \hat{a}_\alpha{}^\dagger\right] = \frac{1}{2}(\sigma_\mu)_{\gamma\alpha}\hat{a}_\gamma{}^\dagger, \tag{2.3.17}$$

so the operators $\hat{a}_\alpha{}^\dagger$ and $\hat{a}_\alpha$ both carry the spin $\frac{1}{2}$ irreducible representation (IRR) of $SU(2)$ and transform as spinors under the action of $SU(2)$. An important and useful implication of this fact is that by taking the N-fold symmetric tensor product of spin-half IRRs, we may reach the angular momentum $j = \frac{N}{2}$ IRR of $SU(2)$ as follows

$$\left(\frac{1}{2}\otimes\frac{1}{2}\otimes ... \otimes\frac{1}{2}\right)_{\text{sym}} \equiv \frac{N}{2}. \tag{2.3.18}$$

In fact, we see that $\left[\widehat{N}, J_\mu\right] = 0$ by (2.3.7), so J_μ spans the spin $j = \frac{N}{2}$ IRR on the subset of states $\left|n_1, n_2\right\rangle$ with $N = n_1 + n_2$. Therefore the full Fock space splits into an infinite direct sum of subspaces each of which is labeled by an $SU(2)$ IRR $j = \frac{N}{2}$ and we may write $\mathscr{F} \equiv \bigoplus_{N=0}^{\infty}\mathscr{H}_N$. The Casimir operator of $SU(2)$ in the spin $\frac{N}{2}$ IRR is

$$\begin{aligned}J_\mu J_\mu \left|N_1, N-N_1\right\rangle &= j\left(j+1\right)\left|N_1, N-N_1\right\rangle \\ &= \frac{N}{2}\left(\frac{N}{2}+1\right)\left|N_1, N-N_1\right\rangle.\end{aligned} \tag{2.3.19}$$

By exploiting (2.3.9), the connection between the angular momentum operators and the fuzzy sphere coordinates can be established as

$$J_\mu \left|N_1, N-N_1\right\rangle = \frac{1}{2}\widehat{N}\hat{x}_\mu \left|N_1, N-N_1\right\rangle$$

$$= \frac{1}{2}\hat{x}_\mu \widehat{N} \left|N_1, N-N_1\right\rangle \tag{2.3.20}$$
$$= \frac{N}{2}\hat{x}_\mu \left|N_1, N-N_1\right\rangle ,$$

or

$$\hat{x}_\mu \left|N_1, N-N_1\right\rangle = \frac{2}{N} J_\mu \left|N_1, N-N_1\right\rangle , \tag{2.3.21}$$

from which one may observe that S_F^2 coordinates satisfy

$$[\hat{x}_\mu, \hat{x}_\nu] = \frac{2i}{N}\epsilon_{\mu\nu\eta}\hat{x}_\eta. \tag{2.3.22}$$

Moreover, it follows from equation (2.3.19) that $\hat{x}_\mu$'s fulfill the relation:

$$\hat{x}_\mu \hat{x}_\mu = \left(1 + \frac{2}{N}\right) \mathbb{1}_{N+1}. \tag{2.3.23}$$

It is clear from equations (2.3.22) and (2.3.23) that in the large-N limit the standard commutative S^2 is recovered. With the scaling

$$\hat{x}_\mu \to \sqrt{\frac{N}{N+2}}\hat{x}_\mu = \frac{1}{\sqrt{j\,(j+1)}} J_\mu, \tag{2.3.24}$$

the last two equations can be put in better-known forms shown below

$$\hat{x}_\mu \hat{x}_\mu = \mathbb{1}_{N+1}, \tag{2.3.25}$$

$$[\hat{x}_\mu, \hat{x}_\nu] = \frac{i}{\sqrt{j\,(j+1)}}\epsilon_{\mu\nu\eta}\hat{x}_\eta. \tag{2.3.26}$$

A general matrix $m \in \textit{Mat}(2j+1)$ is an element of $S_F^2\,(j)$ and can be finitely generated by $\hat{x}_\mu$ as detailed below

$$m = \sum_{\mu_1,\ldots,\mu_l} m_{\mu_1\ldots\mu_l}\hat{x}_{\mu_1}\ldots\hat{x}_{\mu_l}. \tag{2.3.27}$$

We may compare this with equation (2.1.3), we see that, m tends to $\Omega(\vec{\boldsymbol{\rho}})$ in the $j \to \infty$ limit. The scalar product on the fuzzy sphere is defined as

$$(m_1, m_2) = \mathrm{Tr}\Big({m_1}^\dagger m_2\Big), \tag{2.3.28}$$

where $m_1, m_2 \in \textit{Mat}(N+1)$ and Tr stands for the normalized trace given by

$$\mathrm{Tr}(\mathbb{1}_{N+1}) = \frac{1}{N+1}\,\mathrm{tr}(\mathbb{1}_{N+1}) = 1. \tag{2.3.29}$$

It must be clear that the Tr corresponds to the integral $\frac{1}{4\pi}\int \mathrm{d}^3\vec{\boldsymbol{\rho}}$ and the inner product (2.3.28) converges to $\int \mathrm{d}^3\vec{\boldsymbol{\rho}}\;\Omega_1(\vec{\boldsymbol{\rho}})\,\Omega_2(\vec{\boldsymbol{\rho}})$ in the $j\to\infty$ limit. Besides, we may also introduce left and right acting linear operators $\hat{O}^L$ and $\hat{O}^R$ that are defined through their action on $\boldsymbol{Mat}(N+1)$:

$$\hat{O}^L m = om, \quad \hat{O}^R m = mo, \qquad \hat{O}^L, \hat{O}^R \in \boldsymbol{Mat}(N+1), \tag{2.3.30}$$

and satisfy the relations

$$\left[\hat{O}^L, \hat{P}^R\right] = 0, \quad \left(\hat{O}\hat{P}\right)^L = \hat{O}^L\hat{P}^L, \quad \left(\hat{O}\hat{P}\right)^R = \hat{P}^R\hat{O}^R. \tag{2.3.31}$$

A subset of these linear operators, which should be given special emphasis, consist of the angular momentum operators J_μ^L and J_μ^R whose Casimir operators are given by

$$\begin{aligned} J_\mu^R J_\mu^R \left\langle N_1, N-N_1\right| &= \left\langle N_1, N-N_1\right| J_\mu J_\mu \\ &= j\,(j+1)\left\langle N_1, N-N_1\right|, \end{aligned} \tag{2.3.32}$$

$$\begin{aligned} J_\mu^L J_\mu^L \left|N_1, N-N_1\right\rangle &= J_\mu J_\mu \left|N_1, N-N_1\right\rangle \\ &= j\,(j+1)\left|N_1, N-N_1\right\rangle. \end{aligned} \tag{2.3.33}$$

Now that we have introduced the left and right acting operators, it is time to construct a noncommutative analog of the derivative operator, L_μ, of equation (2.1.6). The derivatives on the fuzzy sphere are defined by the adjoint action of the group $SU(2)$ on $\boldsymbol{Mat}(N+1)$ as follows

$$\mathscr{L}_\mu m \equiv adJ_\mu m = \left(J_\mu^L - J_\mu^R\right) m = \left[J_\mu, m\right], \tag{2.3.34}$$

where $\mathscr{L}_\mu$'s satisfy the Leibniz rule

$$\mathscr{L}_\mu\left(m_1 m_2\right) = \left(\mathscr{L}_\mu m_1\right) m_2 + m_1\left(\mathscr{L}_\mu m_2\right), \tag{2.3.35}$$

therefore $\mathscr{L}_\mu$'s are derivations on $\boldsymbol{Mat}(N+1)$. As they contain J_μ^L and J_μ^R, which both carry the spin-j irreducible representations of $SU(2)$, the $\mathscr{L}_\mu$ operators carry the tensor product representation $(j\times j)$ that decomposes into the direct sum of IRRs of $SU(2)$ as

$$j\otimes j = 0\oplus 1\oplus ...\oplus 2j = \bigoplus_{k=0}^{2j} k\,, \tag{2.3.36}$$

which means that there is a cut-off value for the spectrum of the Laplacian $\mathscr{L}^2 = \mathscr{L}_\mu \mathscr{L}_\mu$ on S_F^2. We see that $\mathscr{L}^2$ can take on the eigenvalues $l\,(l+1)$ with $l = 0, 1, ..., 2j$. In fact, we can choose to diagonalize $\mathscr{L}_3$ together with $\mathscr{L}^2 = \mathscr{L}_\mu \mathscr{L}_\mu$. The eigenvectors in this basis are known as the irreducible polarization tensors $T_{lm}(j)$ $(-l \leq m \leq l)$ that carry the spin-l irreducible representation of $SU(2)$. We have

$$\mathscr{L}^2 T_{lm}(j) = \mathscr{L}_\mu \mathscr{L}_\mu T_{lm} = \Big[J_\mu, \Big[J_\mu, T_{lm}\Big]\Big] = l\,(l+1)\,T_{lm}(j), \tag{2.3.37}$$

$$\mathscr{L}_3 T_{lm}(j) = \Big[J_3, T_{lm}\Big] = m T_{lm}(j), \tag{2.3.38}$$

where the polarization tensors are $(2j+1) \times (2j+1)$ matrices. The inner product rule is given by

$$\big(T_{lm}, T_{l'm'}\big) = \mathrm{Tr}\Big({T_{lm}}^\dagger T_{l'm'}\Big) = \delta_{ll'}\delta_{mm'}\,. \tag{2.3.39}$$

For a given value of l, there are $2l+1$ possible values of m, hence in total $T_{lm}(j)$ has

$$\sum_{l=0}^{2j} (2l+1) = 2j\,(2j+1) + 2j + 1 = (2j+1)^2\,, \tag{2.3.40}$$

independent degrees of freedom which leads us to realize that $T_{lm}(j)$ form an orthonormal basis of the matrix algebra $\boldsymbol{Mat}(2j+1)$. As an essential consequence of these facts, generic matrix $M \in \boldsymbol{Mat}(2j+1)$ on the fuzzy S^2 can be decomposed as

$$M = \sum_{l=0}^{2j} \sum_{m=-l}^{l} C_{lm} T_{lm}(j). \tag{2.3.41}$$

We see that, this result is the fuzzy analogue of (2.1.4) and $T_{lm}(j)$ may be thought as the discrete basis replacing the spherical harmonics $Y_{lm}(\theta, \varphi)$ on S^2.

2.3.2 Construction of Fuzzy 4-Sphere

In the preceding subsection, we focused on the construction of the fuzzy two-sphere. In this subsection, we continue our inspection of fuzzy spaces by turning our focus to the discussion of the fuzzy four-sphere S_F^4. Some aspects of construction of S_F^4 resembles the construction of S_F^2. Nevertheless, there are also important distinctions, which does not allow us to give a simple generalization of the discussion leading to the construction of S_F^2.

To begin the construction of S_F^4, we start with the standard definition of a four-sphere. The four-dimensional sphere S^4 can be embedded in five-dimensional Euclidean space $\mathbb{R}^5$ as

$$x_1{}^2 + x_2{}^2 + x_3{}^2 + x_4{}^2 + x_5{}^2 = R^2, \qquad (x_1, x_2, x_3, x_4, x_5) \in \mathbb{R}^5. \tag{2.3.42}$$

Since the coordinates x_a commute by definition, we have

$$\epsilon^{abcde} x_a x_b x_c x_d = 0\,, \tag{2.3.43}$$

where ϵ^{abcde} is the 5-dimensional Levi-Civita tensor. The derivations on 4-sphere are provided by the $SO(5)$ generators that are defined in terms of differential operators as follows

$$L_{ab} = x_a \partial_b - x_b \partial_a\,. \tag{2.3.44}$$

Allowing L_{ab} to operate on an arbitrary coordinate shows readily that

$$L_{ab}(x_c) \equiv [L_{ab}, x_c] = x_a \delta_{cb} - x_b \delta_{ac}, \tag{2.3.45}$$

and the derivations satisfy the usual $SO(5)$ commutation relations given by

$$[L_{ab}, L_{cd}] = \delta_{bc} L_{ad} - \delta_{bd} L_{ac} + \delta_{ad} L_{bc} - \delta_{ac} L_{bd}. \tag{2.3.46}$$

In equation (2.1.26), we provided the description of S^2 as a coset space. The four-sphere can be described as a coset manifold in a similar fashion. To demonstrate this fact, we should consider the action of certain special orthogonal groups on S^4. It is known that $SO(5)$ acts transitively on the 4-sphere. The infinitesimal action of $SO(5)$ on S^4 is already provided by L_{ab} in (2.3.44) and (2.3.45). Let $\vec{x}_{st} = (x_1, x_2, x_3, x_4, x_5)^T$ denote the coordinates of the 4-sphere. From (2.3.42) we can infer that $\vec{x}_{st}$ transforms as a vector under the rotations of $SO(5)$ group. The north pole of S^4 may be given by $\vec{x}_o = (0, 0, 0, 0, 1)^T$. The isotropy group of $\vec{x}_o$ is clearly

$$G \equiv \begin{pmatrix} H & 0 \\ 0 & 1 \end{pmatrix} = \{diag\,(H, 1)\,|\,H \in SO(4)\} \approx SO(4), \tag{2.3.47}$$

since the action of $SO(5)$ is transitive, we have the desired result

$$S^4 \cong \frac{SO(5)}{SO(4)}. \tag{2.3.48}$$

Before giving a detailed construction, we may define the fuzzy four-sphere in terms of noncommutative coordinates χ_a $(a = 1, ..., 5)$ satisfying the conditions

$$\chi_a \chi_a = R^2 \,, \tag{2.3.49a}$$

$$\epsilon^{abcde} \chi_a \chi_b \chi_c \chi_d = C \chi_e \,, \tag{2.3.49b}$$

which can be realized by $N \times N$ matrices such that $N = \frac{1}{6}(n+1)(n+2)(n+3)$ with $n \in \mathbb{Z}^+$. The radius R and the constant C are given by

$$R^2 = \frac{1}{4} n(n+4) r, \quad C = (n+2) r^3, \tag{2.3.50}$$

where r is a constant of dimension length. (2.3.49a) is analogous to (2.3.23) of fuzzy sphere, while (2.3.49b) is new. We also see that not all $N \times N$ matrices can represent S_F^4 but only those of dimension $4, 10, 20, ...$ etc. We may now proceed to discuss the underlying facts.

In order to initiate the formation of a matrix configuration with the symmetry properties of a four-sphere, we recall the Clifford algebra relation (2.2.13), $\{\gamma_a, \gamma_b\} = 2\delta_{ab} \mathbb{1}_4$, where γ_a are the 4×4 gamma-matrices in five dimensions. The generators of the spinor representation $(0, 1)$ (in the Dynkin notation) of $SO(5)$ are given as

$$G_{ab} = -\frac{i}{4} [\gamma_a, \gamma_b], \tag{2.3.51}$$

and fulfills the SO(5) commutation relations, that is

$$[G_{ab}, G_{cd}] = i \left(\delta_{ac} G_{bd} + \delta_{bd} G_{ac} - \delta_{ad} G_{bc} - \delta_{bc} G_{ad} \right). \tag{2.3.52}$$

Let us note that L_{ab} in contrast carry the vector IRR of $SO(5)$ denoted as $(1, 0)$ in Dynkin notation. γ_a act on the four-dimensional spinor space $\mathbb{C}^4$ which is the carrier space of the $(0, 1)$ IRR of SO(5). We define the Hilbert space $\mathscr{H}_n$, which is the carrier space of the $(0, n)$ IRR of SO(5), as the n-fold completely symmetrized tensor product space

$$\mathscr{H}_n = \left(\mathbb{C}^4 \otimes ... \otimes \mathbb{C}^4 \right), \tag{2.3.53}$$

with the dimension N given by

$$N = dim(0, n) = \frac{1}{6}(n+1)(n+2)(n+3). \tag{2.3.54}$$

Now, we consider the n-fold symmetric tensor product

$$X_a^{(n)} = \frac{1}{2} \left(\gamma_a \otimes \mathbb{1}_4 \otimes ... \otimes \mathbb{1}_4 + ... + \mathbb{1}_4 \otimes ... \otimes \mathbb{1}_4 \otimes \gamma_a \right)_{\text{sym}} , \tag{2.3.55}$$

that acts on $\mathscr{H}_n$. The subscript "sym" indicates that X_a are restricted to the completely symmetrized tensor product space. By taking the commutators of X_a's, it is possible to obtain the generators of SO(5) in the $(0,n)$ IRR

$$[X_a, X_b] = iM_{ab}, \tag{2.3.56}$$

which satisfy the SO(5) algebra

$$[M_{ab}, M_{cd}] = i(\delta_{ac}M_{bd} + \delta_{bd}M_{ac} - \delta_{ad}M_{bc} - \delta_{bc}M_{ad}). \tag{2.3.57}$$

The commutation relations of M_{ab} with X_c's show that X_c transform as vectors under the SO(5) transformations generated by M_{ab}

$$[M_{ab}, X_c] = i(\delta_{ac}X_b - \delta_{bc}X_a). \tag{2.3.58}$$

The $N \times N$ Hermitian matrices X_a satisfy the identities (2.3.49) for the fuzzy four-sphere

$$X_aX_a = \frac{1}{4}n(n+4)\mathbb{1}_N, \tag{2.3.59a}$$

$$\epsilon^{abcde}X_aX_bX_cX_d = \frac{1}{4}\epsilon^{abcde}M_{ab}M_{dc} = (n+2)X_e. \tag{2.3.59b}$$

We will compute (2.3.59a) explicitly after stating a few further developments, while we omit the proof of (2.3.59b) and refer the reader to [34]. Note that X_aX_a is an SO(5) invariant operator. Since one can easily check that $[M_{ab}, X_cX_c] = 0$, it is not the Casimir operator of $SO(5)$ though. The latter is given as $M_{ab}M_{ab}$ and in the $(0,n)$ irreducible representation takes the value

$$C_2^{SO(5)}((0,n)) = M_{ab}M_{ab} = \frac{1}{2}n(n+4)\mathbb{1}_N. \tag{2.3.60}$$

The noncommutative coordinates of S_F^4 can be related to X_a via a dimensionful constant r introduced in (2.3.49) as shown below

$$\chi_a = rX_a, \quad R^2 = \frac{1}{4}n(n+4)r^2, \quad C = (n+2)r^3. \tag{2.3.61}$$

The X_a's can also be expressed in terms of quantum oscillators by employing a generalization of the Schwinger's construction. Let $\hat{\mathscr{A}}_\alpha^\dagger$ $\left(\hat{\mathscr{A}}_\alpha\right)$ be the creation (annihilation) operators that correspond to the four bosonic oscillators. They satisfy the bosonic operator algebra

$$\left[\hat{\mathscr{A}}_\alpha, \hat{\mathscr{A}}_{\alpha'}^\dagger\right] = \delta_{\alpha\alpha'}, \quad \left[\hat{\mathscr{A}}_\alpha, \hat{\mathscr{A}}_{\alpha'}\right] = 0, \quad \left[\hat{\mathscr{A}}_\alpha^\dagger, \hat{\mathscr{A}}_{\alpha'}^\dagger\right] = 0. \tag{2.3.62}$$

By allowing the creation operators to act on the vacuum state $|0\rangle \equiv |0000\rangle$, one obtains the Fock space equivalent of (2.3.53), i.e. $\mathscr{H}_n$ is spanned by the states $\hat{\mathscr{A}}^\dagger_{\alpha_1}...\hat{\mathscr{A}}^\dagger_{\alpha_n}|0\rangle$. The realization of X_a in this basis is written by

$$X_a = \frac{1}{2}\hat{\mathscr{A}}^\dagger \gamma_a \hat{\mathscr{A}}, \tag{2.3.63}$$

where the vector $\hat{\mathscr{A}}$ has components given by $\hat{\mathscr{A}} \equiv \left(\hat{\mathscr{A}}_1, \hat{\mathscr{A}}_2, \hat{\mathscr{A}}_3, \hat{\mathscr{A}}_4\right)^T$. Taking the commutators of X_a's yields

$$\begin{aligned}
[X_a, X_b] &= \frac{1}{4}\Big[\left(\hat{\mathscr{A}}^\dagger\right)_\alpha (\gamma_a)_{\alpha\alpha'}\left(\hat{\mathscr{A}}\right)_{\alpha'}, \left(\hat{\mathscr{A}}^\dagger\right)_{\beta'} (\gamma_b)_{\beta'\beta''}\left(\hat{\mathscr{A}}\right)_{\beta''}\Big] \\
&= \frac{1}{4}(\gamma_a)_{\alpha\alpha'}(\gamma_b)_{\beta'\beta''}\left[\hat{\mathscr{A}}^\dagger_\alpha \hat{\mathscr{A}}_{\alpha'}, \hat{\mathscr{A}}^\dagger_{\beta'}\hat{\mathscr{A}}_{\beta''}\right] \\
&= \frac{1}{4}(\gamma_a)_{\alpha\alpha'}(\gamma_b)_{\beta'\beta''}\left(\hat{\mathscr{A}}^\dagger_\alpha \delta_{\alpha'\beta'}\hat{\mathscr{A}}_{\beta''} - \hat{\mathscr{A}}^\dagger_{\beta'}\delta_{\beta''\alpha}\hat{\mathscr{A}}_{\alpha'}\right) \\
&= \frac{1}{4}\left(\hat{\mathscr{A}}^\dagger \gamma_a\gamma_b\hat{\mathscr{A}} - \hat{\mathscr{A}}^\dagger\gamma_b\gamma_a\hat{\mathscr{A}}\right) \\
&= i\hat{\mathscr{A}}^\dagger \frac{1}{4i}[\gamma_a, \gamma_b]\hat{\mathscr{A}} \\
&= iM_{ab},
\end{aligned} \tag{2.3.64}$$

where M_{ab} is

$$M_{ab} = \hat{\mathscr{A}}^\dagger G_{ab}\hat{\mathscr{A}}. \tag{2.3.65}$$

Equations (2.3.57) and (2.3.58) can be verified by the same token. From the analysis of the preceding commutation relations it is found out that the matrix algebra generated by the S_F^4 coordinates, X_a, do not close. Thus, it is not possible to write an expression analogous to (2.3.41) which enables an expansion of functions on S_F^4 in a complete basis.

2.3.2.1 Symmetric Tensor Product of Matrices

With the algebraic background of the fuzzy four-sphere in hand, we shift our view to the calculation of S_F^4 matrices that are defined by (2.3.55). A convenient way of determining the elements of these matrices is to express the symmetric tensor product in terms of an orthonormal basis. To achieve this, we first write the elements of a matrix W as

$$W_{\alpha\beta} = \langle\alpha| W |\beta\rangle . \tag{2.3.66}$$

The tensor product, i.e. Kronecker product, of two matrices may be expressed as [49]

$$(W \otimes V)_{[\alpha\,\beta]} = \langle\alpha_1, \alpha_2|W \otimes V|\beta_1, \beta_2\rangle$$

$$= \langle\alpha_1| \langle\alpha_2| (W \otimes V) |\beta_1\rangle |\beta_2\rangle \tag{2.3.67}$$
$$= \langle\alpha_1| W |\beta_1\rangle \langle\alpha_2| V |\beta_2\rangle ,$$

where $[\alpha\,\beta]$ is a collective notation for $(\alpha_1, \alpha_2, \beta_1, \beta_2)$. Now, consider $|\beta_1, \beta_2\rangle_{\rm sym}$ to be a symmetrized orthonormal state that is given by

$$|\beta_1, \beta_2\rangle_{\rm sym} = |\beta_2, \beta_1\rangle_{\rm sym} = \frac{1}{\gamma_{nr}} \left(|\beta_1\rangle |\beta_2\rangle + |\beta_2\rangle |\beta_1\rangle\right) , \tag{2.3.68}$$

where γ_{nr} is an appropriate constant of normalization. The two-fold symmetric tensor product could be defined by

$$(W \otimes_{\rm S} V)_{[\alpha\,\beta]} = {}_{\rm sym}\langle\alpha_1, \alpha_2|W \otimes V|\beta_1, \beta_2\rangle_{\rm sym}. \tag{2.3.69}$$

As an illustration of the calculation of symmetric product, we may determine a specific element. For instance, consider the case of $[\alpha\,\beta] = (\alpha_1, \alpha_2, \beta_1, \beta_2) = (1, 2, 1, 1)$:

$$\begin{aligned}(W \otimes_{\rm S} V)_{[\alpha\,\beta]} &= {}_{\rm sym}\langle 1, 2|W \otimes V\,|1, 1\rangle_{\rm sym} \\ &= \frac{1}{\sqrt{2}}\Big[\left(\langle 1| \langle 2| + \langle 2| \langle 1|\right) (W \otimes V) \left(|1\rangle |1\rangle\right) \Big] \\ &= \frac{1}{\sqrt{2}}\Big[\langle 1| W |1\rangle \langle 2| V |1\rangle + \langle 2| W |1\rangle \langle 1| V |1\rangle \Big] \\ &= \frac{1}{\sqrt{2}} \left(W_{11}V_{21} + W_{21}V_{11}\right) .\end{aligned} \tag{2.3.70}$$

Besides, an examination of equation (2.3.69) also demonstrates that the symmetric tensor product is commutative. This property is manifest if one substitute (2.3.68) for $|\beta_1, \beta_2\rangle_{\rm sym}$ in (2.3.69)

$$\begin{aligned}(W \otimes_{\rm S} V)_{[\alpha\,\beta]} &= \frac{1}{\gamma_{nr}^2}\Big[\langle\alpha_1| W |\beta_1\rangle \langle\alpha_2| V |\beta_2\rangle + \langle\alpha_1| W |\beta_2\rangle \langle\alpha_2| V |\beta_1\rangle \\ &\qquad + \langle\alpha_2| W |\beta_1\rangle \langle\alpha_1| V |\beta_2\rangle + \langle\alpha_2| W |\beta_2\rangle \langle\alpha_1| V |\beta_1\rangle \Big] \\ &= \frac{1}{\gamma_{nr}^2}\Big[\langle\alpha_2| \langle\alpha_1| (V \otimes W) |\beta_2\rangle |\beta_1\rangle + \langle\alpha_2| \langle\alpha_1| (V \otimes W) |\beta_1\rangle |\beta_2\rangle \\ &\quad + \langle\alpha_1| \langle\alpha_2| (V \otimes W) |\beta_2\rangle |\beta_1\rangle + \langle\alpha_1| \langle\alpha_2| (V \otimes W) |\beta_1\rangle |\beta_2\rangle \Big] \\ &= {}_{\rm sym}\langle\alpha_1, \alpha_2|V \otimes W|\beta_1, \beta_2\rangle_{\rm sym} \\ &= (V \otimes_{\rm S} W)_{[\alpha\,\beta]} .\end{aligned} \tag{2.3.71}$$

Inspecting (2.3.71) we may infer that the minimum number of terms required to evaluate $X_a^{(n)}$ can have two values depending on the parity of n, and it is $\dfrac{n}{2}$ for even n

while it is $\frac{n+1}{2}$ for odd n. We can exemplify this situation by analyzing the case of 5-fold symmetric tensor product:

$$\begin{aligned} X_a^{(5)} = \frac{1}{2}\Big[&\gamma_a \otimes (\mathbb{1}_4 \otimes \mathbb{1}_4 \otimes \mathbb{1}_4 \otimes \mathbb{1}_4) + (\mathbb{1}_4 \otimes \gamma_a \otimes \mathbb{1}_4) \otimes (\mathbb{1}_4 \otimes \mathbb{1}_4) \\ &+ \mathbb{1}_4 \otimes \mathbb{1}_4 \otimes \gamma_a \otimes \mathbb{1}_4 \otimes \mathbb{1}_4 + (\mathbb{1}_4 \otimes \mathbb{1}_4) \otimes (\mathbb{1}_4 \otimes \gamma_a \otimes \mathbb{1}_4) \\ &+ (\mathbb{1}_4 \otimes \mathbb{1}_4 \otimes \mathbb{1}_4 \otimes \mathbb{1}_4) \otimes \gamma_a\Big]_{\text{sym}} \\ = \Big[&\gamma_a \otimes \mathbb{1}_4 \otimes \mathbb{1}_4 \otimes \mathbb{1}_4 \otimes \mathbb{1}_4 + \mathbb{1}_4 \otimes \gamma_a \otimes \mathbb{1}_4 \otimes \mathbb{1}_4 \otimes \mathbb{1}_4 \\ &+ \frac{1}{2}\mathbb{1}_4 \otimes \mathbb{1}_4 \otimes \gamma_a \otimes \mathbb{1}_4 \otimes \mathbb{1}_4\Big]_{\text{sym}}. \end{aligned} \tag{2.3.72}$$

As expected, 3 terms are sufficient to completely evaluate $X_a^{(5)}$. Before concluding the discussion of symmetric tensor product we need to point out that, as suited to the particular needs of the subsequent chapters, $X_a^{(n)}$ matrices for $n = 1, ..., 9$ were numerically evaluated in the basis of γ-matrices provided in appendix A.1. The algorithm, which was developed for the task of the calculation of these matrices, was implemented in the MATLAB code shown in appendix G.

2.3.2.2 Geometry of S_F^4

To conclude this subsection and to further reveal the distinctions between S_F^2 and S_F^4, we move on to a discussion of proper geometric characterization of the fuzzy 4-sphere. Our initial task to reveal the geometry of S_F^4 is to render a reinterpretation of equation (2.2.12). To achieve this, one should first notice that the overall phase of ζ_τ drops out in (2.2.12). Therefore, the second Hopf map is also related to a map from $\mathbb{CP}^3 \cong \frac{S^7}{U(1)}$ to the four-sphere [10, 19]. As it is central to the understanding of this new interpretation, let us consider a definition of $\mathbb{CP}^3$ in terms of projection operators. The relevant projection operator can be defined in Dirac notation as follows [50, 51]

$$P_\zeta = |\zeta\rangle\langle\zeta| = \zeta\zeta^\dagger, \tag{2.3.73}$$

where $\zeta = (\zeta_1, \zeta_2, \zeta_3, \zeta_4)^T$ and $|\zeta\rangle \in \mathbb{C}^4$ is a unit vector modulo an overall phase factor. $\mathbb{CP}^3$ is the space of all projection operators of rank one on $\mathbb{C}^4$:

$$\mathbb{CP}^3 = \left\{ {P_\zeta}^\dagger = P_\zeta \,, {P_\zeta}^2 = P_\zeta \,, \mathrm{Tr}\big(P_\zeta\big) = 1 \,|\, P_\zeta \in \textit{Mat}\,(4, \mathbb{C}) \right\}. \tag{2.3.74}$$

In this regard, we may define the map $\mathscr{M}_4$ as

$$\begin{aligned}\mathscr{M}_4: \quad & \mathbb{CP}^3 \mapsto S^4 \\ & P_\zeta \mapsto \Psi_a = \langle\zeta|\,\gamma_a\,|\zeta\rangle = \zeta^\dagger\gamma_a\zeta.\end{aligned} \tag{2.3.75}$$

The five-dimensional gamma-matrices in the Weyl basis are given by [52]

$$\gamma_0 = \begin{pmatrix} 0 & -\mathbb{1}_2 \\ -\mathbb{1}_2 & 0 \end{pmatrix}, \quad \gamma_\mu = \begin{pmatrix} 0 & \sigma_\mu \\ -\sigma_\mu & 0 \end{pmatrix}, \quad \gamma_5 = \begin{pmatrix} \mathbb{1}_2 & 0 \\ 0 & -\mathbb{1}_2 \end{pmatrix}. \tag{2.3.76}$$

In this basis, a generic column vector ζ is mapped under $\mathscr{M}_4$ to the fifth Euclidean coordinate written by

$$\Psi_5(\zeta) = \zeta^\dagger\gamma_5\zeta = |\zeta_1|^2 + |\zeta_2|^2 - |\zeta_3|^2 - |\zeta_4|^2. \tag{2.3.77}$$

To further clarify the mapping between two manifolds, a specific point can be chosen as the point of reference. Let us pick $\zeta_{rf} = (1,0,0,0)^T$ as the reference point. From (2.3.77), we determine that $\Psi_\alpha\big(\zeta_{rf}\big) = 0$ $(\alpha \neq 4)$ and $\Psi_5\big(\zeta_{rf}\big) = 1$. Therefore, ζ_{rf} is evidently mapped to the S^4 reference point $\Psi_{rf} = (0,0,0,0,1)$ which corresponds to the north pole of the 4-sphere. The isotropy group of Ψ_{rf} is written by

$$H_{rf} = \big\{[h_{rf},\gamma_5] = 0\,|\,h_{rf} \in SO(5)\big\} \approx SO(4) \approx SU(2)_L \times SU(2)_R, \tag{2.3.78}$$

where we have employed the local isomorphism of $SO(4)$ to $SU(2) \times SU(2)$. It is obvious that while $SU(2)_R$ acts on the $-\mathbb{1}_2$ eigenspace of γ_5, $SU(2)_L$ acts on the eigenspace $\mathbb{1}_2$. The fiber over Ψ_{rf} is subject to the condition

$$1 = \langle\zeta_L|\,\gamma_5\,|\zeta_L\rangle = {\zeta_L}^\dagger\gamma_5\zeta_L, \tag{2.3.79}$$

where $\zeta_L = (\zeta_L^1, \zeta_L^2, 0, 0)^T$. Inserting (2.3.76) into (2.3.79) , we find the constraint relation

$$\big|\zeta_L^1\big|^2 + \big|\zeta_L^2\big|^2 = 1, \tag{2.3.80}$$

that defines the three-sphere. In addition, since the overall phase of ζ_L drops out in (2.3.75), it turns out that the fiber is indeed $S^2 \cong \dfrac{S^3}{U(1)}$. Thus, we arrive at the conclusion that $\mathbb{CP}^3$ is an S^2-bundle over S^4.

In order to construct the fuzzy version of this fibration, we start with introducing the map $\mathscr{M}_5$ that describes an embedding of $\mathbb{CP}^3$ to $\mathbb{R}^{15}$ as follows [53]

$$\begin{aligned}\mathscr{M}_5: \quad & \mathbb{CP}^3 \mapsto \mathbb{R}^{15} \\ & P_\zeta \mapsto \Psi_{gh} = \langle\zeta| F_{gh} |\zeta\rangle = \zeta^\dagger F_{gh} \zeta\,, \end{aligned} \tag{2.3.81}$$

where the F_{gh} $(g,h=1,..,6)$ are the generators of $SO(6)$ in the fundamental spinor IRR of $SO(6)$ labeled as $(1,0,0)$. A useful categorization of fifteen generators is $F_{gh} = \{F_{ab}, F_{a6}\}$ where a further identification of F_{a6} with the γ-matrices is also possible [19]

$$\gamma_a = 2F_{a6}\,, \tag{2.3.82}$$

then for Ψ_a coordinates of S^4 in (2.3.75), we have the composition of manifolds:

$$\Psi_a : \mathbb{CP}^3 \to \mathbb{R}^{15} \xrightarrow{\mathscr{H}_{pr}} \mathbb{R}^5\,, \tag{2.3.83}$$

where $\mathscr{H}_{pr}$ is the projection of F_{gh} to the subspace spanned by F_{a6}.

The quantization of (2.3.81) is performed by utilizing Schwinger's construction as

$$\mathscr{F}_{gh} = \hat{\mathscr{A}}^\dagger F_{gh} \hat{\mathscr{A}}\,, \tag{2.3.84}$$

hence, S_F^4 arises from the quantization of the map $\Psi_a : \mathbb{CP}^3 \to S^4$ defined by

$$\chi_a = rX_a = r\mathscr{F}_{a6}\,, \tag{2.3.85}$$

where χ_a and X_a were already defined in equations (2.3.61) and (2.3.63). Summarizing, as we have stated earlier S^4 admits no symplectic structure, so S_F^4 cannot be quantized in the canonical way followed for $S^2 \to S_F^2$. Rather, the fuzzy four-sphere should be thought of as emerging from the quantization of the fibration $S^2 \to \mathbb{CP}^3 \to S^4$. S_F^4 is a squashed fuzzy $\mathbb{CP}^3$ with S_F^2 fibers.

2.4 BFSS Matrix Model

Now that, we have discussed several geometrical aspects of fuzzy two- and four-spheres, it is important to see how they appear in physical context. That brings us to the discussion of matrix gauge theories and the Banks-Fischler-Shenker-Susskind (BFSS) [2] matrix model and its deformations in particular. We will aim to give a

self-contained review of the BFSS matrix model and its deformations which will be referred to throughout the chapter four.

The effective theory describing the dynamics of N coincident $D0$-branes is the BFSS matrix model [2]. In this interpretation of the model, the diagonal elements of the matrices give the positions of these $D0$-branes in 9-dimensional flat space, while the off-diagonal elements describe the interaction of these pointlike objects. Further detailed discussion on this subject may be found in [2, 10, 11, 54]. The BFSS action is a Yang-Mills theory in $0+1$ dimensions which arises from the dimensional reduction of the Yang-Mills theory in $9+1$ dimensions with $\mathscr{N}=1$ supersymmetry. Leaving apart the fermionic part of the action, we focus on the bosonic part of theory, which will be sufficient for our purposes. The starting point of our analysis of the dimensional reduction procedure is then the bosonic part of this ten-dimensional Yang-Mills action and it is given by [11]

$$S_{SY} = -\frac{1}{4g^2}\int \mathrm{d}x^{10}\,\mathrm{Tr}\big(F_{\mu\nu}F^{\mu\nu}\big), \qquad \mu,\nu = 0,..,9. \tag{2.4.1}$$

Here the background of the ten-dimensional space-time is flat, has the Minkowski metric $\eta_{\mu\nu} = diag(-1,1,...,1)$. The field strength tensor is defined as

$$F_{\mu\nu} = \partial_\mu A_\nu - \partial_\nu A_\mu - i[A_\mu, A_\nu]\,, \tag{2.4.2}$$

where A_μ is the gauge field which transforms as

$$A'_\mu = U^\dagger A_\mu U + iU^\dagger \partial_\mu U\,, \tag{2.4.3}$$

under the $U(N)$ gauge transformations. S_{SY} is invariant under this $U(N)$ gauge symmetry. The field components can be written as $A_\mu(t,\vec{\mathbf{x}}) = (A_0(t,\vec{\mathbf{x}}), A_I(t,\vec{\mathbf{x}}))$ where $I = 1,..,9$.

The dimensional reduction procedure is carried out by assuming that all fields and gauge transformations are independent of the spatial coordinates I. Thus we may introduce the notation

$$U \equiv U(t), \quad A_\mu \equiv A_\mu(t) = (A_0(t), B_I(t)). \tag{2.4.4}$$

Under this assumption (2.4.3) implies

$$A'_0(t) = U^\dagger A_0 U + iU^\dagger \partial_t U, \tag{2.4.5a}$$

$$B_I'(t) = U^\dagger B_I U. \tag{2.4.5b}$$

While equation (2.4.5a) demonstrates the transformation property of gauge field $A_0(t)$, (2.4.5b) indicates that B_I transform adjointly under $U(N)$ gauge transformations, that is, B_I's transform as an adjoint non-abelian scalar field with $U(N)$ gauge symmetry.

To proceed further, it is convenient to list the relationships between covariant and contravariant components:

$$A^0 = \eta^{00} A_0 = -A_0, \quad B^I = \eta^{IJ} B_J = B_I, \quad \partial^0 = \eta^{00}\partial_0 = -\partial_0. \tag{2.4.6}$$

Computing the required derivatives with the help of (2.4.6), the components of the field tensor are cast into the following forms

$$\begin{aligned} F_{0I} &= \partial_0 B_I - \partial_I A_0 - i[A_0, B_I] \\ &= \partial_t B_I - i[A_0, B_I] \\ &= D_t B_I, \end{aligned} \tag{2.4.7}$$

$$\begin{aligned} F^{0I} &= \partial^0 B^I - \partial^I A^0 - i[A^0, B^I] \\ &= -\partial_t B_I + i[A_0, B_I] \\ &= -F_{0I}, \end{aligned} \tag{2.4.8}$$

$$\begin{aligned} F^{IJ} = F_{IJ} &= \partial_I B_J - \partial_J B_I - i[B_I, B_J] \\ &= -i[B_I, B_J]. \end{aligned} \tag{2.4.9}$$

Then, utilizing the antisymmetry of $F_{\mu\nu}$, i.e. $F_{\mu\nu} = -F_{\nu\mu}$, it is straightforward to show that

$$\begin{aligned} -\frac{1}{4} F_{\mu\nu} F^{\mu\nu} &= -\frac{1}{4}\left(F_{0I}F^{0I} + F_{I0}F^{I0} + F_{IJ}F^{IJ}\right) \\ &= -\frac{1}{4}\left(-2F_{0I}F_{0I} + F_{IJ}F_{IJ}\right) \\ &= \frac{1}{2}\left(D_t B_I\right)^2 + \frac{1}{4}[B_I, B_J]^2. \end{aligned} \tag{2.4.10}$$

Thus, as a consequence of the dimensional reduction procedure, equation (2.4.1) becomes

$$S_B = \frac{1}{g^2}\int \mathrm{d}t\, \mathrm{Tr}\left(\frac{1}{2}\left(D_t B_I\right)^2 + \frac{1}{4}[B_I, B_J]^2\right). \tag{2.4.11}$$

It must be clear that S_B is invariant under $U(N)$ gauge transformations given by (2.4.5). Besides this gauge symmetry, the $SO(9,1)$ Lorentz symmetry of the original Yang-Mills theory yields to a global $SO(9)$ symmetry of the BFSS model, which is given as

$$B_I' = R_{IJ} B_J, \qquad R \in SO(9)\,. \tag{2.4.12}$$

Let us note in passing that this $SO(9)$ symmetry may be broken by the addition of massive deformations to the action preserving the gauge symmetry. The maximally supersymmetric deformation of the BFSS model is called the Berenstein-Maldacena-Nastase (BMN) [5] model which breaks $SO(9)$ to $SO(6) \times SO(3)$. This leads to a description of coincident $D0$-branes on spherical backgrounds. In particular, fuzzy 2-sphere appears as vacuum configurations in the BMN model. In chapter 4, we will focus on another massive deformation of the BFSS model which breaks $SO(9)$ to $SO(5) \times SO(4)$ and subsequently to $SO(5) \times SO(3) \times \mathbb{Z}_2$.

We see that the gauge field A_0 in the BFSS model is not dynamical as its time derivative does not appear in the action (2.4.11). The variation of S_B with respect to A_0 leads to a constraint equation. To see this explicitly, consider the variation of A_0 given by

$$A_0 \to A_0' = A_0 + \delta A_0\,, \tag{2.4.13}$$

whose effect on the covariant derivative term of the BFSS action can be determined as

$$\begin{aligned} \mathrm{Tr}\big((D_t B_I - i[\delta A_0\,, B_I])^2\big) &= \mathrm{Tr}\big((D_t B_I)^2 - i\{D_t B_I, [\delta A_0\,, B_I]\} + \mathscr{O}\big((\delta A_0)^2\big)\big) \\ &= \mathrm{Tr}\big((D_t B_I)^2\big) - 2i\,\mathrm{Tr}((D_t B_I)\,[\delta A_0\,, B_I]) \\ &= \mathrm{Tr}\big((D_t B_I)^2\big) - 2i\,\mathrm{Tr}([B_I, D_t B_I]\,\delta A_0), \end{aligned} \tag{2.4.14}$$

so the variation of S_B with respect to A_0 is

$$\delta S_B = -\frac{i}{g^2}\int \mathrm{d}t\,\mathrm{Tr}([B_I, D_t B_I]\,\delta A_0) = 0, \tag{2.4.15}$$

which leads to the equation

$$[B_I, D_t B_I] = 0. \tag{2.4.16}$$

Substituting the gauge choice of $A_0 = 0$ into (2.4.16), we obtain the Gauss law constraint written by

$$[B_I, \partial_t B_I] = 0. \tag{2.4.17}$$

In the $A_0 = 0$ gauge, the action is simply given as

$$S_B\Big|_{A_0=0} = \frac{1}{g^2}\int \mathrm{d}t\, \mathrm{Tr}\left(\frac{1}{2}\left(\partial_t B_I\right)^2 + \frac{1}{4}[B_I, B_J]^2\right). \tag{2.4.18}$$

The conjugate momenta of B_I are

$$P_I = \frac{1}{g^2}\,\partial_t B_I \equiv \frac{1}{g^2}\dot{B}_I, \tag{2.4.19}$$

and the associated Hamiltonian takes the form

$$H_{BFSS} = g^2\,\mathrm{Tr}\left(\frac{{P_I}^2}{2} - \frac{1}{4g^4}[B_I, B_J]^2\right). \tag{2.4.20}$$

It is easy to see that H_{BFSS} is invariant under the constant shift of the matrices

$$B_I \to B_I' = B_I + e_T \mathbb{1}_N, \tag{2.4.21}$$

where e_T is a constant. We have

$$P_I' = \frac{1}{g^2}\left(\dot{B}_I + e_T 0_N\right) = \frac{\dot{B}_I}{g^2} = P_I, \tag{2.4.22a}$$

$$\left[B_I', B_J'\right] = [B_I + e_T\mathbb{1}_N, B_J + e_T\mathbb{1}_N] = [B_I, B_J], \tag{2.4.22b}$$

which shows that neither the momentum terms nor the commutators are affected by (2.4.21). Therefore, we deduce that the Hamiltonian has translational symmetry. This means that, center of mass motion of $D0$-branes may be separated out, and we can work with traceless Hermitian matrices, $\mathrm{Tr}\, B^I = 0$, and the $U(1)$ part of the $U(N)$ gauge symmetry separates out, leaving us with the $SU(N)$ gauge symmetry.

The potential part of H_{BFSS} may be written out separately as

$$V_B = \frac{1}{4g^2}\,\mathrm{Tr}(V_{IJ}V_{IJ}), \tag{2.4.23}$$

where $V_{IJ} = i[B_I, B_J]$. Due to the hermiticity of B_I, V_{IJ} are also Hermitian matrices that can be diagonalized with the help of a similarity matrix S:

$$D = SV_{IJ}S^{-1}, \tag{2.4.24}$$

which allows us to write

$$V_B = \frac{1}{4g^2}\,\mathrm{Tr}\left(SV_{IJ}S^{-1}SV_{IJ}S^{-1}\right) = \frac{1}{4g^2}\,\mathrm{Tr}\left(D^2\right). \tag{2.4.25}$$

Then, we conclude that since all elements of the diagonal matrix D are real, V_B must be a non-negative potential, i.e. $V_B \geq 0$.

2.5 Review of Yang-Mills Matrix Models

After comprehensive introductions to fuzzy spheres and the BFSS matrix model, we wish to review some elementary aspects of Yang-Mills matrix models. We start this section with a brief review of 5-matrix model i.e. model with five Hermitian matrices. This can be seen as a subsector of the BFSS model, with first five matrices as dynamical variables, while the remaining four are frozen and essentially set to zero. Then, with the addition of an appropriate massive deformation term, an action with a fuzzy S^4 extremum is constructed.

The action of Yang-Mills 5-matrix model in Minkowski signature can be given as

$$S_{YM} = \frac{1}{g^2}\int \mathrm{d}t\, \mathrm{Tr}\left(\frac{1}{2}(D_t B_a)^2 + \frac{1}{4}[B_a, B_b]^2\right), \tag{2.5.1}$$

where B_a $(a = 1, .., 5)$ are $N \times N$ Hermitian matrices transforming under the adjoint representation of $U(N)$ as

$$B_a \to U^\dagger B_a U, \quad U \in U(N). \tag{2.5.2}$$

Tr stands for the normalized trace and the covariant derivatives are given by

$$D_t B_a = \partial_t B_a - i[A, B_a], \tag{2.5.3}$$

where A is a $U(N)$ gauge field transforming as

$$A \to U^\dagger A U + i U^\dagger \partial_t U. \tag{2.5.4}$$

Action in (2.5.1) is invariant under the $U(N)$ gauge transformations implemented by (2.5.2) and (2.5.4). Besides $U(N)$ gauge transformations, S_{YM} is also invariant under the global $SO(5)$ rotations which are given as

$$B_a \to B'_a = R_{ab} B_b, \quad R \in SO(5), \tag{2.5.5}$$

where R_{ab} are time-independent, rigid rotations.

The potential part of S_{YM} can be written as

$$V_{YM} = -\frac{1}{4g^2}\,\mathrm{Tr}\big([B_a, B_b]^2\big). \tag{2.5.6}$$

There exists a massive deformation term of the form

$$S_\mu = -\frac{1}{g^2}\int \mathrm{d}t\,\mathrm{Tr}\left(\frac{\mu^2}{4}B_a^2\right), \tag{2.5.7}$$

that preserves both the $U(N)$ gauge and $SO(5)$ global symmetries of S_{YM}. With the addition of S_μ, the potential part of the combined action $S = S_{YM} + S_\mu$ can be expressed separately as

$$V = \frac{1}{g^2}\int \mathrm{d}t\,\mathrm{Tr}\left(-\frac{1}{4}[B_a, B_b]^2 + \frac{\mu^2}{4}B_a^2\right). \tag{2.5.8}$$

For the gauge choice of $A = 0$, the covariant derivatives $D_t B_a$ vanish. We may look at the configurations extremizing the potential V in (2.5.8). By letting $B_a \to B_a + \delta B_a$ in equation (2.5.8)

$$\begin{aligned}\delta V &= -\frac{1}{4g^2}\int \mathrm{d}t\Big[4\,\mathrm{Tr}([B_b,[B_a,B_b]]\,\delta B_a) - 2\mu^2\,\mathrm{Tr}(B_a\,\delta B_a)\Big] \\ &= -\frac{1}{g^2}\int \mathrm{d}t\,\mathrm{Tr}\left(\left([B_b,[B_a,B_b]] - \frac{\mu^2}{2}B_a\right)\delta B_a\right) = 0,\end{aligned} \tag{2.5.9}$$

we deduce that V is extremized by the matrices fulfilling

$$[B_b,[B_b,B_a]] + \frac{1}{2}\mu^2 B_a = 0. \tag{2.5.10}$$

Using (2.3.56) and (2.3.58) it is straightforward to demonstrate that by the fuzzy four-sphere configurations $B_a \equiv X_a$, equation (2.5.10) can be put into the form

$$\begin{aligned}0 =& [X_b,[X_b,X_a]] + \frac{1}{2}\mu^2 X_a \\ =& i[M_{ab}, X_b] + \frac{1}{2}\mu^2 X_a \\ =& -\left(\delta_{ab}X_b - \delta_{bb}X_a\right) + \frac{1}{2}\mu^2 X_a \\ =& \left(4 + \frac{1}{2}\mu^2\right)X_a\,.\end{aligned} \tag{2.5.11}$$

(2.5.11) is satisfied for $\mu^2 = -8$ which means that fuzzy four-spheres and their direct sums provide non-trivial solutions of equation (2.5.10). Although such a negative mass squared term may imply an instability, it was shown in [19] that quantum corrections in the pure (i.e. matrices with no time-dependence), five matrix Yang-Mills model stabilizes the radius of the fuzzy four-sphere.

CHAPTER 3

YANG-MILLS 5-MATRIX MODEL AND GENERALIZED FUZZY FOUR-SPHERE

3.1 Overview

In the preceding chapter, we aimed to provide a comprehensive description of fuzzy spaces, focusing on the concrete cases of the fuzzy two-sphere and the fuzzy four-sphere. We have also seen how these fuzzy spaces arise as vacuum solutions to Yang-Mills (YM) matrix models related to massive deformations of the BFSS model.

In this chapter, our main focus is going to be exploring new vacuum solutions of the YM 5-matrix model with a massive deformation term whose essential features were sketched in section 2.5. We look for static matrix configurations i.e. extrema of the potential which carries tensor product representations of $SO(5)$, which solves the classical equations of motion. For this purpose, we essentially generalize and apply an approach followed in [24, 25] which introduces an additive new part to the matrix configuration, which is already satisfying the equations of motion, using a Schwinger type realization of the $SO(5)$ generators with "fermionic" annihilation/creation operators. In [24, 25], this approach has been applied to generate new vacuum configurations in an $SU(N)$ gauge theory coupled to a triplet of adjoint scalar fields and a massive deformation of the bosonic part of the $\mathcal{N} = 4$ SUSY YM model. The new vacuum configurations obtained this way are expressed as direct sums of fuzzy two-spheres or direct sums of products of fuzzy two-spheres. This is because quite straightforwardly tensor products of $SU(2)$ IRRs and likewise that of $SU(2)_L \times SU(2)_R$ IRRs can be expressed as direct sum of IRRs of these groups, and allows one to interpret each block of the matrices carrying an IRR of these groups as generating a fuzzy sphere S_F^2 or a product $S_F^2 \times S_F^2$ at a matrix level specified by the

dimension of the respective IRRs.

For the 5-YM model, the situation becomes much more complex since the direct sum decompositions of the tensor product representations of $SO(5)$ contains not only those IRRs of $SO(5)$ which are carried by the S_F^4 matrices but also more general IRRs of $SO(5)$ which does not appear to be immediately related to S_F^4 matrices. It however turns out that some of these new matrix configurations can be understood as generalized fuzzy four-sphere configurations introduced in [1]. The configurations are denoted as S_Λ^4, where Λ stands for the $SO(5)$ and $SO(6)$ IRR labels carried by these configurations. After the presentation of these new vacuum configurations and discussing in detail how they come about, using the representation theory of $SO(5)$ and $SO(6)$, we will subsequently focus on understanding the connection of our results with the generalized fuzzy four-spheres of [1]. S_Λ^4 has a more involved geomerical structure then S_F^4 and as an alternative to the discussion given in [1], we use the quantization of coadjoint orbits method and quantize a particular 10-dimensional coadjoint orbit O_2 of $SO(6) \approx SU(4)$ to see detailed structure of S_Λ^4. Generalized coherent states associated to $SO(6) \approx SU(4)$ are used to discuss some aspects of the generalized fuzzy four-spheres. While elaborating on these ideas, we also solve the Landau problem on the coset space O_2 and interpret its connection to the fuzzy version of O_2 as well to S_F^4 and S_Λ^4 taking advantage of the general results in the literature [55, 56] that relates the Hilbert space of the lowest Landau level on $\mathbb{CP}^N$, $Gr(2,4)$ etc. to the Hilbert space of the fuzzy spaces $\mathbb{CP}_F^N$ and $Gr_F(2,4)$.

The plan of the chapter is as follows. In section 3.2, we consider the 5-YM matrix model and introduce the new solutions using Schwinger construction of $SO(5)$ IRRs with fermionic oscillators. A detailed group theoretical analysis is provided in the subsection 3.2.2. Section 3.3 presents some warm-up material on the techniques followed to obtain quantization of coadjoint orbits, while some details are relegated to the appendix B. In section 3.4, coadjoint orbit technique is applied to the coset space O_2 and its quantization is obtained.

3.2 New Solutions of the Mass Deformed YM Model

We focus on the mass deformed Yang-Mills 5-matrix model with gauge symmetry group $U(\mathscr{N})$. The action is given as

$$S = \frac{1}{g^2}\int \mathrm{d}t\,\mathrm{Tr}\left(\frac{1}{2}(D_t W_a)^2 + \frac{1}{4}[W_a, W_b]^2 - \frac{\mu^2}{4}{W_a}^2\right), \tag{3.2.1}$$

where W_a are $\mathscr{N}\times\mathscr{N}$ matrices. The potential part of S is extremized by matrices fulfilling (2.5.10)

$$[W_a,[W_a,W_b]] + \frac{1}{2}\mu^2 W_b = 0. \tag{3.2.2}$$

As we have demonstrated in section 2.5 and equation (2.5.11), (3.2.2) has fuzzy 4-sphere solutions given by the matrices(2.3.55) and for the $\mu^2 = -8$ value. In fact, any direct sum of the S_F^4 matrices yield a solution of (3.2.2) in the form

$$W_a = X_a^{(W_1)} \oplus X_a^{(W_2)} \oplus \cdots \oplus X_a^{(W_k)}, \tag{3.2.3}$$

provided that

$$\mathscr{N} = N_1 + N_2 + ... + N_k\,, \tag{3.2.4}$$

where $N_i = \frac{1}{6}(n_i+1)(n_i+2)(n_i+3)$ with i^{th} S_F^4 carrying the $(0,n_i)$ IRR of $SO(5)$. In particular, if all S_F^4's are at the same matrix level, i.e. all N_i are the same and $\mathscr{N} = kN$, the solution may be written as

$$W_a = X_a \otimes \mathbb{1}_k\,. \tag{3.2.5}$$

This is a solution of (3.2.2) consisting of k concentric S_F^4 at the same matrix level. We may wonder if there are other solutions of (3.2.2) which may be expressed in the form

$$W_a = X_a \otimes \mathbb{1}_k + \mathbb{1}_N \otimes Y_a. \tag{3.2.6}$$

with $\mathscr{N} = kN$, $\dim(Y_a) = k$, and Y_a satisying the same commutation relations as X_a. Explicitly, we may write the requirements on Y_a as

$$[Y_a, Y_b] = iZ_{ab}, \tag{3.2.7}$$

$$[Z_{ab}, Y_c] = i(\delta_{ac}Y_b - \delta_{bc}Y_a), \tag{3.2.8}$$

and we have

$$[Z_{ab}, Z_{cd}] = i(\delta_{ac}Z_{bd} + \delta_{bd}Z_{ac} - \delta_{ad}Z_{bc} - \delta_{bc}Z_{ad}), \tag{3.2.9}$$

where Z_{ab} generates the group $SO(5)$. In general, it may carry a reducible representation of $SO(5)$.

Under these assumptions, we may show that (3.2.6) is a solution of equation (3.2.2). We have

$$\begin{aligned}
[W_a, W_b] &= (X_a \otimes \mathbb{1}_k)(X_b \otimes \mathbb{1}_k) - (X_b \otimes \mathbb{1}_k)(X_a \otimes \mathbb{1}_k) \\
&\quad + (\mathbb{1}_N \otimes Y_a)(\mathbb{1}_N \otimes Y_b) - (\mathbb{1}_N \otimes Y_b)(\mathbb{1}_N \otimes Y_a) \\
&= (X_a X_b - X_b X_a) \otimes \mathbb{1}_k + \mathbb{1}_N \otimes (Y_a Y_b - Y_b Y_a) \\
&= i(M_{ab} \otimes \mathbb{1}_k + \mathbb{1}_N \otimes Z_{ab}).
\end{aligned} \tag{3.2.10}$$

Thus

$$\begin{aligned}
[W_a, [W_a, W_b]] &= i([X_a, M_{ab}] \otimes \mathbb{1}_k + \mathbb{1}_N \otimes [Y_a, Z_{ab}]) \\
&= (\delta_{aa} X_b - \delta_{ba} X_a) \otimes \mathbb{1}_k + \mathbb{1}_N \otimes (\delta_{aa} Y_b - \delta_{ba} Y_a) \\
&= (5X_b - X_b) \otimes \mathbb{1}_k + \mathbb{1}_N \otimes (5Y_b - Y_b) \\
&= 4W_b \,,
\end{aligned} \tag{3.2.11}$$

and for $\mu^2 = -8$ we find

$$[W_a, [W_a, W_b]] + \frac{1}{2}\mu^2 W_b = 4W_b - 4W_b = 0 \,. \tag{3.2.12}$$

We now want to focus on a specific form of Y_a, which yields solutions of (3.2.2), whose geometric structure yields to interesting new aspects and become linked to the generalized fuzzy four-sphere S^4_Λ mentioned in the overview section of this chapter.

3.2.1 Reducible Representation of SO(5) and Schwinger Construction

We launch the discussion by introducing four sets of fermionic annihilation-creation operators, fulfilling the anti-commutation relations

$$\left\{b_i, b_j\right\} = 0, \quad \left\{b_i^\dagger, b_j^\dagger\right\} = 0, \quad \left\{b_i, b_j^\dagger\right\} = \delta_{ij}, \tag{3.2.13}$$

where $i, j = 1, 2, 3, 4$. These operators span a 16-dimensional Hilbert space with the basis vectors

$$|n_1, n_2, n_3, n_4\rangle = (b_1^\dagger)^{n_1} (b_2^\dagger)^{n_2} (b_3^\dagger)^{n_3} (b_4^\dagger)^{n_4} \, |0, 0, 0, 0\rangle \,, \tag{3.2.14}$$

where $n_1, n_2, n_3, n_4 = 0, 1$ as a consequnce of the fact that $b_i^2 = 0 = \left(b_i^\dagger\right)^2$. Let us introduce a four-component column matrix as

$$\Psi = \begin{pmatrix} \Psi_1 \\ \Psi_2 \\ \Psi_3 \\ \Psi_4 \end{pmatrix} := \begin{pmatrix} b_1 \\ b_2 \\ b_3 \\ b_4 \end{pmatrix} . \tag{3.2.15}$$

Now by utilizing Schwinger's construction [48] we may form the operators

$$Y_a := \frac{1}{2}\Psi^\dagger \gamma_a \Psi \, . \tag{3.2.16}$$

acting on the Hilbert space spanned by $|n_1, n_2, n_3, n_4\rangle$. Thus, evaluating the matrix elements of Y_a in this basis, we may express each Y_a as an 16×16 matrix. Similarly, using the SO(5) generators

$$G_{ab} = -\frac{i}{4}[\gamma_a, \gamma_b] \, , \tag{3.2.17}$$

in the 4-dimensional spinor IRR of $SO(5)$ given in equation (2.3.51) we may write

$$Z_{ab} := \Psi^\dagger G_{ab} \Psi \, . \tag{3.2.18}$$

The IRR content of Z_{ab} will also be determined.

Using the oscillator algebra (3.2.13) and the Clifford algebra relations for γ-matrices, we may obtain the commutation relations of Y_a's

$$\begin{aligned}
[Y_a, Y_b] &= \frac{1}{4}[b_i^\dagger (\gamma_a)_{ij} b_j, b_k^\dagger (\gamma_b)_{kl} b_l] = \frac{1}{4}(\gamma_a)_{ij}(\gamma_b)_{kl}[b_i^\dagger b_j, b_k^\dagger b_l] \\
&= \frac{1}{4}(\gamma_a)_{ij}(\gamma_b)_{kl}\Big(b_i^\dagger \left\{ b_j, b_k^\dagger \right\} b_l - b_k^\dagger \left\{ b_i^\dagger, b_l \right\} b_j + \left\{ b_i^\dagger, b_k^\dagger \right\} b_l b_j \\
&\quad - b_i^\dagger b_k^\dagger \left\{ b_j, b_l \right\} \Big) \\
&= i\Psi^\dagger \frac{1}{4i}[\gamma_a, \gamma_b]\Psi \\
&= iZ_{ab}.
\end{aligned} \tag{3.2.19}$$

Similarly, it can be demonstrated that

$$[Z_{ab}, Y_c] = i(\delta_{ac} Y_b - \delta_{bc} Y_a), \tag{3.2.20}$$

$$[Z_{ab}, Z_{cd}] = i(\delta_{ac} Z_{bd} + \delta_{bd} Z_{ac} - \delta_{ad} Z_{bc} - \delta_{bc} Z_{ad}). \tag{3.2.21}$$

We see that Y_a transforms as a vector of $SO(5)$ i.e. in the IRR $(1, 0)$ with respect to its index "a", as observed from (3.2.20). Our primary task at this stage is to determine the $SO(5)$ IRR content of the matrices Y_a as well as the generators Z_{ab}.

3.2.2 SO(5) and SO(6) Irreducible Representation Content of Y_a

We start by listing the fermionic number operators and their properties. We have

$$N_i = b_i^\dagger b_i\,, \quad N_i N_i = N_i\,, \quad N_i N_j = N_j N_i\,, \tag{3.2.22a}$$

where no summations over the indices i are implied and N_i could take on the eigenvalues 0 and 1. The total number operator is

$$N := \sum_i N_i = \sum_{i=1}^{4} {b_i}^\dagger b_i\,. \tag{3.2.23}$$

We have that

$$(Y_a)^2 := \sum_{a=1}^{5} Y_a Y_a = (Y_1)^2 + (Y_2)^2 + (Y_3)^2 + (Y_4)^2 + (Y_5)^2, \tag{3.2.24}$$

is an invariant under the action of $SO(5)$. This is easily seen by writing the expression

$$Y_a' Y_a' = (R_{ab} Y_b)(R_{ac} Y_c) = R_{ab} R_{ac} Y_b Y_c = Y_a Y_a \tag{3.2.25}$$

since $R^T = R$. After a long but straightforward calculation, whose details are given in appendix A.2, $(Y_a)^2$ is found to be equal to

$$\begin{aligned}(Y_a)^2 = {} & \frac{5}{4}N - \frac{3}{2}(N_1 + N_2)(N_3 + N_4) + \frac{1}{2}(N_1 N_2 + N_3 N_4) \\ & + 2(b_1^\dagger b_2^\dagger b_3 b_4 + b_1 b_2 b_3^\dagger b_4^\dagger)\,.\end{aligned} \tag{3.2.26}$$

(3.2.26) expresses $(Y_a)^2$ in terms of N_i and $b_i, b_i^\dagger$'s. In an appropriate basis (see appendix A.1) adapted from the Fock basis (3.2.14), (3.2.26) is diagonalized as

$$(Y_a)^2 = diag\left(0, \frac{5}{4}, \frac{5}{4}, \frac{5}{4}, \frac{5}{4}, 5, 1, 1, 1, 1, 1, \frac{5}{4}, \frac{5}{4}, \frac{5}{4}, \frac{5}{4}, 0\right). \tag{3.2.27}$$

Next, let us also look at generators Z_{ab} of $SO(5)$ induced from the 4-dimensional spinor IRR of $SO(5)$ given in (3.2.17) and (3.2.18). We have for the Casimir operator

$$\begin{aligned}\sum_{a<b\leqslant 5} Z_{ab} Z_{ab} = (Z_{ab})^2 = {} & \frac{5}{2}N - 2(b_1^\dagger b_2^\dagger b_3 b_4 + b_1 b_2 b_3^\dagger b_4^\dagger) \\ & - (N_1 + N_2)(N_3 + N_4) - 3(N_1 N_2 + N_3 N_4)\,.\end{aligned} \tag{3.2.28}$$

The detailed derivation of the right hand side of this expression is provided in A.3. By calculating the matrix elements for $(Z_{ab})^2$ operator in the basis given in appendix A.1 its representation is obtained as

$$(Z_{ab})^2 = diag\bigg(0, \frac{5}{2}, \frac{5}{2}, \frac{5}{2}, \frac{5}{2}, 0, 4, 4, 4, 4, 4, \frac{5}{2}, \frac{5}{2}, \frac{5}{2}, \frac{5}{2}, 0\bigg). \tag{3.2.29}$$

We will shortly state the $SO(5)$ IRR content of this representation. Before doing so let us go a step forward and introduce the generators of the group $SO(6)$ by employing the Schwinger's construction as

$$Z_{gh} = \Psi^\dagger G_{gh} \Psi \,, \tag{3.2.30}$$

where $Z_{gh} \equiv (Z_{ab}, Z_{a6})$ and $G_{gh} = (G_{ab}, G_{a6}) \equiv (G_{ab}, \frac{1}{2}\gamma_a)$. The quadratic Casimir operator of $SO(6)$ obtained from these generators takes the form

$$\begin{aligned} \sum_{g<h\leqslant 6} Z_{gh} Z_{gh} = (Z_{gh})^2 = \frac{15}{4} N - \frac{5}{2}(N_1 N_2 + N_3 N_4) \\ - \frac{5}{2}(N_1 + N_2)(N_3 + N_4). \end{aligned} \tag{3.2.31}$$

Details of the calculation leading to the expression in (3.2.31) are presented in the appendix A.4. We can easily see that

$$\begin{aligned} \big[Z_{gh}^2, Z_{ab}^2\big] &= [Y_d Y_d, Z_{ab} Z_{ab}] \\ &= Y_d [Y_d, Z_{ab}] Z_{ab} + Y_d Z_{ab} [Y_d, Z_{ab}] \\ &+ [Y_d, Z_{ab}] Z_{ab} Y_d + Z_{ab} [Y_d, Z_{ab}] Y_d \\ &= i[Y_b, Y_a] Z_{ab} + i Z_{ab} [Y_a, Y_b] \\ &= Z_{ab} Z_{ab} - Z_{ab} Z_{ab} \\ &= 0 \,. \end{aligned} \tag{3.2.32}$$

Therefore, we may diagonalize $(Z_{gh})^2$ in the same basis as that used for $(Z_{ab})^2$ in (3.2.29). This gives

$$(Z_{gh})^2 = diag\bigg(0, \frac{15}{4}, \frac{15}{4}, \frac{15}{4}, \frac{15}{4}, 5, 5, 5, 5, 5, 5, \frac{15}{4}, \frac{15}{4}, \frac{15}{4}, \frac{15}{4}, 0\bigg). \tag{3.2.33}$$

From (3.2.30) we also that $(Y_a)^2$ given in (3.2.24) can be expressed as the difference of the Casimirs of $SO(6)$ and $SO(5)$

$$(Y_a)^2 = (Z_{gh})^2 - (Z_{ab})^2 \tag{3.2.34}$$

$$\equiv diag\bigg(0, \frac{5}{4}, \frac{5}{4}, \frac{5}{4}, \frac{5}{4}, 5, 1, 1, 1, 1, 1, \frac{5}{4}, \frac{5}{4}, \frac{5}{4}, \frac{5}{4}, 0\bigg).$$

the last line easily follows from using (3.2.29) and (3.2.33) and the result (3.2.34) matches with what we have found earlier in (3.2.27).

Since we see that the Casimir operators can be put into block diagonal form, their decompositions in terms of the direct sums of IRRs of SO(5) and SO(6) may be seen by inspecting the Casimir eigenvalues and dimensions in the fundamental IRRs of $SO(5)$ and $SO(6)$. An IRR of SO(5) is labelled in the Dynkin indices (n, m), since it is of rank 2. The dimension of the IRR (n, m) is [19]

$$dim(n, m) = \frac{1}{6}(n + 1)(m + 1)(n + m + 2)(2n + m + 3)\,, \tag{3.2.35}$$

where n and m are positive integers. The trivial representation is $(0, 0)$ which obviously has the dimension $dim(0, 0) = 1$. The fundamental spinor and vector representations have dimensions 4 and 5, respectively

$$dim(0, 1) = 4, \quad dim(1, 0) = 5, \tag{3.2.36}$$

while the corresponding eigenvalues of the Casimir operator are

$$C_2^{SO(5)}((0, 0)) = 0, \quad C_2^{SO(5)}((0, 1)) = \frac{5}{2}, \quad C_2^{SO(5)}((1, 0)) = 4. \tag{3.2.37}$$

Thus, we conclude that the decomposition of $(Z_{ab})^2$ into direct sum of $SO(5)$ IRR is given as

$$\mathbf{3}(0, 0) \oplus \mathbf{2}(0, 1) \oplus (1, 0)\,, \tag{3.2.38}$$

where the coefficients in bold denote the multiplicities of the respective representations in the decomposition. Clearly the total dimension is $3 \times 1 + 2 \times 4 + 5 = 16$.

The IRR of $SO(6) \approx SU(4)$ are labeled by three positive integers (p, q, r) in the Dynkin notation and has the dimension [57]

$$dim(p, q, r) = \frac{1}{12}(p+1)(q+1)(r+1)(p+q+2)(q+r+2)(p+q+r+3)\,. \tag{3.2.39}$$

The fundamental and anti-fundamental spinors are 4-dimensional and the vector representation is 6-dimensional:

$$dim(1, 0, 0) = 4, \quad dim(0, 1, 0) = 6, \quad dim(0, 0, 1) = 4\,. \tag{3.2.40}$$

Eigenvalues of the SO(6) Casimir are

$$C_2^{SO(6)}((0,0,0)) = 0\,, \quad C_2^{SO(6)}((0,1,0)) = 5\,, \tag{3.2.41}$$
$$C_2^{SO(6)}((1,0,0)) = C_2^{SO(6)}((0,0,1)) = \frac{15}{4}\,.$$

Therefore, the IRR decomposition of $(Z_{gh})^2$ under $SO(6)$ is given by

$$\mathbf{2}(0,0,0) \oplus \mathbf{2}(1,0,0) \oplus (0,1,0)\,. \tag{3.2.42}$$

Let us now look at the tensor product of the $(0,n)$ IRR of SO(5) with the fundamental vector and spinor representations. These are given as [58]

$$(0,n) \otimes (1,0) = (1,n) \oplus (0,n) \oplus (1,n-2), \tag{3.2.43a}$$
$$(0,n) \otimes (0,1) = (0,n+1) \oplus (1,n-1) \oplus (0,n-1)\,. \tag{3.2.43b}$$

Our first task is to obtain the $SO(5)$ IRRs carried by the Y_a's. To see that, we introduce the generators H_{ab} of $SO(5)$ related to M_{ab} and Z_{ab} as

$$H_{ab} := M_{ab} \otimes \mathbb{1}_{16} + \mathbb{1}_N \otimes Z_{ab}. \tag{3.2.44}$$

The $SO(5)$ IRR content of H_{ab} is found using (3.2.43)

$$(0,n) \otimes [\mathbf{3}(0,0) \oplus \mathbf{2}(0,1) \oplus (1,0)] = \mathbf{4}(0,n) \oplus \mathbf{2}(0,n+1) \oplus \mathbf{2}(1,n-1)$$
$$\oplus\, \mathbf{2}(0,n-1) \oplus (1,n) \oplus (1,n-2)\,. \tag{3.2.45}$$

From the right hand side of (3.2.45) we observe that there are 4 concentric fuzzy S^4's at the matrix level $dim(0,n) = \frac{1}{6}(n+1)(n+2)(n+3)$, and two concentric S_F^4 at each matrix level $dim(0,n-1)$ and $dim(0,n+1)$ respectively. The remaining $SO(5)$ IRR's in the right hand side of (3.2.45) have higher spin and we cannot interpret them as fuzzy S^4's. This is the matrix algebra content of our new solutions to the YM-matrix model equations of motion.

In order to obtain an enhanced geometrical understanding of these developments, it is useful to consider the $SO(6)$ representation content of these matrix configurations. Proceeding in a similar manner we introduce the $SO(6)$ generator

$$H_{gh} := M_{gh} \otimes \mathbb{1}_{16} + \mathbb{1}_N \otimes Z_{gh}. \tag{3.2.46}$$

where M_{gh} carries the $(n,0,0)$ IRR and Z_{gh} carries the representation given in the direct sum form in (3.2.42). Using the tensor products [58]

$$(n,0,0) \otimes (1,0,0) = (n+1,0,0) \oplus (n-1,1,0), \tag{3.2.47a}$$

$$(n,0,0)\otimes(0,1,0)=(n-1,0,1)\oplus(n,1,0)\,. \tag{3.2.47b}$$

We find that H_{gh} carries the direct sum representation

$$\begin{aligned}(n,0,0)\otimes[\mathbf{2}(0,0,0)\oplus\mathbf{2}(1,0,0)\oplus(0,1,0)] &= \mathbf{2}(n,0,0)\oplus\mathbf{2}(n+1,0,0)\\ &\oplus(n-1,0,1)\oplus\mathbf{2}(n-1,1,0)\oplus(n,1,0)\,.\end{aligned} \tag{3.2.48}$$

We may now notice several facts by inspecting this result. We should first recall that according to branching rules of $SO(6)$ IRRs into $SO(5)$ IRRs, we have that $(n,0,0)$ IRR of $SO(6)$ simply branches to a single IRR of $SO(5)$, which is $(0,n)$ [59]. Thus the matrix algebras representing fuzzy four-spheres carry the generic form $(n,0,0)$. Consequently, we see that from the $SO(6)$ perspective $\mathbf{2}(n,0,0)\oplus\mathbf{2}(n+1,0,0)$ part of the right hand side of (3.2.48) is associated to two concentric S_F^4 at matrix level $dim^{SO(6)}(n,0,0)=dim^{SO(5)}(0,n)$ and two concentric S_F^4 at matrix level $dim^{SO(6)}(n+1,0,0)=dim^{SO(5)}(0,n+1)$, respectively. From the recent developments identifying generalized fuzzy four-spheres as associated to higher dimensional orbits of $SO(6)\approx SU(4)$, we infer that the $(n-1,0,1)$ IRR appearing in the right hand side of (3.2.48) can be related to a particular generalized fuzzy four-sphere which may be denoted as S_Λ^4 in the notation of [1].

Then, we have the result that part of the new matrix configuration (3.2.3) solving the YM 5-matrix model, may be interpreted as the generalized fuzzy 4-spheres recently constructed in [1]. In the next sections, we lay out the structure of these generalized fuzzy 4-spheres using the coadjoint orbit quantization techniques.

3.3 Coadjoint Orbit Method and Fuzzy Spaces

In the following sections, the construction of the basic and the generalized fuzzy four spheres will be explored using the coadjoint orbits method [27]. Our main focus will be on quantum geometries realized as quantized coadjoint orbits embedded in a Euclidean target space. Since S^4 is not a Poisson manifold, it is not realized as a coadjoint orbit of its isometry group. Therefore, the application of the method of coadjoint orbits to S^4 is not direct. The constructions of the basic and generalized fuzzy-four spheres are facilitated by studying the quantization of the coadjoint orbits of $SO(6)\approx SU(4)$.

To start with, we present a brief overview of the technique of coadjoint orbit quantization. The theory of quantization of coadjoint orbits was throughly given by Kirillov in [60] and several related examples were provided in [61]. The development of this section will mostly depend on these sources. To begin with, let G be a Lie group and $\boldsymbol{g}$ be the associated Lie algebra. Now consider $\boldsymbol{g}^*$, which is the vector space dual to $\boldsymbol{g}$, the action of G on $\boldsymbol{g}^*$ is called the coadjoint action. In this regard, a coadjoint orbit is simply the orbit of some point in $\boldsymbol{g}^*$ under the action of G. For compact and semi-simple groups, the adjoint and coadjoint orbits are equivalent. Since the groups $SU(N)$ are compact and semi-simple, their adjoint and coadjoint orbits coincide. From now on we assume that G is compact and semi-simple, hence to determine its coadjoint orbits it suffices to examine the adjoint orbits of G.

For matrix groups such as $SU(N)$, the associated Lie algebra $\boldsymbol{g}$ is a subspace of the matrix algebra $Mat(N)$. Therefore, the adjoint action of G on $\boldsymbol{g}$ is given by the matrix conjugation

$$Ad(g)Y = gYg^{-1}, \tag{3.3.1}$$

where g $\in$ G and Y $\in \boldsymbol{g}$. The coadjoint orbit of G is defined by

$$O_J = \left\{ Ad(g)J = gJg^{-1} \,\middle|\, J \in \boldsymbol{g}\,,\, g \in G \right\} \cong \frac{G}{H_J}\,. \tag{3.3.2}$$

The coadjoint orbit is then considered as a coset space G/H_J where H_J is a subset of G called the isotropy subgroup at J or the stabilizer group of O_J :

$$H_J = \left\{ h \in H_J \,\middle|\, J = Ad(h)J = hJh^{-1} \right\}. \tag{3.3.3}$$

3.3.1 Warmup

To get started, let us quickly look at the coadjoint orbits of SU(2). An arbitrary element $J \in$ ***su(2)*** can be written as

$$J = i\vec{u}\cdot\vec{\sigma} = \begin{pmatrix} iu^3 & u^2 + iu^1 \\ -u^2 + iu^1 & -iu^3 \end{pmatrix} \tag{3.3.4}$$

where $\vec{\sigma}$ is the vector of Pauli matrices. To follow the convention of [61], we pick J to be anti-Hermitian in this section. The eigenvalues of J can be found from the characteristic equation

$$\lambda^2 - tr(J)\lambda + det(J) = 0, \tag{3.3.5}$$

with $\mathrm{tr}(J) = 0$ and $\det(J) =: r_e^2 = \vec{u} \cdot \vec{u}$ as

$$\lambda_{\pm} = \pm i r_e \,, \tag{3.3.6}$$

therefore the diagonal matrix is

$$J_D = \begin{pmatrix} i r_e & 0 \\ 0 & -i r_e \end{pmatrix}, \tag{3.3.7}$$

which spans the $U(1)$ subalgebra of $SU(2)$. Recall from (2.1.15), a general element g of $SU(2)$ is given as

$$g = \begin{pmatrix} s_1 & -{s_2}^* \\ s_2 & {s_1}^* \end{pmatrix}, \qquad (s_1, s_2) \in \mathbb{C}^2,\ \det(g) = 1 \,. \tag{3.3.8}$$

From equations (3.3.8) and (3.3.7) we have

$$g_1 J_D {g_1}^{-1} = g_1 J_D {g_1}^{\dagger} = \begin{pmatrix} s_1 & -{s_2}^* \\ s_2 & {s_1}^* \end{pmatrix} \begin{pmatrix} i r_e & 0 \\ 0 & -i r_e \end{pmatrix} \begin{pmatrix} {s_1}^* & {s_2}^* \\ -s_2 & s_1 \end{pmatrix}, \tag{3.3.9}$$

$$g_1 J_D {g_1}^{-1} = \begin{pmatrix} i(|s_1|^2 - |s_2|^2) r_e & i2 r_e s_1 {s_2}^* \\ i2 r_e (s_1 {s_2}^*)^* & -i(|s_1|^2 - |s_2|^2) r_e \end{pmatrix}. \tag{3.3.10}$$

Let $s_1 = a_1 + i b_1$, $s_2 = a_2 + i b_2$ and rename the parameters as follows

$$w_1 = 2r_e(a_1 a_2 + b_1 b_2), \quad w_2 = 2r_e(a_1 b_2 - b_1 a_2), \quad w_3 = (|s_1|^2 - |s_2|^2) r_e \,, \tag{3.3.11}$$

then we obtain

$$g_1 J_D {g_1}^{-1} = \begin{pmatrix} i w_3 & w_2 + i w_1 \\ -w_2 + i w_1 & -i w_3 \end{pmatrix}. \tag{3.3.12}$$

By comparing this equation with equation (3.3.4) , we observe that $g J_D g^{-1}$ is an element of ***su(2)***. Hence we have

$$J = g_1 J_D {g_1}^{-1}, \tag{3.3.13}$$

for some $g_1 \in G$. From (3.3.13) we deduce that every element of ***su(2)*** can be diagonalized by means of an SU(2) matrix.

By using (3.3.13), orbits of $SU(2)$ can be described as

$$O_J = g J g^{-1} = g(g_1 J_D {g_1}^{-1}) g^{-1} = (g g_1) J_D (g g_1)^{-1}, \tag{3.3.14a}$$

$$O_J = g_2 J_D {g_2}^{-1}, \qquad g_2 := g g_1. \tag{3.3.14b}$$

The stabilizer of these orbits should be a subgroup of $SU(2)$ leaving J_D invariant under the adjoint action. That is satisfying

$$J_D = g_s J_D {g_s}^{\dagger}, \tag{3.3.15}$$

Explicitly we have

$$J_D = \begin{pmatrix} s_1 & -{s_2}^* \\ s_2 & {s_1}^* \end{pmatrix} \begin{pmatrix} ir_e & 0 \\ 0 & -ir_e \end{pmatrix} \begin{pmatrix} {s_1}^* & {s_2}^* \\ -s_2 & s_1 \end{pmatrix}, \tag{3.3.16a}$$

$$\begin{pmatrix} ir_e & 0 \\ 0 & -ir_e \end{pmatrix} = ir_e \begin{pmatrix} |s_1|^2 - |s_2|^2 & 2s_1{s_2}^* \\ 2s_2{s_1}^* & -|s_1|^2 + |s_2|^2 \end{pmatrix}. \tag{3.3.16b}$$

There are two cases to be considered:

Case 1: $r_e = 0$

This is the trivial case. The stabilizer is SU(2). Therefore, the orbit is a just a single point specified by $e^{iJ_D}\Big|_{r_e=0} = \mathbb{1}_2$. Adjoint actions by all group elements $g \in SU(2)$ leave the point fixed.

Case 2: $r_e \neq 0$

Let $s_1 = r_1 e^{i\gamma_1}$, $s_2 = r_2 e^{i\gamma_2}$, $\quad 0 = s_1{s_2}^* = r_1 r_2 e^{i(\gamma_1 - \gamma_2)}$ If we pick $r_2 = 0$ then $s_2 = 0$. This gives $det(g_s) = 1$ and therefore we have $r_1 = 1$, hence $s_1 = e^{i\gamma_1}$

$$g_s = \begin{pmatrix} e^{i\gamma_1} & 0 \\ 0 & e^{-i\gamma_1} \end{pmatrix}. \tag{3.3.17}$$

The stabilizer is $U(1) \subset SU(2)$ and the orbit is $SU(2)/U(1) \cong \mathbb{CP}^1 \cong S^2$.

Following the same line of developments, coadjoint orbits of $SU(3)$, $SU(4)$ and in general $SU(N)$ can be constructed. For the examples of coadjoint orbits of $SU(3)$ we refer the reader to the appendix B. Since we need to know the coadjoint orbits of $SU(4)$ for the developments in this chapter, we direct our attention to these spaces. The coadjoint orbits of SU(4) can also be found by using (3.3.15). They are given in [62] as follows

$$O_1 = \frac{SU(4)}{U(1) \times U(1) \times U(1)}, \qquad O_2 = \frac{SU(4)}{SU(2) \times U(1) \times U(1)}, \tag{3.3.18a}$$

$$O_3 = \frac{SU(4)}{S(U(2)\times U(2))}\,, \quad O_4 = \frac{SU(4)}{SU(3)\times U(1)} \cong \mathbb{CP}^3, \tag{3.3.18b}$$

with corresponding dimensions

$$\dim(O_1) = 12\,, \quad \dim(O_2) = 10\,, \quad \dim(O_3) = 8\,, \quad \dim(O_4) = 6\,. \tag{3.3.19}$$

3.4 Quantization of O_2

General technique of the quantization of coadjoint orbits was developed in [26]. Among the four coadjoint orbits of SU(4) given in (3.3.18) we are particularly interested in the quantizations of O_2 and O_4. The quantization of O_4, which is diffeomorphic to $\mathbb{CP}^3$, was achieved by Bernevig et. al. [27]. The general formalism of quantization [38] is given in appendix C. Some of the intermediate steps used during the quantization of $O_2 = \frac{SU(4)}{SU(2)\times U(1)\times U(1)}$ are provided in appendix D. Here, we employ the method outlined in [26] and use the Dirac constraint analysis formalism [63] to perform the quantization of O_2.

In the previous chapter, we have seen how $\mathbb{CP}^3$ and S^4 are related through an S^2 fibration and the corresponding relations between the fuzzy $\mathbb{CP}^3$ and fuzzy spheres S^4_F and S^2_F. By studying the quantization of O_2, we would like to understand and elaborate on the relation between this quantized space and the generalized fuzzy four-spheres S^4_Λ, which are introduced in the work [1] and encountered in our search for new solutions to the YM matrix model, discussed earlier in this chapter. Although, several aspects of S^4_Λ are discussed in detail in [1], we feel that coadjoint orbit quantization technique allows us to gain a useful and practical perspective to its structure, and at the same time allows us to exploit the connection between fuzzy spaces and Landau problem [64, 65, 66] which is discussed later on in this section.

The starting point is the Wess-Zumino term defined by

$$L = -i\,\mathrm{tr}\Big(\Lambda S^{-1}\dot{S}\Big), \tag{3.4.1}$$

where $S \in SU(4)$, $\dot{S} = \frac{\mathrm{d}S}{\mathrm{d}t}$ and t is a parameter with respect to which group elements are parametrized. Let us denote by T_k $(k = 1, ..., 15)$ 15 generators of SU(4) satisfying [67]

$$[T_k, T_l] = i f_{klm} T_m\,, \tag{3.4.2}$$

f_{klm} being the structure constants for $SU(4)$ and Λ be a linear combination of Cartan generators that will be specified shortly. If the general group element S is parametrized by the set of real variables $\xi(t) \equiv (\xi_1, \xi_2, ..., \xi_{15})$, it can be expressed as

$$S(\xi) = e^{i\sum_k T_k \xi_k}. \tag{3.4.3}$$

The momenta conjugate to ξ_k are

$$\begin{aligned}\pi_k = \frac{\partial L}{\partial \dot{\xi}_k} &= -i\frac{\partial}{\partial \dot{\xi}_k}\,\mathrm{tr}\left(\Lambda S^{-1}\frac{\partial S}{\partial \xi_l}\frac{\mathrm{d}\xi_l}{\mathrm{d}t}\right) \\ &= -i\,\mathrm{tr}\left(\Lambda S^{-1}\frac{\partial S}{\partial \xi_l}\frac{\partial \dot{\xi}_l}{\partial \dot{\xi}_k}\right) \\ &= -i\,\mathrm{tr}\left(\Lambda S^{-1}\frac{\partial S}{\partial \xi_k}\right).\end{aligned} \tag{3.4.4}$$

Local coordinates and conjugate momenta satisfy the following Poisson brackets as usual

$$\{\xi_k, \pi_l\} = \delta_{kl}\,, \quad \{\xi_k, \xi_l\} = \{\pi_k, \pi_l\} = 0\,. \tag{3.4.5}$$

We may introduce a 15×15 matrix E whose elements are functions of ξ_k and write

$$S^{-1}\frac{\partial S}{\partial \xi_k} = iT_{k'}E_{k'k}\,. \tag{3.4.6}$$

Since $E_{k'k}$ is non-singular [26, 27] we may multiply both sides of (3.4.4) with E^{-1} to write

$$\pi_{k'}E^{-1}_{k'k} = -i\,\mathrm{tr}\big(\Lambda i T_{k''}E_{k''k'}E^{-1}_{k'k}\big). \tag{3.4.7}$$

Introducing $\Lambda_k = \pi_{k'}E^{-1}_{k'k}$, this gives

$$\Lambda_k = \mathrm{tr}(\Lambda T_k)\,. \tag{3.4.8}$$

Λ_k generate $SU(4)$ since we can easily see that

$$\{\Lambda_k, \Lambda_l\} = f_{klm}\Lambda_m, \tag{3.4.9}$$

as a consequence of the commutation relations of T_k's given above. We also see that

$$\{\Lambda_k, S\} = -iST_k, \tag{3.4.10}$$

since T_k acts on the right of $S \in SU(4)$. In this expression, it is customary to call Λ_k the right acting generators of $SU(4)$.

The Cartan generators of $SU(4)$ in the 4-dimensional fundamental representation are usually taken to be

$$T_3 = \frac{1}{2} diag(1, -1, 0, 0), \tag{3.4.11a}$$

$$T_8 = \frac{1}{2\sqrt{3}} diag(1, 1, -2, 0), \tag{3.4.11b}$$

$$T_{15} = \frac{1}{2\sqrt{6}} diag(1, 1, 1, -3)\,. \tag{3.4.11c}$$

in a notation generalizing the Gell-Mann matrices in $SU(3)$. However, for our purposes it is more convenient to use the Cartan subalgebra basis (h_1, h_2, h_3) which is given as

$$h_1 = \frac{\sqrt{3}}{2} T_8 = \frac{1}{4} diag(1, 1, -2, 0), \tag{3.4.12a}$$

$$h_2 = \frac{\sqrt{3}}{6} T_8 + \sqrt{\frac{2}{3}} T_{15} = \frac{1}{4} diag(1, 1, 0, -2), \tag{3.4.12b}$$

$$h_3 = T_3\,. \tag{3.4.12c}$$

We would like to quantize O_2 by considering the $U(1) \times U(1)$ part of the isotropy subgroup of $SU(4)$ in the coset space realization of O_2. For this purpose we take

$$\Lambda = n_1 h_1 + n_2 h_2, \tag{3.4.13}$$

where $n_1, n_2 \in \mathbb{Z}$ are the corresponding $U(1)$ charges. For the choice of Λ given above, the right acting generators take the form

$$\Lambda_k = n_1 \frac{\sqrt{3}}{4}\, \delta_{8,k} + n_2 \left\{ \frac{\sqrt{3}}{12}\, \delta_{8,k} + \frac{1}{\sqrt{6}}\, \delta_{15,k} \right\}. \tag{3.4.14}$$

Since the Lagrangian is first order in derivatives, equation (3.4.14) actually defines a set of constraints for the conjugate momenta which is expressed as

$$\Lambda_k - \frac{n_1}{2} \left\{ \frac{\sqrt{3}}{2}\, \delta_{8,k} \right\} - \frac{n_2}{2} \left\{ \frac{\sqrt{3}}{6}\, \delta_{8,k} + \sqrt{\frac{2}{3}}\, \delta_{15,k} \right\} \approx 0\,, \tag{3.4.15}$$

where $\approx$ is the weak equality sign indicating that the equality is valid on the constraint surface only. The classification of constraints can be performed by calculating Poisson brackets among Λ_k. We have

$$\{\Lambda_1, \Lambda_2\} = f_{123} \Lambda_3 = \Lambda_3 \approx 0, \tag{3.4.16}$$

$$\{\Lambda_1, \Lambda_4\} = f_{147}\Lambda_7 = \frac{1}{2}\Lambda_7 \approx 0, \tag{3.4.17}$$

$$\{\Lambda_4, \Lambda_5\} = f_{458}\Lambda_8 = \frac{\sqrt{3}}{2}\Lambda_8 \approx \frac{3}{2}\left(\frac{n_1}{4} + \frac{n_2}{12}\right), \tag{3.4.18}$$

$$\{\Lambda_9, \Lambda_{10}\} = f_{(9)(10)(15)}\Lambda_{15} = \sqrt{\frac{2}{3}}\Lambda_{15} \approx \frac{n_2}{3}. \tag{3.4.19}$$

If we keep on calculating the Poisson brackets, we observe that the brackets of Λ_1, Λ_2, Λ_3, Λ_8 and Λ_{15} with all constraints are weakly equal to zero. Therefore, we infer that while Λ_1, Λ_2, Λ_3, Λ_8 and Λ_{15} are first-class constraints, while all the remaining constraints are second-class constraints.

The second-class constraints can be rearranged to form a complete set of first-class constraints by taking the appropriate linear combinations $\phi_m^{\pm}$:

$$\phi_m^{\pm} = \Lambda_m \pm i\Lambda_{m+1}, \tag{3.4.20}$$

where $m = 4, 6, 9, 11, 13$. For instance,

$$\begin{aligned} \left\{\Lambda_8, \phi_6^{\pm}\right\} &= \{\Lambda_8, \Lambda_6\} \pm i\{\Lambda_8, \Lambda_7\} \\ &= f_{8,6,7}\Lambda_7 \pm i f_{8,7,6}\Lambda_6 \\ &= \frac{\sqrt{3}}{2}\Lambda_7 \mp i\frac{\sqrt{3}}{2}\Lambda_6 \approx 0. \end{aligned} \tag{3.4.21}$$

We may take either ϕ_m^+ or ϕ_m^- as the first-class constraints. Aside from this fact, their Poisson brackets with Λ_3, Λ_8 and Λ_{15} also provide the following results

$$\begin{aligned} \left\{\Lambda_3, \phi_4^{\pm}\right\} &= \{\Lambda_3, \Lambda_4\} \pm i\{\Lambda_3, \Lambda_5\} \\ &= f_{345}\Lambda_5 \pm i f_{354}\Lambda_4 \\ &= \frac{1}{2}(\Lambda_5 \mp i\Lambda_4) \\ &= \mp\frac{i}{2}\phi_4^{\pm}, \end{aligned} \tag{3.4.22}$$

$$\left\{\Lambda_3, \phi_6^{\pm}\right\} = \pm\frac{i}{2}\phi_6^{\pm}, \qquad \left\{\Lambda_3, \phi_9^{\pm}\right\} = \mp\frac{i}{2}\phi_9^{\pm}, \tag{3.4.23}$$

$$\left\{\Lambda_3, \phi_{11}^{\pm}\right\} = \pm\frac{i}{2}\phi_{11}^{\pm}, \qquad \left\{\Lambda_3, \phi_{13}^{\pm}\right\} = 0\,, \tag{3.4.24}$$

$$\begin{aligned}\left\{\Lambda_8, \phi_4^{\pm}\right\} &= \{\Lambda_8, \Lambda_4\} \pm i\,\{\Lambda_8, \Lambda_5\} \\ &= f_{845}\Lambda_5 \pm i f_{854}\Lambda_4 \\ &= \frac{\sqrt{3}}{2}(\Lambda_5 \mp i\Lambda_4) \\ &= \mp\frac{i\sqrt{3}}{2}\phi_4^{\pm},\end{aligned} \tag{3.4.25}$$

$$\left\{\Lambda_8, \phi_6^{\pm}\right\} = \mp\frac{i\sqrt{3}}{2}\phi_6^{\pm}, \qquad \left\{\Lambda_8, \phi_9^{\pm}\right\} = \mp\frac{i}{2\sqrt{3}}\phi_9^{\pm}, \tag{3.4.26}$$

$$\left\{\Lambda_8, \phi_{11}^{\pm}\right\} = \mp\frac{i}{2\sqrt{3}}\phi_{11}^{\pm}, \qquad \left\{\Lambda_8, \phi_{13}^{\pm}\right\} = \pm\frac{i}{\sqrt{3}}\phi_{13}^{\pm}\,, \tag{3.4.27}$$

$$\left\{\Lambda_{15}, \phi_4^{\pm}\right\} = 0\,, \quad \left\{\Lambda_{15}, \phi_6^{\pm}\right\} = 0\,, \quad \left\{\Lambda_{15}, \phi_9^{\pm}\right\} = \mp i\sqrt{\frac{2}{3}}\phi_9^{\pm}, \tag{3.4.28}$$

$$\left\{\Lambda_{15}, \phi_{11}^{\pm}\right\} = \mp i\sqrt{\frac{2}{3}}\phi_{11}^{\pm}, \quad \left\{\Lambda_{15}, \phi_{13}^{\pm}\right\} = \mp i\sqrt{\frac{2}{3}}\phi_{13}^{\pm}\,. \tag{3.4.29}$$

From these Poisson brackets we may interpret $\phi_m^{\pm}$ $(m = 4, 6, 9, 11, 13)$ as the ladder operators of $SU(4)$ with respect to the Weyl-Cartan basis.

The usual procedure of quantization can be followed at this stage. Namely, we must have that first class constraints annihilating the physical states. This means that the physical states must be $SU(2)$ singlets and carry the $U(1)$ charges n_1 and n_2, respectively. The $SU(4)$ IRRs carried by the physical states are therefore given as (n_1, q, n_2) in the Dynkin notation.

The natural wave-functions on the group manifold of $SU(4)$ are given by the Wigner D-functions $D^{(p,q,r)}_{[L][R]}(S)$, $S \in SU(4)$, where $[L]$ and $[R]$ denote collectively the appropriate left and right quantum numbers that uniquely label these states. $D^{(p,q,r)}_{[L][R]}(S)$ are the matrix elements of the group elements $D^{(p,q,r)}(S)$ of $SU(4)$ in the IRR (p, q, r). On these wave-functions, the Dirac quantization procedure following the given constraint analysis requires that

$$h_1\, D(S) = \frac{1}{2} n_1\, D(S), \tag{3.4.30a}$$

$$h_2\, D(S) = \frac{1}{2} n_2\, D(S), \tag{3.4.30b}$$

$$h_3\, D(S) = 0. \tag{3.4.30c}$$

Let us take θ_1 and θ_2 as two real parameters, then the $U(1)$ rotations generated by the Cartan generators h_1, h_2 and h_3 may be given as

$$V_1 := e^{i\theta_1 h_1} = \begin{pmatrix} e^{i\theta_1/4} & 0 & 0 & 0 \\ 0 & e^{i\theta_1/4} & 0 & 0 \\ 0 & 0 & e^{-i\theta_1/2} & 0 \\ 0 & 0 & 0 & 1 \end{pmatrix}, \tag{3.4.31a}$$

$$V_2 := e^{i\theta_2 h_2} = \begin{pmatrix} e^{i\theta_2/4} & 0 & 0 & 0 \\ 0 & e^{i\theta_2/4} & 0 & 0 \\ 0 & 0 & 1 & 0 \\ 0 & 0 & 0 & e^{-i\theta_2/2} \end{pmatrix}, \tag{3.4.31b}$$

$$V_3 := e^{i\theta_3 h_3} = \begin{pmatrix} e^{i\theta_3/2} & 0 & 0 & 0 \\ 0 & e^{-i\theta_3/2} & 0 & 0 \\ 0 & 0 & 1 & 0 \\ 0 & 0 & 0 & 1 \end{pmatrix}. \tag{3.4.31c}$$

Since $D(S)$ satisfies the group homomorphism property, we may write $D(S_1 S_2) = D(S_1)D(S_2)$. Thus, we may also express (3.4.30) as

$$D(SV_1) = D(S)D(V_1) = D(S)e^{-\frac{i}{2}n_1\theta_1}, \tag{3.4.32a}$$

$$D(SV_2) = D(S)D(V_2) = D(S)e^{-\frac{i}{2}n_2\theta_2}, \tag{3.4.32b}$$

$$D(SV_3) = D(S)D(V_3) = D(S). \tag{3.4.32c}$$

In order to consider the physical states that are annihilated by the first class constraints, it is sufficient to consider $SU(4)$ IRRs with $q = 0$. At this stage, it is most convenient to use tensor operators in a Cartesian basis rather than the Wigner D-functions to give a concrete demonstration. Let us denote by Z^p_r an irreducible tensor in the IRR $(p, 0, r)$ of $SU(4)$. We may write

$$Z^p_r = Z^{j_1\cdots j_p}_{i_1\ldots i_r}, \tag{3.4.33}$$

where $i, j = 1, 2, 3, 4$ and the indices j_a, i_b take the values $a = 1, \ldots, p$ and $b = 1, \ldots, r$. Under the SU(4) rotations S, Z^p_r transforms as

$$(Z')^{j_1\cdots j_p}_{i_1\ldots i_r} = S^{j_1\cdots}_{o_1\ldots} S^{j_p}_{o_p} \bar{S}^{i_1\cdots}_{l_1\ldots} \bar{S}^{i_r}_{l_r} Z^{o_1\cdots o_p}_{l_1\ldots l_r}. \tag{3.4.34}$$

Applying V_1 on Z^p_r gives the eigenvalues of V_1 acting on the upper index appearing as p_1, p_2, p_3, p_4 respectively so that $p = p_1 + p_2 + p_3 + p_4$ and eigenvalues of V_1 acting on the lower index appearing as r_1, r_2, r_3, r_4 respectively so that $r = r_1 + r_2 + r_3 + r_4$. We have

$$exp\Big(-\frac{i}{2}n_1\theta_1\Big)Z^{j_1\cdots}_{i_1\cdots} = exp\Big(i\Big(\frac{p_1}{4}+\frac{p_2}{4}-\frac{p_3}{2}-\frac{r_1}{4}-\frac{r_2}{4}+\frac{r_3}{2}\Big)\theta_1\Big)Z^{j_1\cdots}_{i_1\cdots}\,, \quad (3.4.35)$$

which gives

$$2n_1 = 2p_3 - p_1 - p_2 - 2r_3 + r_1 + r_2\,. \quad (3.4.36)$$

Likewise, for V_2 acting on Z^p_r we find

$$exp\Big(-\frac{i}{2}n_2\theta_2\Big)Z^{j_1\cdots}_{i_1\cdots} = exp\Big(i\Big(\frac{p_1}{4}+\frac{p_2}{4}-\frac{p_4}{2}-\frac{r_1}{4}-\frac{r_2}{4}+\frac{r_4}{2}\Big)\theta_2\Big)Z^{j_1\cdots}_{i_1\cdots}\,, \quad (3.4.37)$$

which requires

$$2n_2 = 2p_4 - p_1 - p_2 - 2r_4 + r_1 + r_2\,, \quad (3.4.38)$$

and V_3 acting on Z^p_r gives

$$0 = p_1 - p_2 - r_1 + r_2\,. \quad (3.4.39)$$

We have not yet imposed all the constraints on the physical states and it is rather tedious to explicitly work out the equations for p_i and r_i coming from these as the corresponding generators for the constraints are not diagonal. Nevertheless, the rest of the analysis can be completed by determining the eigenvalues of

$$H = \frac{1}{2m}\Big(C_2^{SU(4)}(p,0,r) - C_2^{SU(2)}(0) - T_8^2 - T_{15}^2\Big), \quad (3.4.40)$$

which is a linear function of n_1 and n_2 only when acting on $D^{(p,0,r)}$. Here

$$C_2^{SU(4)}(p,0,r) = \frac{3}{8}(r^2+p^2) + \frac{1}{4}(pr+6p+6r), \quad (3.4.41)$$

are the eigenvalues of the Casimir operator in the $(p,0,r)$ IRR of $SU(4)$ and $C_2^{SU(2)}(0) = 0$ is the Casimir eigenvalue in the spin-0 IRR of $SU(2)$ and we have

$$\Big(T_8^2 + T_{15}^2\Big)D^{(p,0,r)} = \left(\frac{3}{8}\Big(n_1^2+n_2^2\Big) - \frac{1}{4}n_1n_2\right)D^{(p,0,r)}, \quad (3.4.42)$$

since $h_1 = \frac{\sqrt{3}}{2}T_8$ and $h_2 = \frac{\sqrt{3}}{6}T_8 + \sqrt{\frac{2}{3}}T_{15}$ as already noted in (3.4.12).

Equation (3.4.40) may be interpreted as the Hamiltonian of the particles on $O_2 = \frac{SU(4)}{SU(2)\times U(1)\times U(1)}$ charged under $U(1)\times U(1)$ and subject to non-vanishing $U(1)$

fluxes. This is the Landau problem of O_2 [27, 68]. From the known correspondences on the Hilbert space of the Lowest Landau levels (LLL) with fuzzy spaces it is expected that LLL corresponds to the generalized fuzzy S^4 which is to obtained as a quantization of O_2. The LLL energy is expected to be linear in the $U(1)$ fluxes n_1 and n_2. Taking

$$p_1 = p_2 = p_4 = 0, \qquad r_1 = r_2 = r_3 = 0, \tag{3.4.43}$$

in (3.4.36), (3.4.38) and (3.4.40), we have

$$E = \frac{1}{2m}\left[\frac{3}{8}(r_4^2 + p_3^2) + \frac{1}{4}(p_3 r_4 + 6p_3 + 6r_4) - \frac{3}{8}\Big(p_3^2 + r_4^2\Big) - \frac{1}{4}p_3 r_4\right], \tag{3.4.44}$$

$$n_1 = p_3 = p, \qquad n_2 = -r_4 = -r, \tag{3.4.45}$$

and these give

$$\begin{aligned} E &= \frac{1}{2m}\left[\frac{3}{8}(n_1^2 + n_2^2) + \frac{1}{4}(-n_1 n_2 + 6n_1 - 6n_2) - \frac{3}{8}\Big(n_1^2 + n_2^2\Big) + \frac{1}{4}n_1 n_2\right] \\ &= \frac{3}{4m}(n_1 - n_2) \\ &= \frac{3}{4m}(n_1 + |n_2|)\,, \end{aligned} \tag{3.4.46}$$

which is the LLL energy and linear in n_1 and n_2. The wavefunctions are in the form $D^{(n_1,0,|n_2|)}(S)$ carrying the $SU(4)$ IRRs as we wanted to demonstrate.

3.5 Fuzzy Spheres and Coherent States

In this section, the relationships between the coherent states on $\mathbb{CP}^3$ and O_2 coadjoint orbits of $SU(4)$ and fuzzy spheres are examined. A review of canonical coherent states can be found in appendix E.

3.5.1 CP^3 Coherent States and S_F^4

In order to provide a better grasp of the mathematical structure of S_F^4, we should give an explicit derivation of the continuum limit of coherent state expectation values of SU(4) generators T_k. In appendix D, we have shown that the quantization procedure transforms $\Phi^{\pm}_{n'}(n' = 9, 11, 13)$ constraints into ladder operators. Therefore, $\mathbb{CP}^3$ coherent states for the defining representation $(p, q, r) = (1, 0, 0)$ can be given as

follows [69]

$$
\begin{aligned}
|M\rangle &= exp\big[i(aT_9 + bT_{10} + cT_{11} + dT_{12} + eT_{13} + fT_{14})\big]\,\big|v_{(1,0,0)}\big\rangle \\
&=: e^{-iH}\,\big|v_{(1,0,0)}\big\rangle\ ,
\end{aligned}
\tag{3.5.1}
$$

where $\big|v_{(1,0,0)}\big\rangle = |v\rangle$ is the highest weight state for the defining representation and a, b, c, d, e, f are some real parameters. The coherent states $|M\rangle$ are in one-to-one correspondence with the points M of $\mathbb{CP}^3$ [53]. This is analogous to the fact that canonical coherent states $|z\rangle$ are in one-to-one correspondence with the complex plane $\mathbb{C}$. Let us note also that a point $M \in \mathbb{CP}^3$ can be described by three complex numbers as

$$
\mathbb{CP}^3 = \big\{ z \equiv (z_1, z_2, z_3) \in \mathbb{C}^3 \setminus \{0\}\ |\, z_i z_i = |z|^2 = 1\,, z \equiv \lambda z\,, \lambda \in \mathbb{C}\,, |\lambda| = 1 \big\}\,.
\tag{3.5.2}
$$

$\mathbb{CP}^3$ has complex dimensions 3 and real dimensions 6. The three complex coordinates (z_1, z_2, z_3) in (3.5.2) and the six real numbers a, b, c, d, e, f in (3.5.1) are two equivalent ways to describe $\mathbb{CP}^3$. In fact we see that with $\hat{a} = \dfrac{a}{r}, \hat{b} = \dfrac{b}{r} \ldots$, we have $\hat{a}^2 + \hat{b}^2 + \cdots + \hat{f}^2 = 1$, where $r^2 = \hat{a}^2 + \hat{b}^2 + \cdots + \hat{f}^2$, which is equivalent to the condition $|z|^2 = z_i z_i = 1$.

For the coherent states $|M\rangle$, we may introduce the rank 1 projection operators as

$$
P_M = |M\rangle\langle M|\ , \quad {P_M}^2 = P_M\,, \quad {P_M}^\dagger = P_M\,.
\tag{3.5.3}
$$

Clearly, this is also in one-to-one correspondence with the points on $\mathbb{CP}^3$. Our task is to understand how the manifold $\mathbb{CP}^3$ is embedded in the group manifold of $SU(4)$. To this end, we may start with computing the expectation values of $SU(4)$ generators with respect to the $\mathbb{CP}^3$ coherent states. We have

$$
\begin{aligned}
y_k &\coloneqq \mathrm{Tr}(P_M T_k) \\
&= \mathrm{Tr}(|M\rangle\langle M|\, T_k) \\
&= \langle M|\, T_k\, |M\rangle \\
&= \langle v|\, e^{iH} T_k e^{-iH}\, |v\rangle \\
&= p_{k,l}\, \langle v|\, T_l\, |v\rangle\,,
\end{aligned}
\tag{3.5.4}
$$

where sum over repeated indices is implied and the last line follows as a consequence of the Baker–Campbell–Hausdorff formula [70], which allows us to express

$e^{iH}\,T_k\,e^{-iH}$ as a linear combination $\sum p_{k,l}T_l$ of the generators T_k of $SU(4)$ [69]. The Cartan generator matrices are given in (3.4.12). Since only the eigenvalue of the fifteenth generator is nonzero, i.e. $T_{15}\,|v\rangle = t_{15}\,|v\rangle$, we have

$$y_k = \langle v|\, p_{k,15}T_{15}\,|v\rangle = p_{k,15}\,\langle v|\, t_{15}\,|v\rangle = p_{k,15}\,t_{15}\,. \tag{3.5.5}$$

The highest weight state for the defining representation is $|v\rangle = \big|1/2, 1/(2\sqrt{3}), 1/(2\sqrt{6})\big\rangle$, so $t_{15} = \frac{1}{2\sqrt{6}}$ and y_k are

$$y_k = \langle M|\, T_k\,|M\rangle = \frac{1}{2\sqrt{6}}\,p_{k,15}. \tag{3.5.6}$$

By applying the lowering operator to $|v\rangle$, the rest of the states in the $(1,0,0)$ IRR of $SO(6)$ can be obtained. In (3.5.6), y_k $(k = 1,..,15)$ are called the trigonometric embedding functions that parametrize the coset space $O_4 \cong \mathbb{CP}^3$. The technique used for the derivation of these functions can be found in appendix F. y_k are given as follows

$$\begin{gathered} y_1 = -\frac{1}{3}(ac+bd)\frac{\sin^2(r)}{r^2}, \quad y_2 = -\frac{1}{3}(bc-ad)\frac{\sin^2(r)}{r^2}\,, \\ y_3 = -\frac{1}{6}(a^2+b^2-c^2-d^2)\frac{\sin^2(r)}{r^2}, \end{gathered} \tag{3.5.7}$$

$$\begin{gathered} y_4 = -\frac{1}{3}(ae+bf)\frac{\sin^2(r)}{r^2}, \quad y_5 = \frac{1}{3}(af-be)\frac{\sin^2(r)}{r^2}\,, \\ y_6 = -\frac{1}{3}(ce+df)\frac{\sin^2(r)}{r^2}, \end{gathered} \tag{3.5.8}$$

$$\begin{gathered} y_7 = \frac{1}{3}(cf-de)\frac{\sin^2(r)}{r^2}, \quad y_8 = \frac{1}{6\sqrt{3}}\left[3(e^2+f^2)-r^2\right]\frac{\sin^2(r)}{r^2}\,, \\ y_9 = -\frac{b}{3}\frac{\sin(2r)}{2r}, \end{gathered} \tag{3.5.9}$$

$$y_{10} = \frac{a}{3}\frac{\sin(2r)}{2r}, \quad y_{11} = -\frac{d}{3}\frac{\sin(2r)}{2r}, \quad y_{12} = \frac{c}{3}\frac{\sin(2r)}{2r}, \tag{3.5.10}$$

$$y_{13} = -\frac{f}{3}\frac{\sin(2r)}{2r}, \quad y_{14} = \frac{e}{3}\frac{\sin(2r)}{2r}, \quad y_{15} = \frac{1}{2\sqrt{6}}\left[1-\frac{4}{3}\sin^2(r)\right], \tag{3.5.11}$$

where $r^2 = a^2+b^2+c^2+d^2+e^2+f^2$.

The sum of the squares of y_k is

$$\sum_{k=1}^{15} y_k^2 = \sum_{k=1}^{8} y_k^2 + \sum_{k=9}^{15} y_k^2 = \frac{\sin^4(r)}{27} + \left[\frac{1}{24} - \frac{\sin^4(r)}{27}\right] = \frac{1}{24}. \tag{3.5.12}$$

There is another identity satisfied by the embedding functions, which may be written as

$$d^{kls} y_l y_s = -\frac{1}{12} y_k, \tag{3.5.13}$$

where d^{kls} is the totally symmetric tensor defined through

$$T_k T_l = \frac{1}{2}\left[\frac{1}{4}\delta_{kl}\mathbb{1}_4 + (d^{kls} + if^{kls})T_s\right]. \tag{3.5.14}$$

In appendix A.1, the generators in the fundamental spinor representation $(1,0,0)$ of $SO(6)$ are given. These generators can be expressed in terms of $SU(4)$ generators as

$$F_{gh} = \sum \eta_{gh}{}^{i} T_i, \tag{3.5.15}$$

where $\eta_{gh}{}^{i}$ are the 't Hooft symbols [1]. F_{gh}'s can be written explicitly as

$$F_{12} = \frac{1}{2}T_3 - \frac{\sqrt{3}}{6}T_8 + \frac{\sqrt{6}}{6}T_{15}, \quad F_{13} = \frac{1}{2}T_2 + \frac{1}{2}T_{14}, \quad F_{14} = -\frac{1}{2}T_1 + \frac{1}{2}T_{13}, \tag{3.5.16}$$

$$F_{15} = \frac{1}{2}T_7 + \frac{1}{2}T_{10}, \quad F_{16} = -\frac{1}{2}T_6 - \frac{1}{2}T_9, \quad F_{23} = -\frac{1}{2}T_1 - \frac{1}{2}T_{13}, \tag{3.5.17}$$

$$F_{24} = -\frac{1}{2}T_2 + \frac{1}{2}T_{14}, \quad F_{25} = \frac{1}{2}T_6 - \frac{1}{2}T_9, \quad F_{26} = \frac{1}{2}T_7 - \frac{1}{2}T_{10}, \tag{3.5.18}$$

$$F_{34} = \frac{1}{2}T_3 + \frac{\sqrt{3}}{6}T_8 - \frac{\sqrt{6}}{6}T_{15}, \quad F_{35} = -\frac{1}{2}T_5 + \frac{1}{2}T_{12}, \quad F_{36} = \frac{1}{2}T_4 - \frac{1}{2}T_{11}, \tag{3.5.19}$$

$$F_{45} = \frac{1}{2}T_4 + \frac{1}{2}T_{11}, \quad F_{46} = \frac{1}{2}T_5 + \frac{1}{2}T_{12}, \quad F_{56} = \frac{\sqrt{3}}{3}T_8 + \frac{\sqrt{6}}{6}T_{15}. \tag{3.5.20}$$

Using the projection operator $P_M = |M\rangle\langle M|$ of (3.5.3), we may compute the expectation values of the $SO(6)$ generators as

$$w_{gh} \coloneqq \frac{1}{2}\,\mathrm{Tr}\big(P_M F_{gh}\big)$$

[1] A general basis for the 't Hooft symbols can be found in [71].

$$= \frac{1}{2}\,\mathrm{Tr}\big(|M\rangle\langle M|\,F_{gh}\big) \tag{3.5.21}$$
$$= \frac{1}{2}\,\langle M|\,F_{gh}\,|M\rangle\,.$$

This means that we can write

$$P_M = \sum_{g<h} w_{gh}F_{gh} = \frac{1}{2}\sum w_{gh}F_{gh}\,, \tag{3.5.22}$$

where w_{gh} are the embedding functions of $\mathbb{CP}^3$ to $SU(4)$ group manifold using the $SO(6)$ generator basis. By combining equations (3.5.16) to (3.5.20) with equations (3.5.6) to (3.5.11), w_{gh} can be given as

$$w_{12} = \frac{1}{2}y_3 - \frac{\sqrt{3}}{6}y_8 + \frac{\sqrt{6}}{6}y_{15}\,, \quad w_{13} = \frac{1}{2}y_2 + \frac{1}{2}y_{14}\,, \quad w_{14} = -\frac{1}{2}y_1 + \frac{1}{2}y_{13}\,, \tag{3.5.23}$$

$$w_{15} = \frac{1}{2}y_7 + \frac{1}{2}y_{10}\,, \quad w_{16} = -\frac{1}{2}y_6 - \frac{1}{2}y_9\,, \quad w_{23} = -\frac{1}{2}y_1 - \frac{1}{2}y_{13}\,, \tag{3.5.24}$$

$$w_{24} = -\frac{1}{2}y_2 + \frac{1}{2}y_{14}\,, \quad w_{25} = \frac{1}{2}y_6 - \frac{1}{2}y_9\,, \quad w_{26} = \frac{1}{2}y_7 - \frac{1}{2}y_{10}\,, \tag{3.5.25}$$

$$w_{34} = \frac{1}{2}y_3 + \frac{\sqrt{3}}{6}y_8 - \frac{\sqrt{6}}{6}y_{15}\,, \quad w_{35} = -\frac{1}{2}y_5 + \frac{1}{2}y_{12}\,, \quad w_{36} = \frac{1}{2}y_4 - \frac{1}{2}y_{11}\,, \tag{3.5.26}$$

$$w_{45} = \frac{1}{2}y_4 + \frac{1}{2}y_{11}\,, \quad w_{46} = \frac{1}{2}y_5 + \frac{1}{2}y_{12}\,, \quad w_{56} = \frac{\sqrt{3}}{3}y_8 + \frac{\sqrt{6}}{6}y_{15}\,. \tag{3.5.27}$$

Let us consider the embedding functions associated to the five generators $F_{a6} = -\frac{1}{2}\gamma_a$ $(a = 1, ..., 5)$ of $SO(6)$. We have

$$v_a \coloneqq w_{a6} = \langle M|\,F_{a6}\,|M\rangle = -\frac{1}{2}\,\langle M|\,\gamma_a\,|M\rangle\,. \tag{3.5.28}$$

From the expression of w_{e6} in ((3.5.24)-(3.5.27)) and expression for relevant y_k, we see that the sum of the squares of v_e is

$$\sum_{e=1}^{5}(v_e)^2 = \left(\frac{1}{12}\right)^2. \tag{3.5.29}$$

It is also straightforward but rather tedious to show that

$$\sum_{e=1}^{5} w_{ge}v_e = 0\,, \tag{3.5.30a}$$

$$\epsilon^{abcde} v_a v_b v_c v_d = 0\,, \tag{3.5.30b}$$

$$\epsilon^{abcde} v_a v_b w_{cd} = 0\,, \tag{3.5.30c}$$

$$\epsilon^{abcde} w_{ab} w_{cd} = -\frac{1}{18}\left[\cos(2r) + 2(e^2+f^2)\frac{\sin^2(r)}{r^2}\right]. \tag{3.5.30d}$$

From these considerations it is possible to see how the fuzzy 4-sphere emerges by comparing these expressions with those given in subsection 2.3.2.

Referring to equation (2.3.51) we recall

$$[\gamma_a, \gamma_b] = 4iG_{ab}\,, \tag{3.5.31}$$

and therefore,

$$[F_{a6}, F_{b6}] = \left[-\frac{\gamma_a}{2}, -\frac{\gamma_b}{2}\right] = \left[\frac{\gamma_a}{2}, \frac{\gamma_b}{2}\right] = iG_{ab}\,, \tag{3.5.32}$$

where G_{ab} generate the $(0,1)$ IRR of $SO(5)$. Moreover, as it is shown in subsection 2.3.2, M_{ab} generators given in equation (2.3.56) generate the $(0,n)$ IRR of$SO(5)$.

Now, let us relabel the $\mathbb{CP}^3$ coherent states in the defining representation $(0,1)$ as

$$|z,1\rangle \equiv |M\rangle\,. \tag{3.5.33}$$

In this new notation, equation (3.5.28) can be rewritten as

$$\langle z,1|\, F_{a6}\, |z,1\rangle = v_a\,. \tag{3.5.34}$$

By taking the n-fold symmetric tensor product of these coherent states, we obtain

$$|z,n\rangle \equiv (|z,1\rangle \otimes |z,1\rangle \otimes ... \otimes |z,1\rangle)_{Sym}. \tag{3.5.35}$$

n-fold symmetric tensor product of γ_a's, i.e. the X_a generators of equation (2.3.55) are then mapped to the embedding functions v_a via (3.5.35) as

$$\langle z,n|\, X_a\, |z,n\rangle = nv_a\,. \tag{3.5.36}$$

Let us denote $\widehat{X_a} = \frac{1}{n}X_a$, then the embedding functions into S^4 are

$$v_a = \frac{1}{n}\,\langle z,n|\, X_a\, |z,n\rangle = \langle z,n|\, \widehat{X_a}\, |z,n\rangle\,, \tag{3.5.37}$$

and the coherent state maps for the commutators $[\widehat{X_a}, \widehat{X_b}]$ are

$$\langle z,n|\, [\widehat{X_a}, \widehat{X_b}]\, |z,n\rangle = \langle z,n|\, \frac{1}{n^2}[X_a, X_b]\, |z,n\rangle$$

$$= \langle z, n| \frac{i}{n} \frac{M_{ab}}{n} |z, n\rangle \tag{3.5.38}$$
$$= \langle z, n| \frac{i}{n} \widehat{M_{ab}} |z, n\rangle ,$$

which is consistent with

$$[\widehat{X_a}, \widehat{X_b}] = \frac{i}{n} \widehat{M_{ab}}, \tag{3.5.39}$$

where $\widehat{M_{ab}} = \frac{1}{n} M_{ab}$. Likewise, we have

$$\langle z, n| [\widehat{M_{ab}}, \widehat{M_{cd}}] |z, n\rangle = \langle z, n| \frac{i}{n} (\delta_{ac} \widehat{M_{bd}} + \delta_{bd} \widehat{M_{ac}} - \delta_{bc} \widehat{M_{ad}} - \delta_{ad} \widehat{M_{bc}}) |z, n\rangle$$
$$[\widehat{M_{ab}}, \widehat{M_{cd}}] = \frac{i}{n} (\delta_{ac} \widehat{M_{bd}} + \delta_{bd} \widehat{M_{ac}} - \delta_{bc} \widehat{M_{ad}} - \delta_{ad} \widehat{M_{bc}}), \tag{3.5.40}$$

$$\langle z, n| [\widehat{M_{ab}}, \widehat{X_c}] |z, n\rangle = \langle z, n| \frac{i}{n} (\delta_{ac} \widehat{X_b} - \delta_{bc} \widehat{X_a}) |z, n\rangle$$
$$[\widehat{M_{ab}}, \widehat{X_c}] = \frac{i}{n} (\delta_{ac} \widehat{X_b} - \delta_{bc} \widehat{X_a}). \tag{3.5.41}$$

3.5.2 O_2 Coherent States and S^4_Λ

In section 3.4, we have investigated the Dirac quantization of the coadjoint orbit $O_2 = \frac{SU(4)}{SU(2)\times U(1)\times U(1)}$ and revealed that as a result of the quantization procedure, $\phi^{\pm}_m$ $(m = 4, 6, 9, 11, 13)$ constraint can be interpreted as the ladder operators i.e. generators associated to the roots in the Cartan-Weyl decomposition of $SO(6) \approx SU(4)$. Thus, O_2 coherent states for the irreducible representation $(p, q, r) = (1, 0, 1)$ of $SO(6)$ can be defined as follows

$$|G\rangle = exp\big[i(g_1 T_4 + g_2 T_5 + g_3 T_6 + g_4 T_7 + g_5 T_9 + g_6 T_{10} + g_7 T_{11} + g_8 T_{12} + g_9 T_{13} + g_{10} T_{14})\big] \left|w_{(1,0,1)}\right\rangle$$
$$=: e^{ig_i T_{i+3}} \left|w_{(1,0,1)}\right\rangle , \tag{3.5.42}$$

where $\left|w_{(1,0,1)}\right\rangle = |w\rangle$ is the highest weight state for $(1, 0, 1)$ IRR and g_r $(r = 1, .., 10)$ are all real parameters.

Now consider the tensor product $(n, 0, 0) \otimes (0, 0, 1)$ which can be decomposed as

$$(n, 0, 0) \otimes (0, 0, 1) = (n, 0, 1) \oplus (n - 1, 0, 0). \tag{3.5.43}$$

For the case of $n = 1$ we have

$$(1, 0, 0) \otimes (0, 0, 1) = (1, 0, 1) \oplus (0, 0, 0). \tag{3.5.44}$$

The tensor product given in equation (3.5.44) is carried by U_a which is given by

$$U_a = \gamma_a \otimes I + I \otimes (-\gamma_a^*). \tag{3.5.45}$$

The coherent state maps for U_a's are

$$u_a = \langle G| U_a |G\rangle = \langle G| \gamma_a \otimes I - I \otimes \gamma_a^* |G\rangle . \tag{3.5.46}$$

If we denote the generators of $SO(6)$ in the product representation $(n,0,0)\otimes(0,0,1)$ as D_{gh} then the quadratic Casimir operator C_u is

$$C_u = D_{gh} D_{gh}. \tag{3.5.47}$$

In view of the right hand side of (3.5.46), C_u can be put to block diagonal form

$$C_u = \begin{pmatrix} C_u(1,0,1) & 0 \\ 0 & C_u(0,0,0) \end{pmatrix} = \begin{pmatrix} [diag(4,\ldots,4)]_{15\times 15} & 0 \\ 0 & 0 \end{pmatrix}, \tag{3.5.48}$$

then the projection operators into the $(1,0,1)$ and $(0,0,0)$ representations are [72]

$$P_1 = \frac{C_u}{4}, \qquad P_2 = \frac{C_u - 4I}{-4}. \tag{3.5.49}$$

u_a are the embedding functions that parametrize the coset space O_2. An alternative derivation of u_a that depends on $\mathbb{CP}^3$ coherent states $|z,1\rangle$ can also be provided:

$$|z,1\rangle = exp\big[i(aT_9 + bT_{10} + cT_{11} + dT_{12} + eT_{13} + fT_{14})\big] \left|v_{(1,0,0)}\right\rangle, \tag{3.5.50}$$

$$\begin{aligned} |\bar{z},1\rangle = exp\big[i(a\big(T_9\big)^* + b\big(T_{10}\big)^* + c\big(T_{11}\big)^* + d\big(T_{12}\big)^* + e\big(T_{13}\big)^* \\ + f\big(T_{14}\big)^*)\big] \left|v_{(1,0,0)}\right\rangle. \end{aligned} \tag{3.5.51}$$

By employing $|z,n\rangle$ coherent states given in equation (3.5.35), we may define $|G\rangle$ as

$$(|z,n\rangle \otimes |\bar{z},1\rangle)_{Sym} = P_1(|z,n\rangle \otimes |\bar{z},1\rangle) \equiv |G\rangle , \tag{3.5.52}$$

so u_a's are

$$u_a = \langle G| U_a |G\rangle = (\langle z,n| \otimes \langle \bar{z},1|) P_1(\gamma_a \otimes I - I \otimes \gamma_a^*) P_1(|z,n\rangle \otimes |\bar{z},1\rangle). \tag{3.5.53}$$

CHAPTER 4

BFSS MODEL WITH MASS DEFORMATIONS

This chapter opens with an introduction that provides the necessary background information on a Yang-Mills (YM) matrix model with two distinct mass deformation terms which may be contemplated as a double mass deformation of the bosonic part of the BFSS model. As the first step, it is demonstrated that due to the presence of quadratic deformation terms, this newly introduced YM model subsequently breaks the global $SO(9)$ symmetry of the BFSS action down to $SO(5) \times SO(4) \times \mathbb{Z}_2$. Since our main objective is to examine the nature of emerging chaotic dynamics from the YM matrix models, as the next step, we propose an ansatz configuration in section 4.2 involving fuzzy two- and four-spheres with collective time dependence that can be employed to obtain reduced models with a few phase space degrees of freedom whose dynamics can be investigated in considerable detail. The chaotic dynamics emerging from these reduced models are revealed by calculating their Lyapunov spectrum, Poincaré sections and mean largest Lyapunov exponents by using numerical solutions to their Hamiltonian equations of motion.

As there is room for the choice of the values of massive deformation parameters, in subsection 4.2.3 we consider the same ansatz configuration with different masses and obtain another set of reduced models. In order to investigate the effects of mass parameters on the emerging chaotic dynamics; the Lyapunov spectrum, Poincaré sections and mean largest Lyapunov exponents for these new models are also calculated and comparisons between the two cases are made. Furthermore, in order to discuss the consequences of changing the fuzzy two-sphere part of the first ansatz, we propose a second ansatz configuration in section 4.3 and investigate its chaotic dynamics. Lastly, in section 4.4, we examine the dynamics of the motion when the two real func-

tions with collective time dependence are taken to be equal to each other. This leads to quasi-periodic motion.

4.1 Yang-Mills Matrix Models with Double Mass Deformation

As thoroughly discussed in section 2.5, gauge invariant deformations of YM matrix models are possible. Such a gauge invariant double mass deformation of (2.4.11) may be specified as

$$S_{MD} = \frac{1}{g^2}\int dt\, Tr\left(\frac{1}{2}(D_t B_I)^2 + \frac{1}{4}[B_I, B_J]^2 - \frac{1}{2}\mu_1^2 B_a^2 - \frac{1}{2}\mu_2^2 B_i^2\right), \qquad (4.1.1)$$

where the indices a and i take on the values $a = 1, .., 5$ and $i = 6, 7, 8$, respectively. In (4.1.1) the terms proportional to μ_1 and μ_2 are the quadratic deformations, which respect the $U(N)$ gauge symmetry, but altogether break the $SO(9)$ down to $SO(5) \times SO(3) \times \mathbb{Z}_2$. The discrete $\mathbb{Z}_2$ factor is present for $B_9 \to -B_9$ symmetry. In what follows, we are going to consider the sector in which B_9 is set equal to the zero matrix, or equally well, taken as the zero matrix as a part of the ansatz configuration which will be introduced shortly. Since, we are going to be essentially concerned with the classical dynamics of (4.1.1), we absorb the coupling constant in the definition of $\hbar$, as it only determines the overall scale of energy classically.

In the $A_0 = 0$ gauge, the equations of motion for B_I take the form

$$\ddot{B}_a + [B_I, [B_I, B_a]] + \mu_1^2 B_a = 0\,, \qquad (4.1.2a)$$

$$\ddot{B}_i + [B_I, [B_I, B_i]] + \mu_2^2 B_i = 0\,, \qquad (4.1.2b)$$

$$\ddot{B}_9 + [B_I, [B_I, B_9]] = 0\,, \qquad (4.1.2c)$$

while the Gauss law constraint remains unchanged in the form as given in (2.4.17).

The massive deformation of the BFSS model, which preserves maximal amount of supersymmetry is already known to be the BMN matrix model [5], which possesses fuzzy two-spheres and their direct sums as possible vacuum configurations. However, in this thesis, our focus is directed toward exploring the emerging chaotic dynamics from the Yang-Mills matrix models which could allow for not only fuzzy two-sphere configurations but also more exotic fuzzy sphere, and in particular a fuzzy four-sphere[1].

[1] In this section, we employ scaled versions of S_F^4 matrices that are defined as $H_a^{(n)} = 2X_a^{(n)}$.

It is possible to conceive deformations of (2.4.11) including two separate mass terms, which break the $SO(9)$ symmetry down to several different product subgroups. The underlying motivation for introducing the specific massive deformation in (4.1.1) comes from the fact that in two distinct limiting cases the equations of motion can be solved by either with fuzzy two-sphere our fuzzy four-sphere configurations. To be more precise, we have for $B_i = 0$, $B_9 = 0$, (4.1.2b) and (4.1.2c) satisfied identically, while (4.1.2a) takes the form

$$\ddot{B}_a + [B_b, [B_b, B_a]] + \mu_1^2 B_a = 0\,, \tag{4.1.3}$$

which is satisfied by the fuzzy four-sphere configurations $B_a \equiv H_a$ for $\mu_1^2 = -16$. H_a are $N \times N$ matrices carrying the $(0, n)$ UIR of $SO(5)$ so that $N = \frac{1}{6}(n+1)(n+2)(n+3)$. Whereas, in the other extreme, one may set $B_a = 0$, $B_9 = 0$, with the only remaining non-trivial equation of motion

$$\ddot{B}_i + [B_j, [B_j, B_i]] + \mu_2^2 B_i = 0\,, \tag{4.1.4}$$

which is solved by fuzzy two-sphere configurations $B_i \equiv Z_i$ or their direct sum for $\mu_2^2 = -2$. In this case, Z_z are $N \times N$ matrices carrying the spin $j = \frac{N-1}{2}$ UIR of $SO(3) \approx SU(2)$.

In view of these observations we consider ansätze configurations involving fuzzy two- and four- spheres with collective time dependence, which fulfill the Gauss law constraint given in (2.4.17). Tracing over the fuzzy two- and four-sphere configurations, we aim to obtain reduced models with a few phase space degrees of freedom, whose dynamics can be investigated in considerable detail.

4.2 Ansatz *I* and the Effective Action

A reasonably simple, yet non-trivial, configuration is constructed by introducing two separate collective time-dependent functions multiplying the fuzzy four- and two-sphere matrices. Concretely, we have

$$B_a = r(t)\, H_a\,, \quad B_i = y(t)\, Z_i\,, \quad B_9 = 0\,, \tag{4.2.1}$$

where $r(t)$ and $y(t)$ are real functions of time. In this ansatz, we consider a single spin-$j = \frac{N-1}{2}$ IRR of $SU(2)$ as the fuzzy S^2 configuration, while taking direct

sums of fuzzy two spheres with different IRRs of $SU(2)$, i.e. forming Z_i as a block-diagonal matrix composed of a direct sum of different IRRs of $SU(2)$ with spin less than j remains an open possibility which will be discussed later in section 4.3. Z_i exist at every matrix level, while this is not so for H_a. Fuzzy four-spheres exist at the matrix levels $4, 10, 20 \cdots$ as given by the dimension $N = \frac{1}{6}(n+1)(n+2)(n+3)$ of the IRR $(0, n)$ of $SO(5)$. Accordingly the fuzzy two-spheres are taken at the matrix levels matching these dimensions of the fuzzy-four sphere. In what follows, we initially keep the mass parameters μ_1^2 and μ_2^2 as unspecified in some of the key equations, but will investigate the detailed dynamics for $\mu_1^2 = -16$ and $\mu_2^2 = -2$, which emerge as the limiting values for the static solutions of (4.1.3) and (4.1.4) and subsequently will also briefly investigate the consequences of taking another set of values for the masses, namely $\mu_1^2 = -8$ and $\mu_2^2 = 1$ on the chaotic dynamics of the reduced models.

Substituting the (4.2.1) configuration in the action (4.1.1), we perform the trace over the fuzzy four- and two-sphere matrices at each of the matrix levels $N = \frac{1}{6}(n+1)(n+2)(n+3)$ for $n = 1, 2, \cdots, 7$. Using Matlab to evaluate the traces we obtain the Lagrangian for the reduced in the form

$$L_n = c_1 \dot{r}^2 + c_2 \dot{y}^2 - 8c_1 r^4 - c_2 y^4 - c_1 {\mu_1}^2 r^2 - c_2 {\mu_2}^2 y^2 - c_3 r^2 y^2 \,, \qquad (4.2.2)$$

where the coefficients $c_\mu = c_\mu(n)$ ($\mu = 1, 2, 3$) depend on n and their values (given up to one digit after the decimal point at most) for $n = 1, 2, \cdots, 7$ are listed in the table 4.1 given below. We suppress the label n of the coefficients $c_\mu(n)$ in (4.2.2) in order not to clutter the notation. Coefficients given for $n = 7$ in table (4.1) are evaluated by obtaining a polynomial function of n approximating[2] $c_\mu(n)$ for $n = 1, 2, \cdots, 6$ and interpolating this result to $n = 7$.

---

[2] These polynomial functions are given as

$$c_1(n) = \frac{1}{2} n(n+4)\,,$$
$$c_2(n) = \frac{1}{288}(n^6 + 12n^5 + 58n^4 + 144n^3 + 193n^2 + 132n)\,,$$
$$c_3(n) = 0.0093n^7 + 0.20n^6 + 1.35n^5 + 4.22n^4 + 6.99n^3 + 5.44n^2 + 2.43n + 0.36\,.$$

Table 4.1: $c_\mu(n)$ values for Ansatz 1 and $n = 1, \ldots, 7$

	$n=1$	$n=2$	$n=3$	$n=4$	$n=5$	$n=6$	$n=7$
c_1	2.5	6	10.5	16	22.5	30	38.5
c_2	1.9	12.4	49.9	153	391.9	881.9	1800
c_3	21	207.7	1080	3970	11691	29493	66345

The corresponding Hamiltonian is easily obtained from (4.2.2) and it is given by

$$\begin{aligned} H_n(r, y, p_r, p_y) \;&=\; \frac{p_r^2}{4c_1} + \frac{p_y^2}{4c_2} + 8c_1\, r^4 + c_2\, y^4 + c_1\, \mu_1^2 r^2 + c_2\, \mu_2^2 y^2 + c_3\, r^2 y^2 \\ &=: \frac{{p_r}^2}{4c_1} + \frac{{p_y}^2}{4c_2} + V_n(r, y)\,, \end{aligned} \tag{4.2.3}$$

where $V_n(r, y)$ denotes the potential function.

To explore the dynamics of the models governed by H_n, we first evaluate the Hamilton's equations of motion. These take the form

$$\dot{r} - \frac{p_r}{2c_1} = 0\,, \qquad \dot{y} - \frac{p_y}{2c_2} = 0\,, \tag{4.2.4a}$$

$$\dot{p_r} + 32c_1 r^3 + 2c_1\mu_1^2 r + 2c_3 r y^2 = 0\,, \tag{4.2.4b}$$

$$\dot{p_y} + 4c_2 y^3 + 2c_2\mu_2^2 y + 2c_3 r^2 y = 0\,. \tag{4.2.4c}$$

Taking the mass parameter values as $\mu_1^2 = -16$ & $\mu_2^2 = -2$, (4.2.4) becomes

$$\dot{r} - \frac{p_r}{2c_1} = 0\,, \qquad \dot{y} - \frac{p_y}{2c_2} = 0\,, \tag{4.2.5a}$$

$$\dot{p_r} + 32c_1 r^3 - 32c_1 r + 2c_3 r y^2 = 0\,, \tag{4.2.5b}$$

$$\dot{p_y} + 4c_2 y^3 - 4c_2 y + 2c_3 r^2 y = 0\,. \tag{4.2.5c}$$

In order to investigate the dynamics of these models governed by (4.2.5) in detail, it is quite useful to start the analysis by determining the fixed points corresponding to the equations of motion in (4.2.5) and addressing their stability at the linear order. The dynamical system reaches equilibrium states at the fixed points. This fact can be equivalently stated by the set of equations specified as [73, 74]

$$(\dot{r}, \dot{y}, \dot{p_r}, \dot{p_y}) \equiv (0, 0, 0, 0)\,. \tag{4.2.6}$$

Using (4.2.6) in (4.2.5) leads to four algebraic equations, two of which are trivially solved by $(p_r, p_y) \equiv (0,0)$, which means that all the fixed points are confined to the $(p_r, p_y) \equiv (0,0)$ plane in the phase space. The remaining two equations are

$$\begin{aligned} -32c_1 r^3 + 32c_1 r - 2c_3 r y^2 = 0\,, \\ -4c_2 y^3 + 4c_2 y - 2c_3 r^2 y = 0\,, \end{aligned} \tag{4.2.7}$$

and have the general set of solutions given as

$$(r, y) \equiv \{(0,0)\,, (\pm 1, 0)\,, (0, \pm 1)\,, (\pm h_1, \pm h_2)\,, (\pm h_1, \mp h_2)\}\,, \tag{4.2.8}$$

where h_1 and h_2 are given in terms of c_μ as

$$h_1 = -\sqrt{2}i\frac{\sqrt{-c_2 c_3 + 16 c_1 c_2}}{\sqrt{c_3^2 - 32 c_1 c_2}}\,, \quad h_2 = -4i\frac{\sqrt{2c_1 c_2 - c_1 c_3}}{\sqrt{c_3^2 - 32 c_1 c_2}}\,. \tag{4.2.9}$$

Clearly, only real solutions of (4.2.7) are physically acceptable. From table 4.1 it is straightforward to compute that both h_1 and h_2 are real except at $n = 1$. For $n > 1$ the set of fixed points are given as

$$\begin{aligned} (r, y, p_r, p_y) \equiv \{&(0,0,0,0), (\pm 1, 0, 0, 0)\,, (0, \pm 1, 0, 0))\,, \\ &(\pm h_1(n), \pm h_2(n), 0, 0)\,, (\pm h_1(n), \mp h_2(n), 0, 0)\}\,, \end{aligned} \tag{4.2.10}$$

where the values of h_1 and h_2 are presented in the table 4.2 below

Table 4.2: h_1 and h_2 values for $n = 2, \ldots, 7$

	$n=2$	$n=3$	$n=4$	$n=5$	$n=6$	$n=7$
h_1	0.26	0.28	0.27	0.26	0.24	0.23
h_2	0.6	0.38	0.25	0.17	0.12	0.093

while for the $n = 1$ model we only have

$$(r, y, p_r, p_y) \equiv \{(0,0,0,0)\,, (\pm 1, 0, 0, 0)\,, (0, \pm 1, 0, 0)\}\,, \tag{4.2.11}$$

as the fixed points.

Let us note that (4.2.8) corresponds to the critical points of the potential V_n, since (4.2.7) are the equations determining the extrema of the latter. From the eigenvalues

of the matrix $\frac{\partial^2 V_n}{\partial g_i \partial g_j}$, $(g_1, g_2) \equiv (r, y)$, we see that the points $(\pm 1, 0)$ and $(0\,, \pm 1)$ are local minima, $(0, 0)$ is a local maximum, while $(\pm h_1(n), \pm h_2(n))$, $(\pm h_1(n), \mp h_2(n))$ are all saddle points of V_n. Evaluating V_n at the local minima, we find $V_n(\pm 1, 0) = -8c_1$ and $V_n(0, \pm 1) = -c_2$. From table 4.1, we easily conclude that $(\pm 1, 0)$ is the absolute minimum of V_n for $n = 1, 2, 3$, while $(0, \pm 1)$ is the absolute minima for the models with $n = 4, 5, 6$. From now on we add to the Hamiltonian's, H_n, the constant term $8c_1$ for $n = 1, 2, 3$, and c_2 for $n = 4, 5, 6$, respectively, to shift the minimum value of the potentials V_n to zero and use the notation

$$H_{n<4} = H_n + 8c_1\,, \quad H_{n\geq 4} = H_n + c_2\,. \tag{4.2.12}$$

Fixed point energies are readily evaluated using (4.2.10), (4.2.11) and the mass squared values $\mu_1^2 = -16$ and $\mu_2^2 = -2$ in the Hamiltonian's $H_{n<4}$, $H_{n\geq 4}$ and they are

$$\begin{aligned} E_F(0,0,0,0) &= 8c_1\,, & E_F(\pm 1,0,0,0) &= 0\,, \\ E_F(0,\pm 1,0,0) &= 8c_1 - c_2\,, & 1 \leq n &\leq 3\,, \end{aligned} \tag{4.2.13a}$$

$$\begin{aligned} E_F(0,0,0,0) &= c_2\,, & E_F(\pm 1,0,0,0) &= c_2 - 8c_1\,, \\ E_F(0,\pm 1,0,0) &= 0\,, & 4 \leq n &\leq 6\,. \end{aligned} \tag{4.2.13b}$$

Table 4.3: Fixed point energies for $n = 2, \ldots, 7$

	$n=2$	$n=3$	$n=4$	$n=5$	$n=6$	$n=7$
$E_F(\pm h_1(n), \pm(\mp) h_2(n), 0, 0)$	39.4	70.2	134.6	368.9	854.2	1767.7

4.2.1 Linear Stability Analysis in the Phase Space

It must be clear that the properties of extrema of V_n does not provide sufficient information to decide on the stability of the fixed points. We now perform a first order stability analysis around the fixed points of H_n given in (4.2.10) and (4.2.11). Together with the Lyapunov spectrum and the Poincare sections that will be determined in the next subsection, this analysis, will allow us to comment on the outset and variation of chaos, that is, the increase and decrease in the amount of chaotic orbits in the phase spaces of H_n, with respect to energy.

For the phase space coordinates, it is useful to introduce the notation

$$(g_1, g_2, g_3, g_4) \equiv (r, y, p_r, p_y)\,. \tag{4.2.14}$$

From g_α and $\dot{g}_\alpha$, we may form the Jacobian matrix

$$J_{\alpha\beta} \equiv \frac{\partial \dot{g}_\alpha}{\partial g_\beta}\,, \tag{4.2.15}$$

whose eigenvalue structure allows us to decide on the stability character of the fixed points [75]. Written in explicit form, we have

$$J(r,y) \equiv \begin{pmatrix} 0 & 0 & \frac{1}{2c_1} & 0 \\ 0 & 0 & 0 & \frac{1}{2c_2} \\ J_{31} & -2c_3 ry & 0 & 0 \\ -2c_3 ry & J_{42} & 0 & 0 \end{pmatrix}\,, \tag{4.2.16}$$

where J_{31} and J_{42} are

$$\begin{aligned} J_{31} &= 32c_1 - 96c_1 r^2 - 2c_3 y^2\,, \\ J_{42} &= 4c_2 - 12c_2 y^2 - 2c_3 r^2\,. \end{aligned} \tag{4.2.17}$$

Eigenvalues of $J(r,y)$ at the fixed points (4.2.10) are easily evaluated and listed in the table 4.4 below.

Table 4.4: Eigenvalues of the fixed points for Ansatz 1

Fixed Points	Eigenvalues of $J(r,y)$
$(0,0,0,0)$	$\pm 4, \pm\sqrt{2}$
$(\pm 1,0,0,0)$	$(\pm 4i\sqrt{2}, \pm i\frac{\sqrt{c_3 c_2 c_1^2 - 2c_2^2 c_1^2}}{c_1 c_2})$
$(0,\pm 1,0,0)$	$(\pm 2i, \pm i\frac{\sqrt{c_3 c_1 c_2^2 - 16 c_1^2 c_2^2}}{c_1 c_2})$
$(h_1(2), h_2(2), 0, 0)$	$(\pm 2.5, \pm i 3.2)$
$(h_1(3), h_2(3), 0, 0)$	$(\pm 2.9, \pm i 3.4)$
$(h_1(4), h_2(4), 0, 0)$	$(\pm 3.1, \pm i 3.5)$
$(h_1(5), h_2(5), 0, 0)$	$(\pm 3.1, \pm i 3.5)$
$(h_1(6), h_2(6), 0, 0)$	$(\pm 3.2, \pm i 3.5)$

General criterion of the linear stability analysis states that a fixed point is stable if all the real eigenvalues of the Jacobian are negative, and unstable if the Jacobian has

at least one real positive eigenvalue [75, 76]. It may that all the eigenvalues of the Jacobian matrix are imaginary. This is called the borderline case and an analysis beyond first order is necessary to decide if the system is stable or unstable at such a point. Accordingly, we see that $(0, 0, 0, 0)$ and $(h_1(n), h_2(n), 0, 0)$ are all unstable fixed points as the corresponding Jacobian's have at least one real positive eigenvalue, as readily seen from the table 4.4. From the same table and the values of $c_\mu(n)$ given in table (4.1), we see that $(\pm 1, 0, 0, 0)$ and $(0, \pm 1, 0, 0)$ are borderline cases. We are not going to explore the structure of these borderline fixed points any further, as we expect that their impact on the chaotic dynamics should be rather small compared to those of the unstable fixed points which we just identified at the linear level. Our numerical results on the Lyapunov spectrum indeed corroborates with this expectation as will be discussed shortly.

4.2.2 Chaotic Dynamics

4.2.2.1 Lyapunov Spectrum

In order to probe the presence and analyze the structure of chaotic dynamics of the models described by the Hamiltonian's H_n, we will examine their Lyapunov spectrum. A detailed description of the technique used to compute the Lyapunov exponents is included in appendix J. In a dynamical system, presence of at least one positive Lyapunov exponent is sufficient to conclude the presence of chaotic motion. In Hamiltonian systems, due to the symplectic structure of the phase space, Lyapunov exponents appear in λ_i and $-\lambda_i$ pairs, a pair of the Lyapunov exponents vanishes as there is no exponential growth in perturbations along the direction of the trajectory specified by the initial condition and sum of all the Lyapunov exponents is zero as a consequence of the Liouville's theorem. These facts are well-known and their details may be found in many of the excellent books on chaos [75, 77].

In order to obtain the Lyapunov spectrum for our models we run a Matlab code, which numerically solves the Hamilton's equations of motion in (4.2.5) for all H_n $(1 \leq n < 7)$ at several different values of the energy. We run the code 40 times with randomly selected initial conditions satisfying a given energy and calculate the mean of the time series for all runs for each of the Lyapunov exponents at each value

of n. In order to give certain effectiveness to the random initial condition selection process we developed a simple approach which we briefly explain next. Let us denote a generic set of initial conditions at $t = 0$ by $(r(0), y(0), p_r(0), p_y(0))$. For $H_{n<4}$ we take $y(0) = 0$ and for $H_{n\geq 4}$, $r(0) = 0$ as part of the initial condition and subsequently generate three random numbers ω_i $(i = 1, 2, 3)$ and define $\Omega_i = \frac{\omega_i}{\sqrt{\omega_i^2}}\sqrt{E}$ for a given energy E of the system, so that $E = \Omega_i^2 = \Omega_1^2 + \Omega_2^2 + \Omega_3^2$. Subsequently, we take positive roots in the expressions[3]

$$p_r(0) = \sqrt{4c_1\Omega_1^2}\,, \quad p_y(0) = \sqrt{4c_2\Omega_2^2}\,, \tag{4.2.18}$$

and the real roots of

$$\begin{aligned} 8c_1r^4(0) - 16c_1r^2(0) + 8c_1 - \Omega_3^2 = 0 \quad &\text{for} \quad H_{n<4} \\ c_2y^4(0) - 2y^2(0) + c_2 - \Omega_3^2 = 0 \quad &\text{for} \quad H_{n\geq 4}\,, \end{aligned} \tag{4.2.19}$$

where in the last step of the process our code randomly selects from the available real roots of the equations (4.2.19). In the computations we use a time step of 0.25 and run the code for a sufficient amount of computer time to clearly observe the values that the Lyapunov exponents converge to. We present sample plots for these time series of Lyapunov exponents at each value of n in the following pages. From the figures 4.2, chaotic dynamics of the models are clearly observed, as in each case (except in figure 4.2b) a positive Lyapunov exponent is present. We also observe that the properties of Lyapunov spectrum for Hamiltonian systems summarized at the end of the first paragraph of this section are readily satisfied. Let us immediately note that the model at $n = 1$ have distinct features from the rest. This is already observed from the first two plots (figures 4.2a and 4.2b); for $E = 30$ there is a positive Lyapunov exponent, while at $E = 500$ all the Lyapunov exponents appear to be converging to zero indicating that very little chaos remains at this energy. The distinct features of the $n = 1$ model will also be seen in the ensuing discussions.

In order to see the dependence of the mean largest Lyapunov exponent (MLLE), (denoted as λ_n in figures and tables) to energy, we obtain the MLLE at several different values of energy in a range, which appears to be best suited to observe the onset and progression of chaotic dynamics in these models. As may be expected, the energies

[3] We have checked that randomly selecting positive and negative roots in (4.2.18) does not cause any significant impact on our results.

determined for the unstable fixed points in the previous section are of central importance here. From the figures 4.4, we see that appreciable amount of chaotic dynamics starts to develop once the energy of the systems exceeds the energy E_F of the models at the fixed points $(\pm h_1(n), \pm(\mp)h_2(n), 0, 0)$. The onset of the chaotic dynamics as observed from progression of the MLLE values with increasing energy is highlighted by the blow-up figures provided in the insets of the plots in figures 4.4. Error bars at each data point is found by evaluating mean square error using MLLE and the LLE values of each of the 40 runs.

Table 4.5: α_n and β_n values for the fitting curve (4.2.20)

$\lambda_i(E)$	α_n	β_n
$\lambda_2(E)$	1.7	-8.5
$\lambda_3(E)$	2.4	-18.2
$\lambda_4(E)$	2.9	-32.0
$\lambda_5(E)$	3.4	-63.8
$\lambda_6(E)$	3.69	-101.9
$\lambda_7(E)$	4.3	-180.4

Several observations can be made from these numerical results. Firstly, we see that in the $n = 1$ model the MLLE acquires a peak value of about ≈ 0.55 at an energy around ≈ 32 and rapidly decreases toward zero with increasing energy. From the profile of MLLE with respect to energy in figure 4.4a as well as the time series plot (4.2b) of the model at $E = 500$, we conclude that this model is not chaotic for energies $E \geq 500$. These conclusions are also fully supported by the Poincaré sections given in figures 4.3.

In order to elaborate on the data obtained for the MLLE values, it is useful to explore the dependence of the LLEs at a given level n with respect to the energy. We find that the function

$$\lambda_n(E) = \alpha_n + \beta_n \frac{1}{\sqrt{E}}\,, \tag{4.2.20}$$

gives not perfect but essentially very good fits to our data as can be seen from the figures 4.4. For consistency, we consider the fits to the data starting from the energies

corresponding to an MLLE value[4] of ≈ 0.1. The coefficients for the fits are provided in the table 4.5. Extrapolating these fits, we find that the energies at which the MLLE vanish are given approximately as $25, 58, 122, 352, 799, 1760$ for $n = 2, 3, 4, 5, 6, 7$, respectively. We find that these are somewhat less than the E_F's given in table 4.3. As previously noted, the latter are marking the onset of chaotic dynamics in our models and the comparatively lower values of energy found for vanishing MLLE is expected and consistent with this fact. Results of this extrapolation appear to be also consistent with the Poincaré sections obtained at nearby energies as can be seen from the figures 4.3. We may use (4.2.20) to compare the relative rate at which the chaotic dynamics tends to develop once the systems reach their respective fixed point energies in table 4.3. Defining

$$R_n := \left.\frac{d\lambda_n(E)}{dE}\right|_{E_F} = -\beta_n \frac{1}{2E_F^{3/2}}\,, \tag{4.2.21}$$

as the quantity measuring this relative rate, we find that R_n takes on the values 0.017, 0.015, 0.010, 0.005, 0.002, 0.0012 for $n = 2, 3, 4, 5, 6, 7$, respectively. Thus, as n increases, R_n values indicate a slow decrease in the rate at which MLLE increases with energy. This suggests that the models at low values of n become chaotic somewhat more rapidly. It is also interesting to note that MLLE values show essentially the same functional relationship with the energy, as that was found in the Yang-Mills 5-matrix models with a mass term, which was studied in [20].

Let us also remark on a feature of the models $H_{n\geq 4}$ which is observed from the plots in figures 4.4d - 4.4g at energies $E \gtrapprox 2500$. We see that for a range of energy values in these models there is an observable decrease in the value of MLLE and the mean square errors appear to be considerably larger than those computed for the rest of the data points. A closer analysis of the Lyapunov time series at these data points reveal that LLE values of less than a quarter of the 40 initial conditions approach to zero, leading to the observed decrease in MLLE values and the increase in the mean square errors. From a physical point of view, approach of some of the LLE values to zero implies that the systems' development in time, starting from these initial conditions are of either periodic or quasi-periodic type and not chaotic. Nevertheless, the overall MLLE values are still quite large and the sample Poincaré sections taken at one of

[4] The numerically determined best fits to the functional form (4.2.20) do not necessary start at MLLE ≈ 0.1. They actually start somewhat above this MLLE value; In the figures 4.4, the best fits are extrapolated to start at MLLE ≈ 0.1.

these energies are densely chaotic, showing no sign of KAM tori signaling the presence of quasi-periodic orbits. Thefore, we are inclined to think that such periodic or quasi-periodic orbits occur only at comparatively very small regions of the phase space and evaluated the MLLE values at these energies by excluding the initial conditions leading to vanishing LLE. The results of MLLE obtained this way are given in the plots in the figures 4.4d - 4.4g in yellow color for comparison and used to obtain the fits given in the table 4.5.

4.2.2.2 Poincaré Sections

In order to supplement the results of the previous subsubsection, we have obtained the Poincaré sections at several different values of the energy. For each model we plot the Poincaré sections at energies below, around and above the energy of unstable the fixed points $(\pm h_1(n), \pm(\mp)h_2(n), 0, 0)$ to visualize how the phase spaces trajectories develop and capture the onset of chaotic dynamics. As in the calculation of Lyapunov spectrum we use 40 randomly selected initial conditions for each model at a given energy and the same procedure as in the analysis of the Lyapunov spectrum is followed. For $H_{n<4}$, $y(0) = 0$ is a part of the initial conditions and for $H_{n\geq 4}$, $r(0) = 0$ is so, therefore it is convenient to look at the Poincaré sections on the $r - p_r$-plane and the $y - p_y$-plane, respectively in these cases. Our plots for $n = 1, \ldots, 6$ cases are given in figures 4.3.

4.2.3 Other Mass Values

We now consider assigning different values to the mass parameters and their impact on the dynamics of our models. Let us first note that $\mu_1^2 = -16$ and $\mu_2^2 = -2$ is a suitable and immediate guiding choice for the mass values due to the reasons discussed around equations (4.1.3) and (4.1.4), but surely not canonical in the sense that they are not enforced on us by the full set of equations of motion (4.1.2). Considering Chern-Simons-type terms, i.e. a cubic term in B_i's as in the BMN model and a fifth order term in B_a's [34] alter the equations of motion given in (4.1.3) and (4.1.4) and lead to solutions with $\mu_1^2 > -16$ and $\mu_2^2 > -2$. It is not our aim in this subsection to provide a detailed analysis of such possibilities, but simply confine ourselves to examining another choice for the mass values and to serve this purpose we take

$\mu_1^2 = -8$ and $\mu_2^2 = 1$.

With the Lagrangian and Hamiltonian given in the form (4.2.2) and (4.2.3) and the corresponding Hamilton's equations given as in (4.2.4), we find that the fixed points of the phase space are

$$(r, y, p_r, p_y) = \{(0,0,0,0)\,, (\pm\frac{1}{\sqrt{2}}, 0, 0, 0)\} \tag{4.2.22}$$

with the corresponding energies

$$E_F(0,0,0,0) = 2c_1 = n(n+4)\,, \quad E_F(\pm\frac{1}{\sqrt{2}}, 0, 0, 0) = 0\,. \tag{4.2.23}$$

Linear stability analysis shows that $(0,0,0,0)$ is an unstable fixed point while $(\pm\frac{1}{\sqrt{2}}, 0, 0, 0)$ are of the borderline type that we encountered previously and play no significant role in the numerical analysis that follows next. For convenience of comparison to numerical data for $n = 1\,, \cdots 6$, the fixed point energies are given in the same order as $12, 21, 32, 45, 60, 77$.

Following the same steps of the numerical analysis for the Lyapunov spectrum as outlined previously, we find that, in this case too, the models exhibit chaotic dynamics for $n = 2, 3, 4, 5, 6$, while the model at the level $n = 1$ is essentially not chaotic for energies $E \gtrapprox 100$, but retain some chaos only in a narrow band of energy from around $E \approx 12$ (i.e. the fixed point energy) to $E \gtrapprox 100$ (See the figures 4.7). The transition to chaos for $n = 2, 3, 4, 5, 6$ appears to happen around the fixed point energies as can be clearly seen from the blow-up insets of these figures and the time series plots given in figures 4.5. This fact is also captured by inspecting the Poincaré sections taken at energies somewhat below and above those of the fixed points.

In contrast to the previous case, MLLE values fluctuate and the mean square errors are comparatively larger at a narrow band of energies after E_F. Due to this reason, for each model, we consider fits to the data starting at end of this transient band, where the change in MLLE with respect to energy starts to settle in a steady pattern of development and do not attempt to extrapolate them all the way to zero MLLE value as it would clearly be misleading to do so. We find that a logarithmic fit of the form

$$\lambda_n(E) = \tilde{\alpha}_n + \tilde{\beta}_n \log(E)\,, \tag{4.2.24}$$

with

Table 4.6: $\tilde{\alpha}_n$ and $\tilde{\beta}_n$ values for the fitting curve (4.2.24)

	$\tilde{\alpha}_n$	$\tilde{\beta}_n$
$\lambda_2(E)$	-0.84	0.34
$\lambda_3(E)$	-0.79	0.35
$\lambda_4(E)$	-0.81	0.37
$\lambda_5(E)$	-2.19	0.56
$\lambda_6(E)$	-2.47	0.58

appears to be well-suited to model the dependence of MLLE to energy after transient band is passed. Let us also note that within the transient band of energies, chaotic and quasi-periodic motion coexist, this is clearly seen from those of the Poincaré sections in figure 4.6 that are taken at energies somewhat above the E_F. Using (4.2.24) we have

$$\tilde{R}_n = \frac{\tilde{\beta}_n}{E_F}\,, \tag{4.2.25}$$

measuring the relative rate of the development of chaos at E_F. We find that R_n takes the values $0.016, 0.011, 0.008, 0.009, 0.007$ for $n = 2, 3, 4, 5, 6$, respectively, which essentially indicates that there is not any significant difference at the rate in which chaos develops in these models once the systems have energies around those of the fixed points.

4.3 Ansatz *II*

We would like to briefly discuss the consequences of changing the fuzzy two sphere part of ansatz *I*. Namely, we consider the configurations

$$B_a = r(t)\, H_a\,, \quad B_i = y(t)\, Z_i\,, \quad B_9 = 0\,, \tag{4.3.1}$$

at the matrix levels $N = \frac{1}{6}(n+1)(n+2)(n+3)$ for $n = 2, 3, 5$. In (4.3.1), H_a are the same as in ansatz *I*, while we take $Z_i = \oplus_{k=1}^{K_n} \Sigma_i(k)$, with $\Sigma_i(k)$ spanning the spin $\frac{1}{2}$ UIR of $SU(2)$, in the k^{th} block of the direct sum and K_n is the number of 2×2 blocks, which are $5, 10, 28$ for $n = 2, 3, 5$, respectively. Thus, we have a direct sum of 2×2 fuzzy two spheres.[5] We call this the ansatz *II*.

[5] For odd values of N, it is not possible to form Z_i's by 2×2 blocks only. In this case we can fill the last block of the matrices simply with the 0-matrix, i.e. the trivial representation of $SU(2)$.

The Lagrangian and Hamiltonian are given in the same form as in (4.2.2) and (4.2.3), where now the coefficients c_β are given in the table 4.7

Table 4.7: $c_\mu(n)$ values for Ansatz 2 and $n = 2, 3, 5$

	$n=2$	$n=3$	$n=5$
c_1	6	$21/2$	$45/2$
c_2	$3/8$	$3/8$	$3/8$
c_3	7	11.45	3.44

Corresponding fixed points and their energies are

$$(r, y, p_r, p_y) \equiv \{(0,0,0,0), (\pm 1,0,0,0), (0,\pm 1,0,0)\}, \tag{4.3.2}$$

$$E_F(0,0,0,0) = 8c_1,\ E_F(\pm 1,0,0,0) = 8c_1 - c_2,\ E_F(0,\pm 1,0,0) = 0. \tag{4.3.3}$$

Linear stability analysis reveals that $(0,0,0,0)$ is the only unstable fixed point in these models.

We have numerically studied the Lyapunov spectrum at several different values of the energy in these systems and determined that for an interval starting around the fixed point energies $E_F = 48, 84, 180$, respectively and going up to ≈ 500 for the first two cases and ≈ 1000 for $n = 5$, there is a positive Lyapunov exponent indicating the presence of chaotic motion. From the times series plots in figure 4.8 and the Poincaré sections in figure 4.9 taken at energies within these ranges, we see that chaos is not dense, coexists together with quasi periodic motion and remains local in the phase space. At higher energies chaos ceases to exist and the phase space becomes dominated by periodic and/or quasi-periodic orbits.

4.4 Effective Action with Single Time-Dependence

While specifying the fuzzy two- and four-sphere configurations of Ansatz *I* given in (4.2.1), we have introduced two real functions with collective time dependence, namely $r(t)$ and $y(t)$. In this section, we examine the dynamics of motion when $r(t)$ is taken to be equal to $y(t)$. Let us keep the values of mass parameters as $\mu_1^2 = -8$

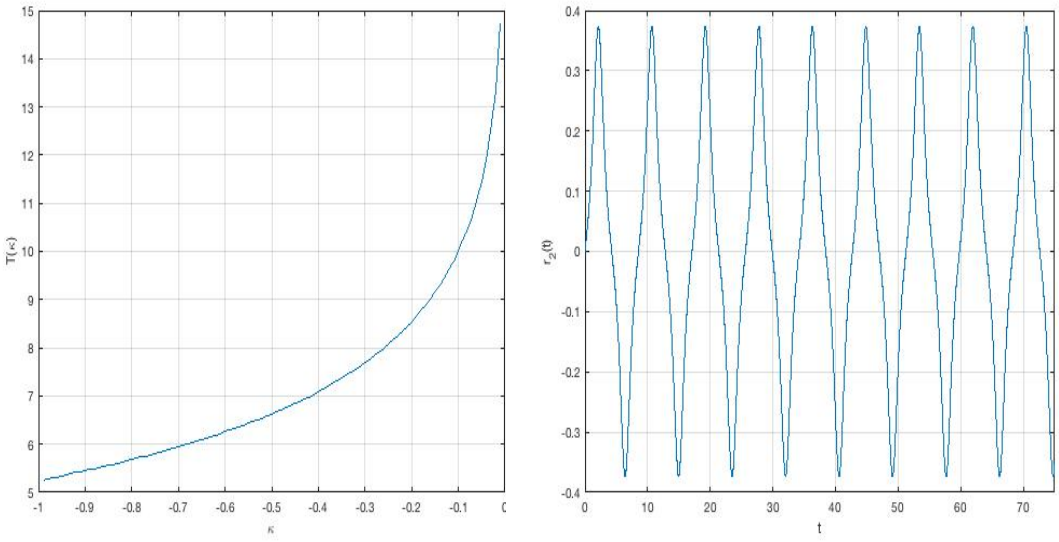

(a) $T(\kappa)$ vs. κ (b) $r_2(t)$ vs. time

Figure 4.1: $T(\kappa)$ vs. κ and $r_2(t)$ vs. time

and $\mu_2^2 = 1$, i.e. as selected in subsection 4.2.3. In this case, (4.2.2) becomes

$$\widetilde{L}_n(r, \dot{r}) = (c_1 + c_2)\dot{r}^2 - (8c_1 + c_2 + c_3)r^4 + (8c_1 - c_2)r^2 - 2\,c_1\,, \tag{4.4.1}$$

from which the Lagrange's equations of motion can be determined as follows

$$\ddot{r}(t) = -e_1 r^3 + e_2 r\,, \tag{4.4.2}$$

where e_1 and e_2 are explicitly given by

$$e_1 = \frac{2(8c_1 + c_2 + c_3)}{c_1 + c_2}, \quad e_2 = \frac{8c_1 - c_2}{c_1 + c_2}\,. \tag{4.4.3}$$

As a concrete example, let us take initial conditions as $r(0) = 0\,,\, \dot{r}(0) = 0.1$, the general solution of (4.4.2) can be written in terms of the Jacobi elliptic function sn of modulus k, denoted by $sn(z|k)$

$$r(t) = (\epsilon - i\zeta)sn((\epsilon + i\phi)t| - \eta)\,, \tag{4.4.4}$$

where ζ, ϕ, η are positive real numbers and ϵ is a real number which is very close to zero. A review of some properties of Jacobi elliptic functions can be found in appendix H. For all practical purposes, ϵ can be considered to be equal to zero. Moreover, for the sake of simplicity, let us concentrate on the case of unit frequency

($\phi = 1$) and redefine the elliptic modulus as $\kappa = -\eta$. Applying these changes to equation (4.4.4) yields

$$r(t) = -i\,\zeta sn(it|\kappa). \tag{4.4.5}$$

The complete elliptic integral of the first kind is defined by [78]

$$K(k) = \int_0^{\frac{\pi}{2}} \Big(1 - k^2 sin^2(\theta)\Big)^{-\frac{1}{2}} d\theta, \tag{4.4.6}$$

with $0 \leq k < 1$. The complementary elliptic modulus is defined by $k_c = (1-k^2)^{\frac{1}{2}}$. For the interval of $-2K\big(k_c\big) < t < 2K\big(k_c\big)$, Jacobi's imaginary transformations relate the elliptic functions with complex arguments to the elliptic functions with real arguments. For the case of sn, we have

$$sn(it|k) = \frac{isn(t|k_c)}{cn(t|k_c)}\,, \tag{4.4.7}$$

where $cn\big(t|k_c\big)$ is the Jacobi elliptic function cn of modulus k_c. As an immediate consequence of (4.4.7), for the time interval of $-2K_c < t < 2K_c$, equation (4.4.5) can be put in the form

$$r = \zeta \frac{sn(t|\kappa_c)}{cn(t|\kappa_c)}\,, \tag{4.4.8}$$

with $\kappa_c = \sqrt{1-\kappa^2}$ and $K_c = K(\kappa_c)$.

Let us denote with T the period of (4.4.5). The calculations of the T values for the range of modulus values $0 > \kappa > -1$ were performed utilizing a MATLAB script and graphed in figure 4.1a. Since the numerical values (given up to two significant digits after the decimal point at most) of the c_μ coefficients for the model at the level $n = 2$ are given by

$$c_1 = 6\,, \quad c_2 = 12.38\,, \quad c_3 = 207.66\,, \tag{4.4.9}$$

and e_α coefficients of (4.4.3) take the values

$$e_1 = 29.17, \quad e_2 = 1.94\,, \tag{4.4.10}$$

(4.4.2) takes the form

$$\ddot{r_2} = -29.17\,{r_2}^3 + 1.94\,r_2\,, \tag{4.4.11}$$

whose solution can be written as

$$r_2(t) = -i\,0.071\,sn(i\,1.42\,t| - 0.036)\,. \tag{4.4.12}$$

Using Mathematica it can be verified that the maximum value of the imaginary part of $r_2(t)$ is on order of 10^{-13}. Therefore, the imaginary part of $r_2(t)$ may be ignored for practical purposes, and we may write

$$r_2(t) \cong Re[-i\,0.071\,sn(i\,1.42\,t| - 0.036)]\,. \tag{4.4.13}$$

A graph of $r_2(t)$ versus time is shown in figure 4.1b. By reading the numerical value of $T(\kappa = -0.036)$, which corresponds to the period of $-i\,sn(i\,t| - 0.036)$, from figure 4.1a, the period of $r_2(t)$ can be computed as

$$T_2 = \frac{T(-0.036)}{1.42} = \frac{12.11}{1.42} = 8.53\,. \tag{4.4.14}$$

Summarizing the above considerations, choosing collective time dependence in terms of a single function $r(t)$ results in periodic motion whose variation in time can be completely described by the Jacobi elliptic function sn.

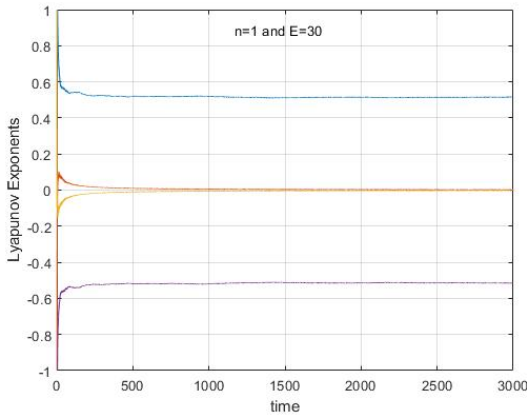

(a) $n = 1$ and $E = 30$

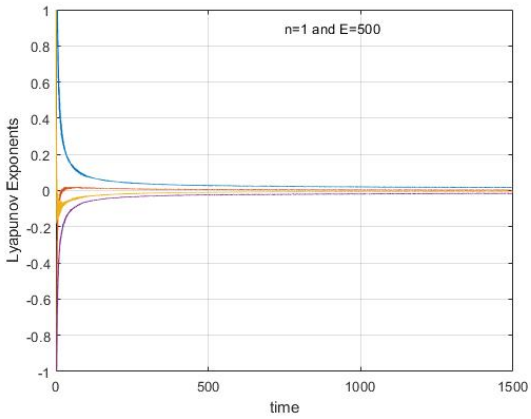

(b) $n = 1$ and $E = 500$

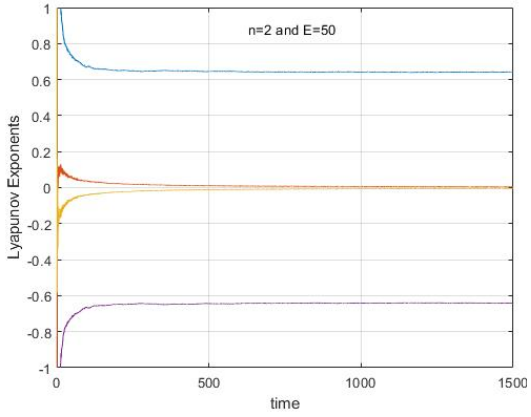

(c) $n = 2$ and $E = 50$

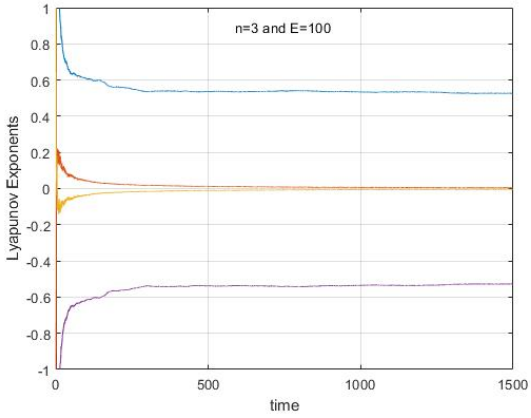

(d) $n = 3$ and $E = 100$

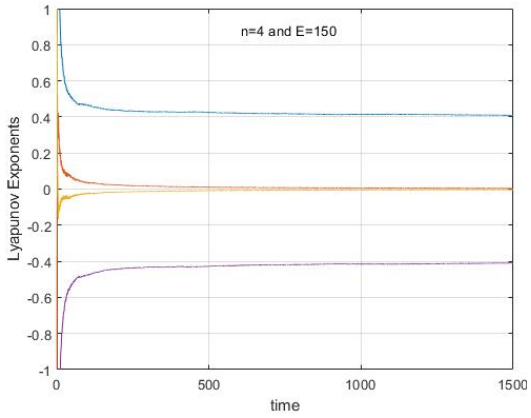

(e) $n = 4$ and $E = 150$

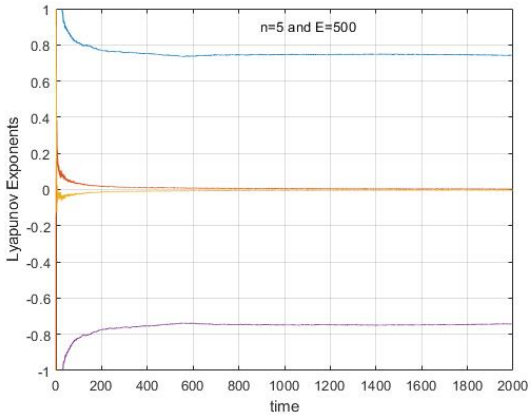

(f) $n = 5$ and $E = 500$

Figure 4.2: Lyapunov exponents vs. time for Ansatz 1 at $\mu_1^2 = -16$ and $\mu_2^2 = -2$

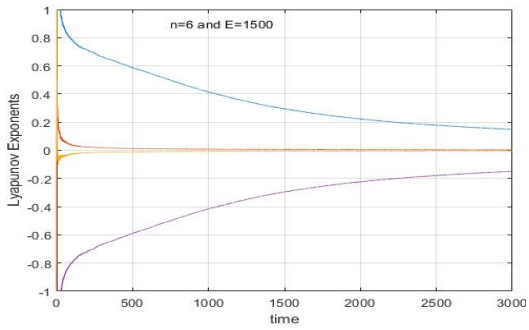

(g) $n = 6$ and $E = 1500$

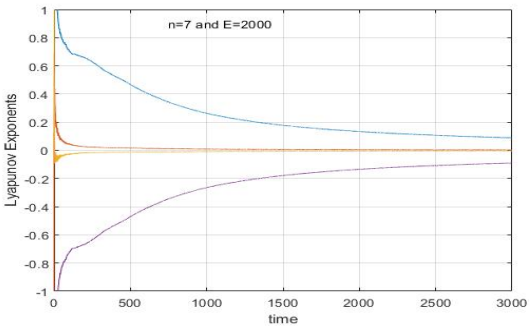

(h) $n = 7$ and $E = 2000$

Figure 4.2: Lyapunov exponents vs. time for Ansatz 1 at $\mu_1^2 = -16$ and $\mu_2^2 = -2$

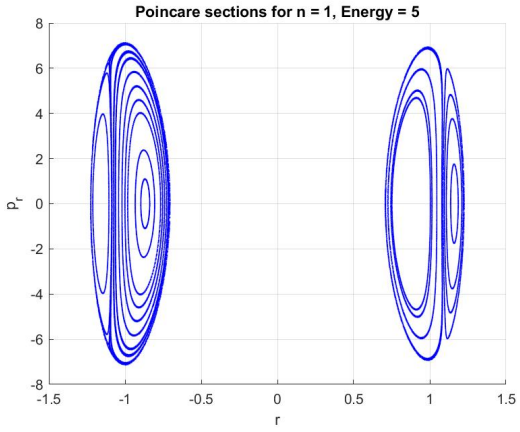

(a) $n = 1$ and $E = 5$

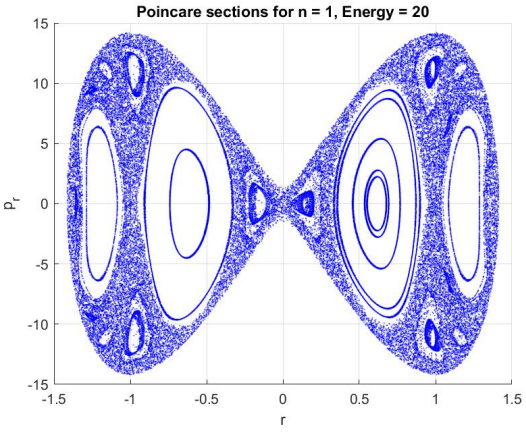

(b) $n = 1$ and $E = 20$

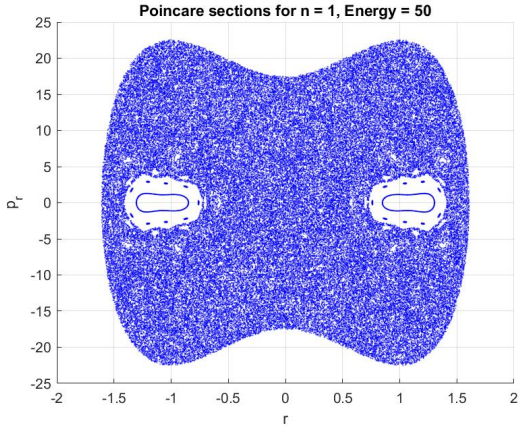

(c) $n = 1$ and $E = 50$

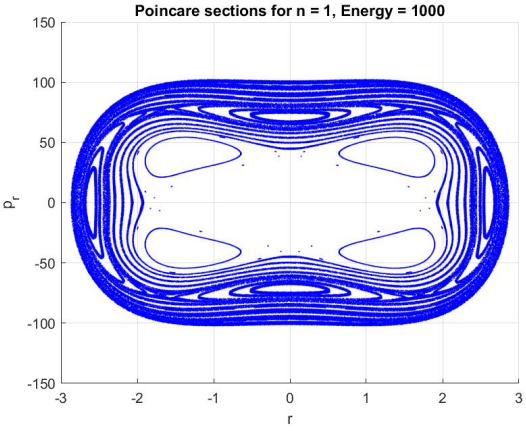

(d) $n = 1$ and $E = 1000$

Figure 4.3: Poincaré Sections for Ansatz 1 at $\mu_1^2 = -16$ and $\mu_2^2 = -2$

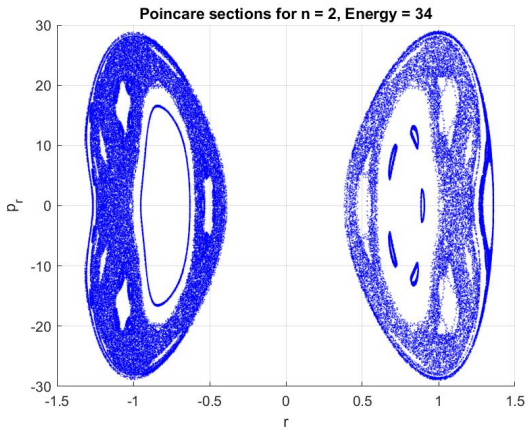

(e) $n = 2$ and $E = 34$

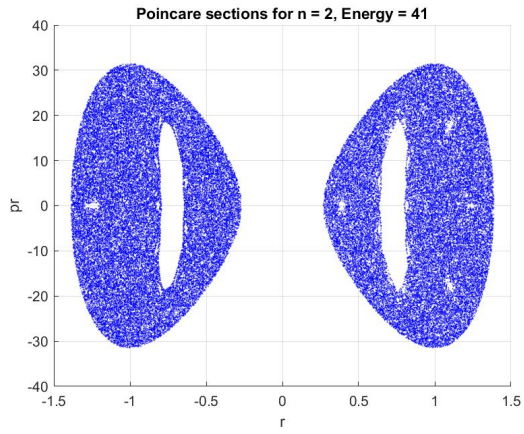

(f) $n = 2$ and $E = 41$

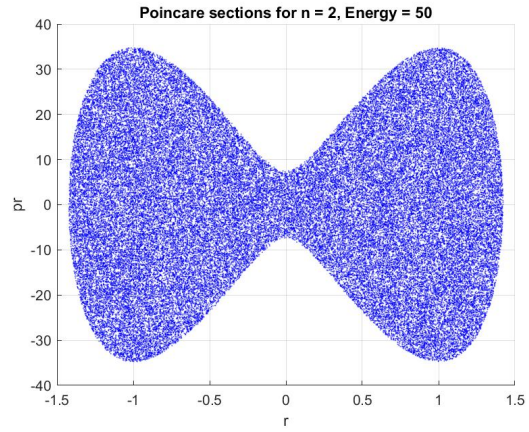

(g) $n = 2$ and $E = 50$

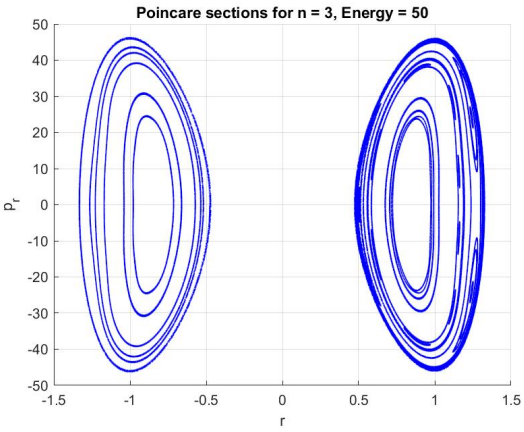

(h) $n = 3$ and $E = 50$

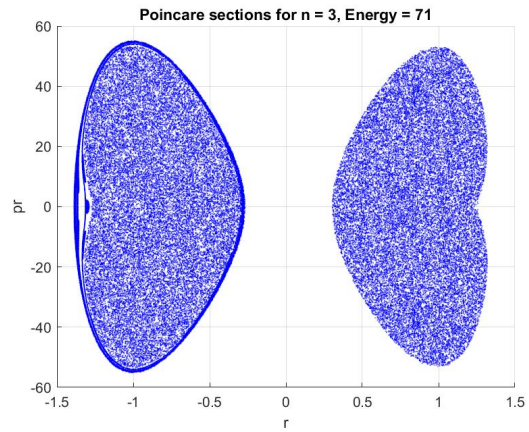

(i) $n = 3$ and $E = 71$

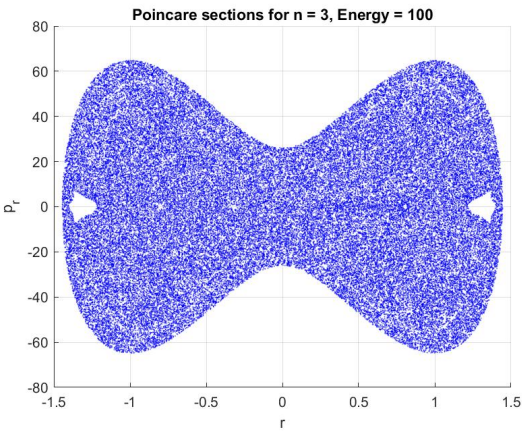

(j) $n = 3$ and $E = 100$

Figure 4.3: Poincaré Sections for Ansatz 1 at $\mu_1^2 = -16$ and $\mu_2^2 = -2$

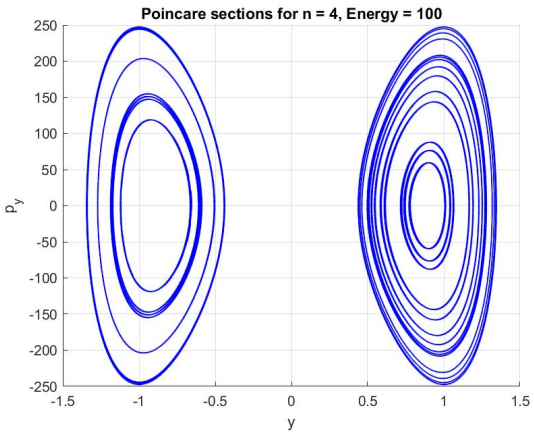

(k) $n = 4$ and $E = 100$

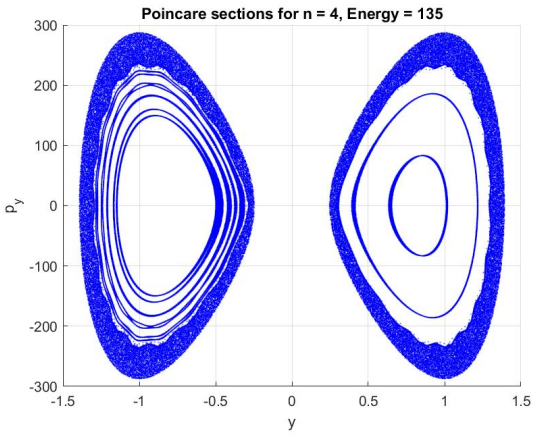

(l) $n = 4$ and $E = 135$

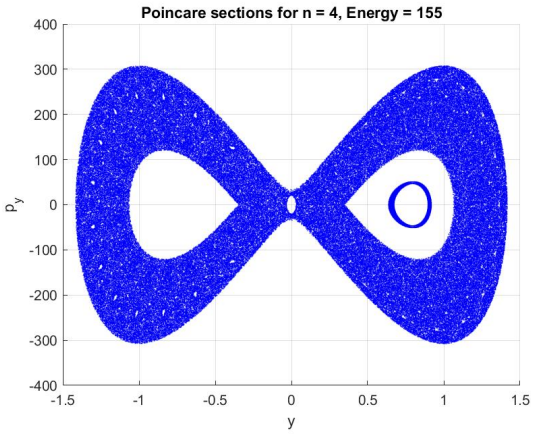

(m) $n = 4$ and $E = 155$

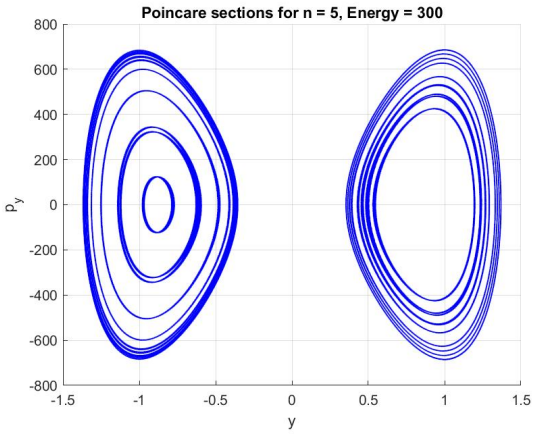

(n) $n = 5$ and $E = 300$

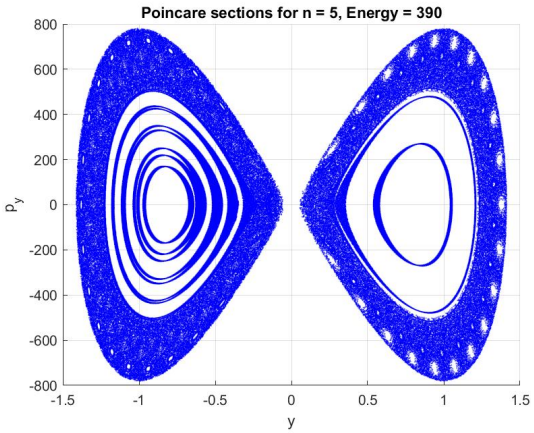

(o) $n = 5$ and $E = 390$

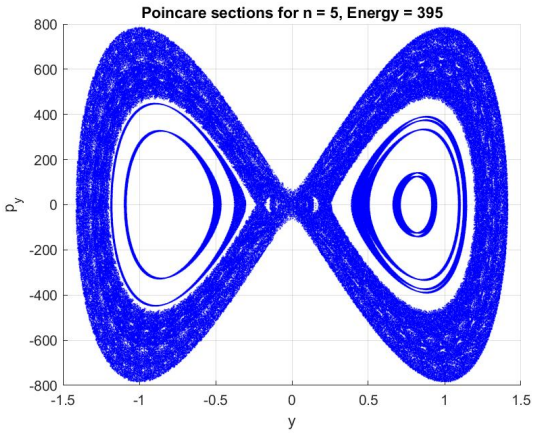

(p) $n = 5$ and $E = 395$

Figure 4.3: Poincaré Sections for Ansatz 1 at $\mu_1^2 = -16$ and $\mu_2^2 = -2$

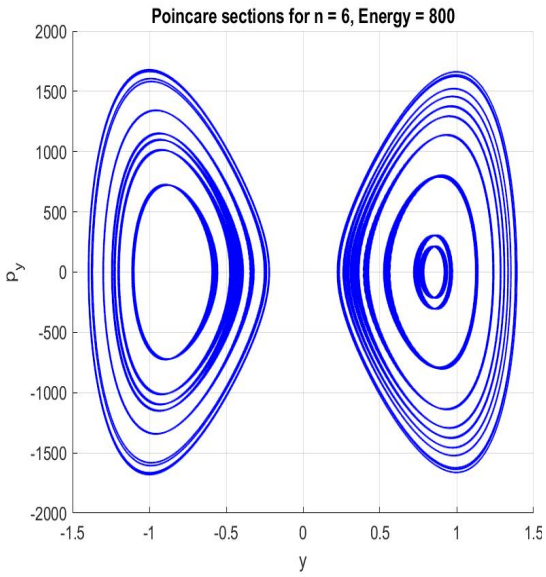

(q) $n = 6$ and $E = 800$

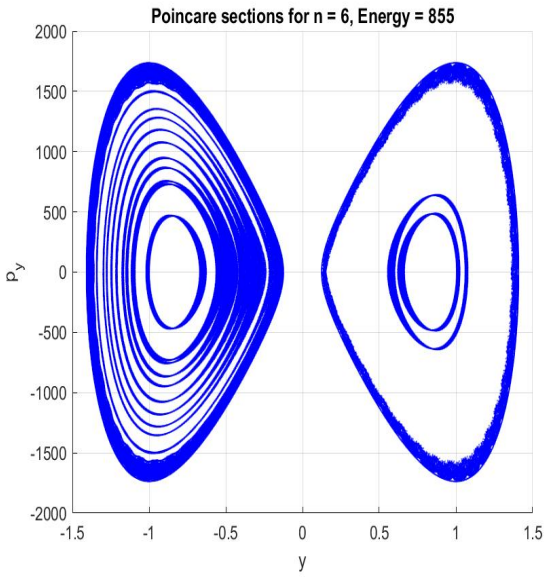

(r) $n = 6$ and $E = 855$

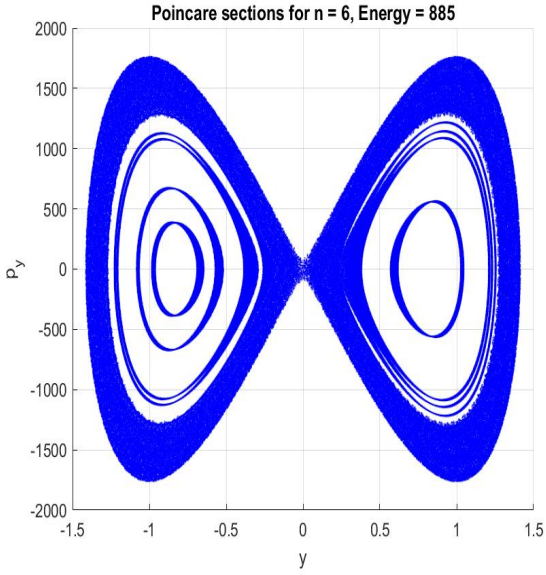

(s) $n = 6$ and $E = 885$

Figure 4.3: Poincaré Sections for Ansatz 1 at $\mu_1^2 = -16$ and $\mu_2^2 = -2$

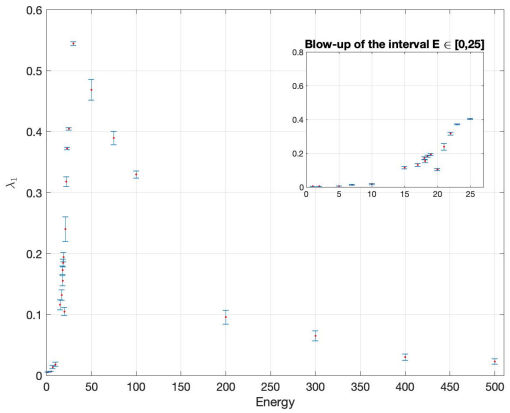

(a) λ_1 vs. Energy

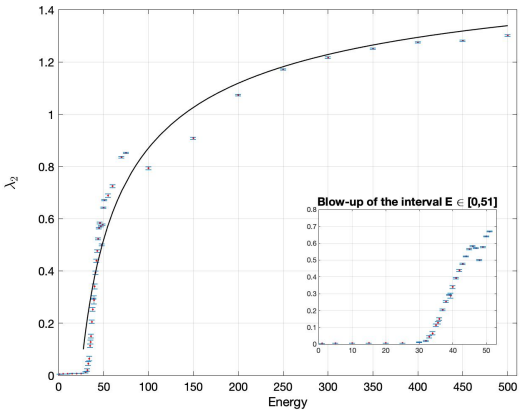

(b) λ_2 vs. Energy

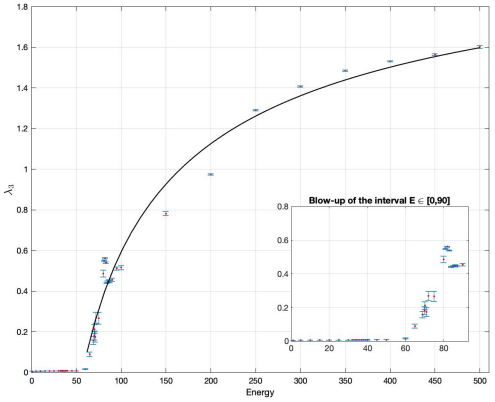

(c) λ_3 vs. Energy

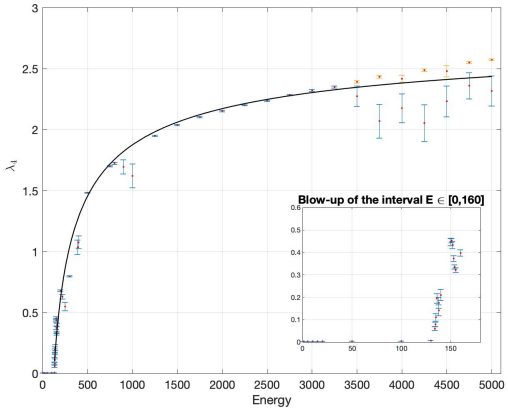

(d) λ_4 vs. Energy

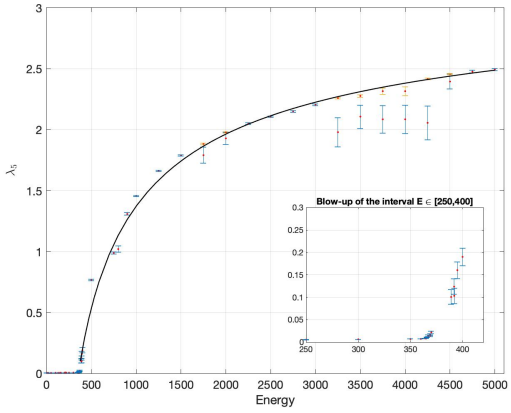

(e) λ_5 vs. Energy

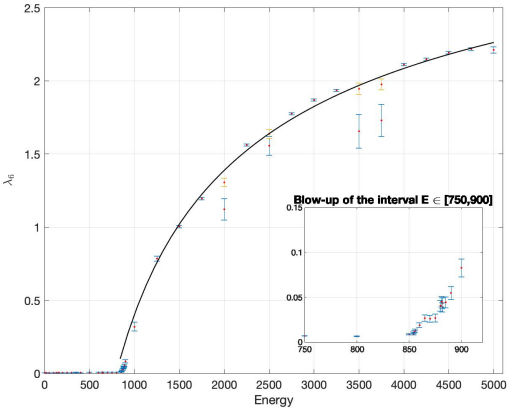

(f) λ_6 vs. Energy

Figure 4.4: MLLE vs. Energy for Ansatz 1 at $\mu_1^2 = -16$ and $\mu_2^2 = -2$

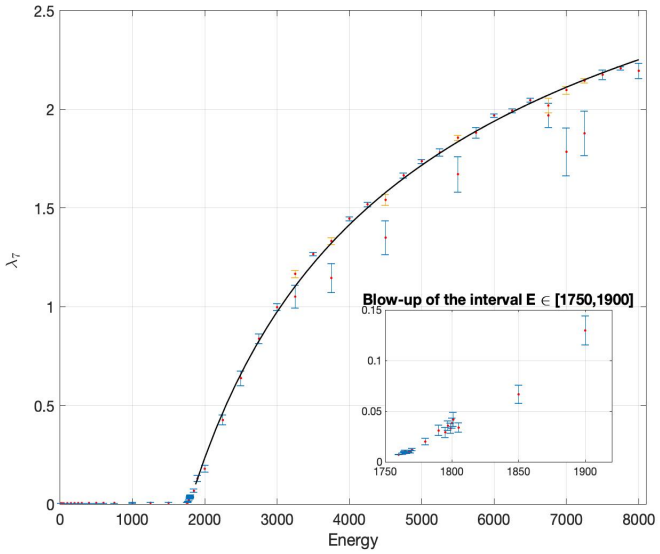

(g) λ_7 vs. Energy

Figure 4.4: MLLE vs. Energy for Ansatz 1 at $\mu_1^2 = -16$ and $\mu_2^2 = -2$

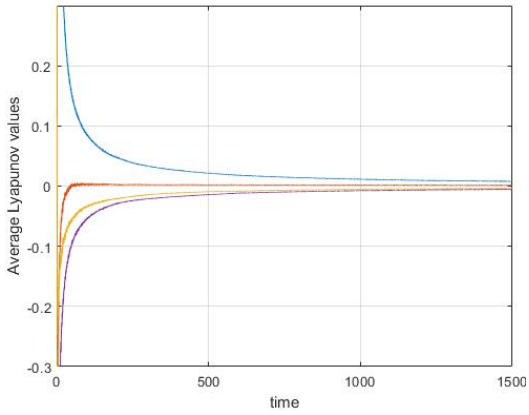

(a) $n = 1$ and $E = 5$

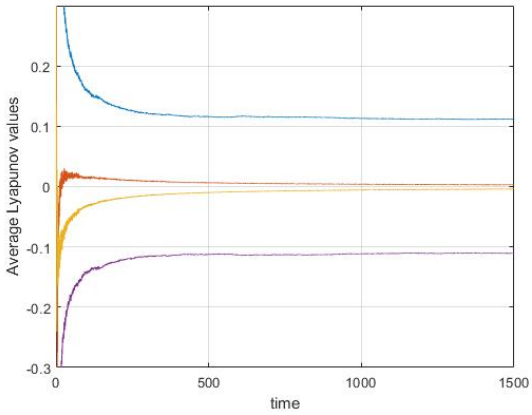

(b) $n = 1$ and $E = 6$

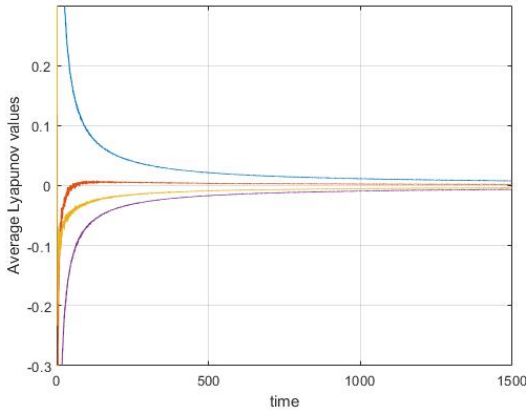

(c) $n = 2$ and $E = 12$

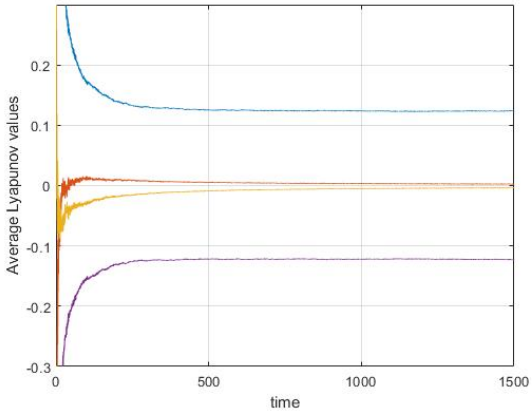

(d) $n = 2$ and $E = 15$

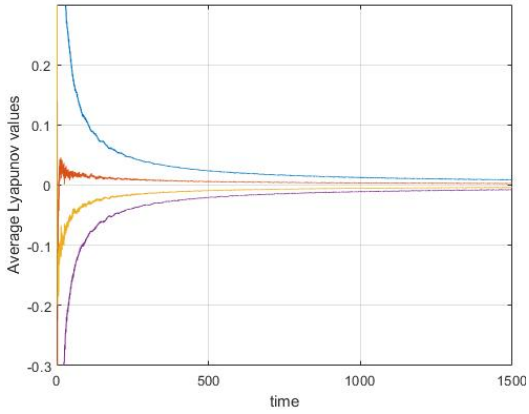

(e) $n = 3$ and $E = 21$

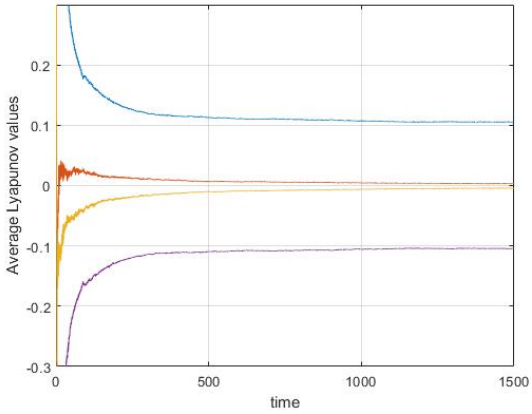

(f) $n = 3$ and $E = 22$

Figure 4.5: Lyapunov exponents vs. time for Ansatz 1 at $\mu_1^2 = -8$ and $\mu_2^2 = 1$

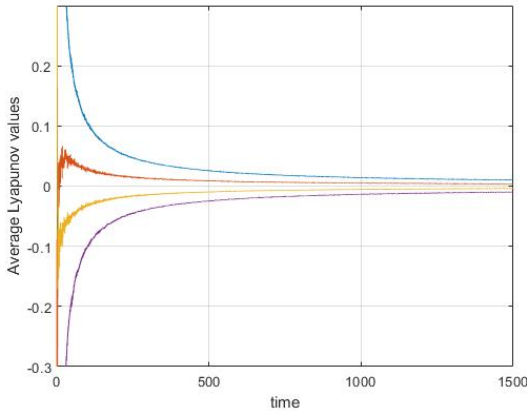

(g) $n = 4$ and $E = 32$

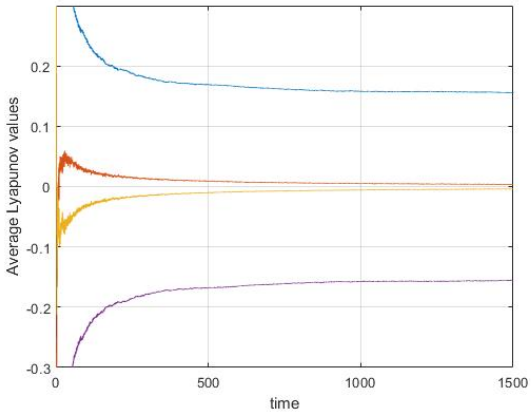

(h) $n = 4$ and $E = 34$

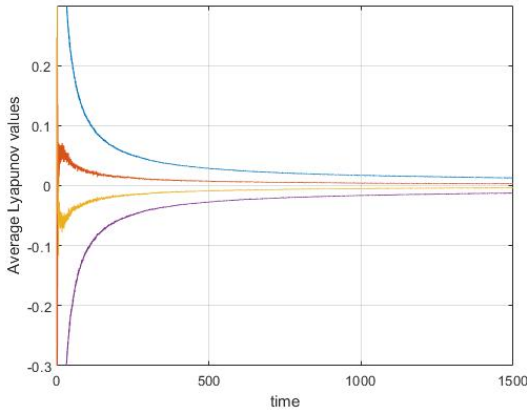

(i) $n = 5$ and $E = 45$

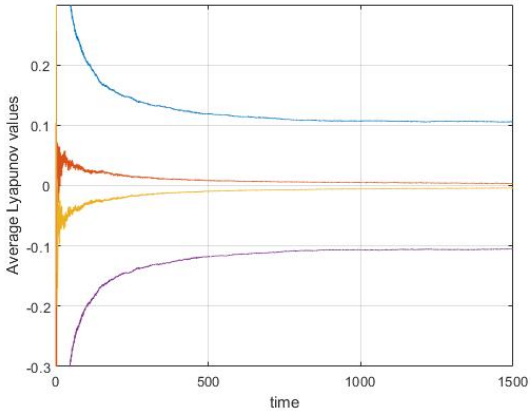

(j) $n = 5$ and $E = 47$

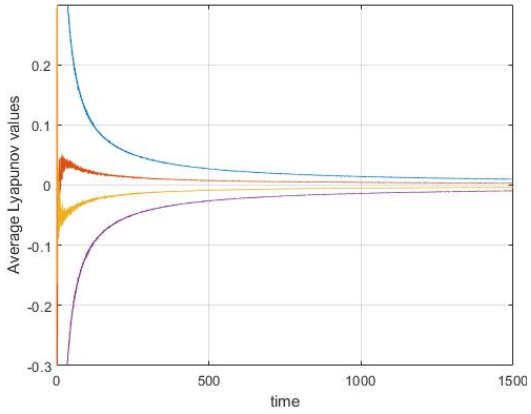

(k) $n = 6$ and $E = 60$

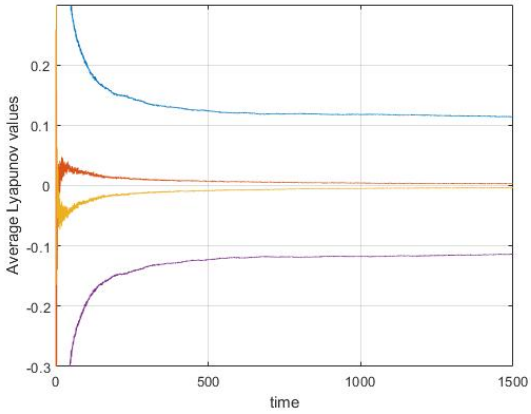

(l) $n = 6$ and $E = 63$

Figure 4.5: Lyapunov exponents vs. time for Ansatz 1 at $\mu_1^2 = -8$ and $\mu_2^2 = 1$

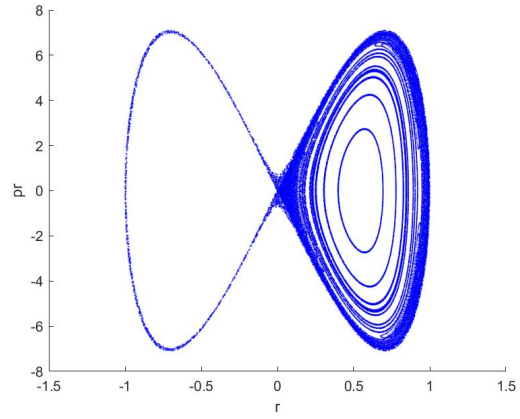

(a) $n = 1$ and $E = 5$

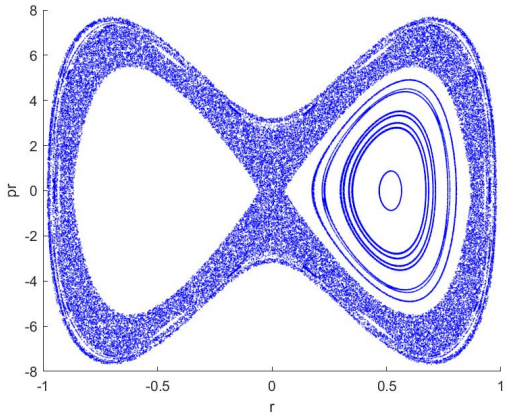

(b) $n = 1$ and $E = 6$

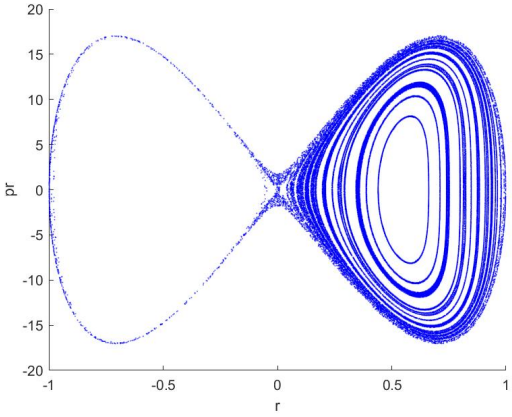

(c) $n = 2$ and $E = 12$

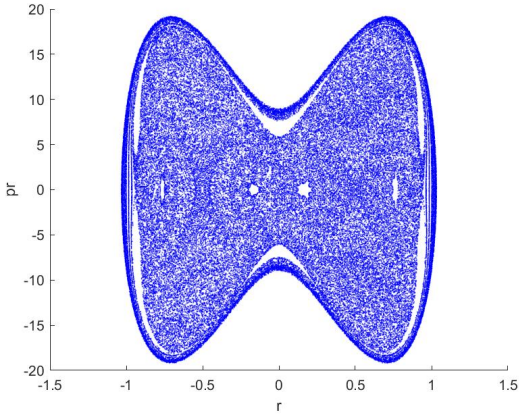

(d) $n = 2$ and $E = 15$

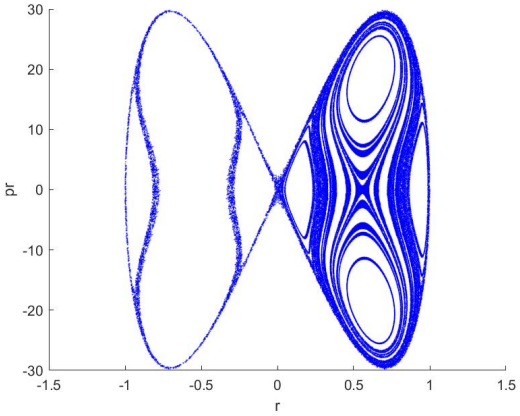

(e) $n = 3$ and $E = 21$

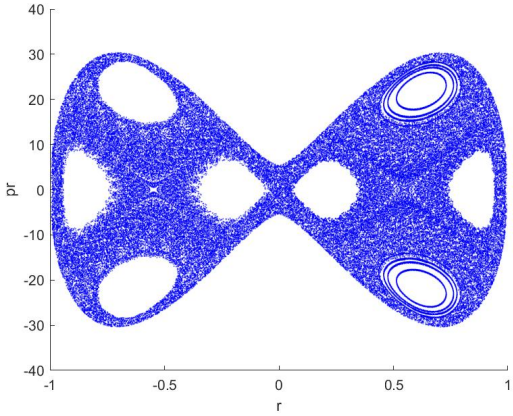

(f) $n = 3$ and $E = 22$

Figure 4.6: Poincaré Sections for Ansatz 1 at $\mu_1^2 = -8$ and $\mu_2^2 = 1$

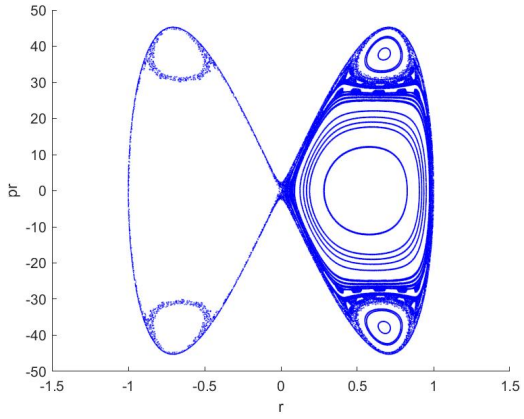

(g) $n = 4$ and $E = 32$

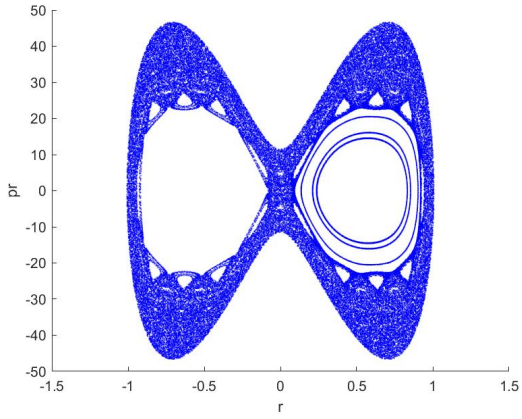

(h) $n = 4$ and $E = 34$

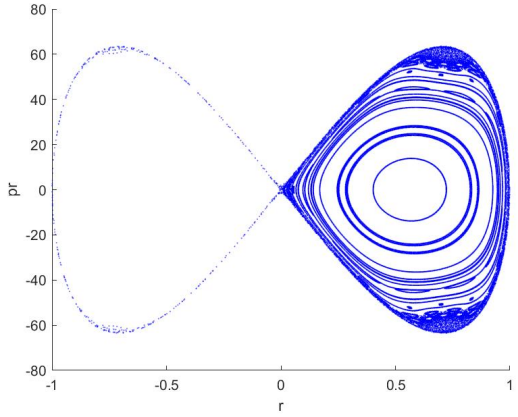

(i) $n = 5$ and $E = 45$

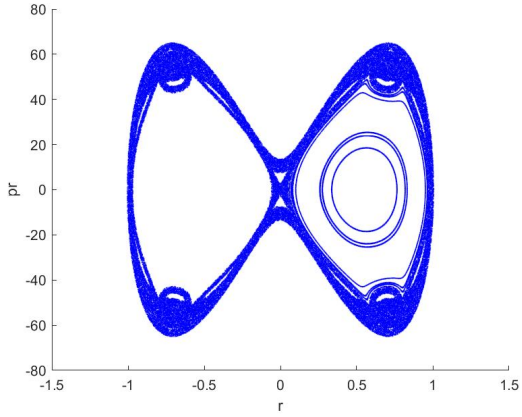

(j) $n = 5$ and $E = 47$

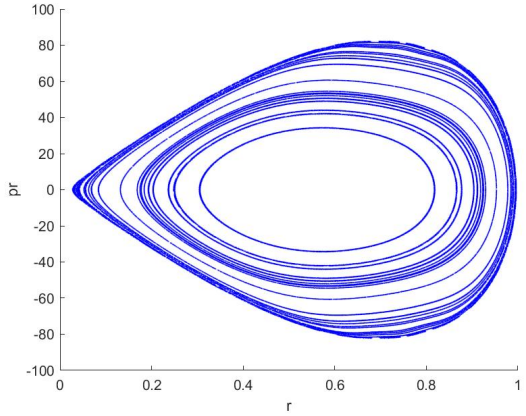

(k) $n = 6$ and $E = 60$

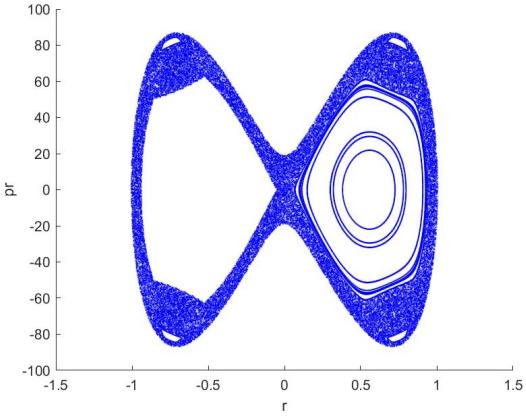

(l) $n = 6$ and $E = 63$

Figure 4.6: Poincaré Sections for Ansatz 1 at $\mu_1^2 = -8$ and $\mu_2^2 = 1$

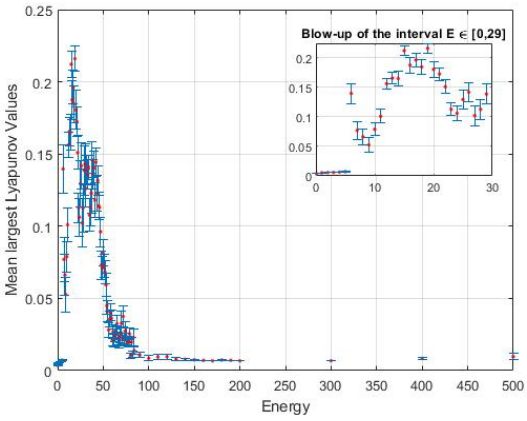

(a) $n = 1$

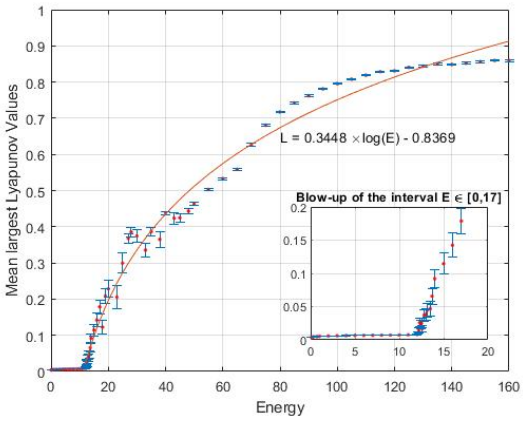

(b) $n = 2$

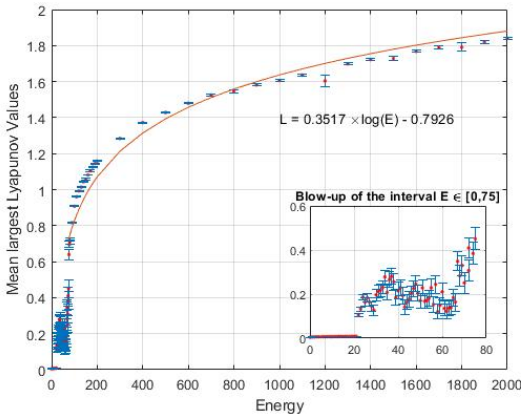

(c) $n = 3$

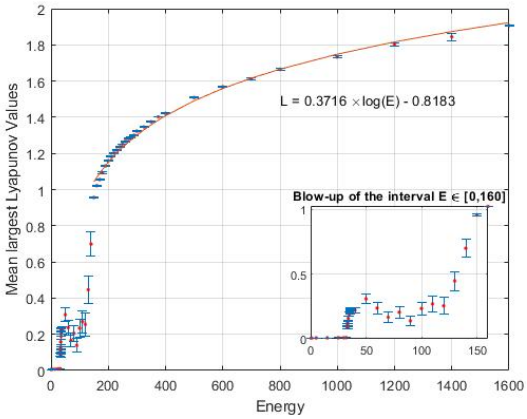

(d) $n = 4$

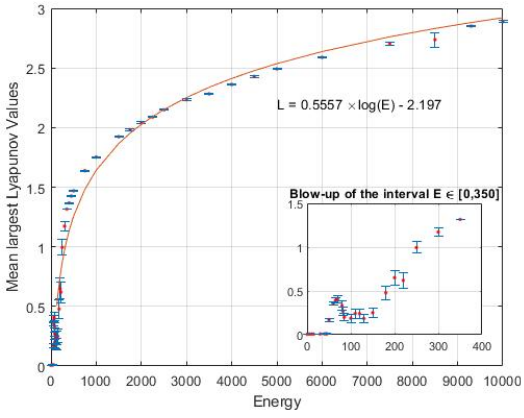

(e) $n = 5$

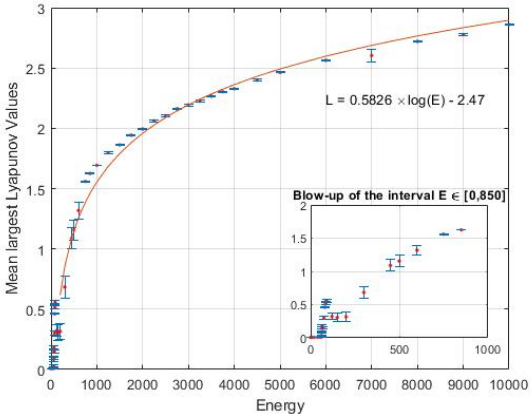

(f) $n = 6$

Figure 4.7: MLLE vs. Energy for Ansatz 1 at $\mu_1^2 = -8$ and $\mu_2^2 = 1$

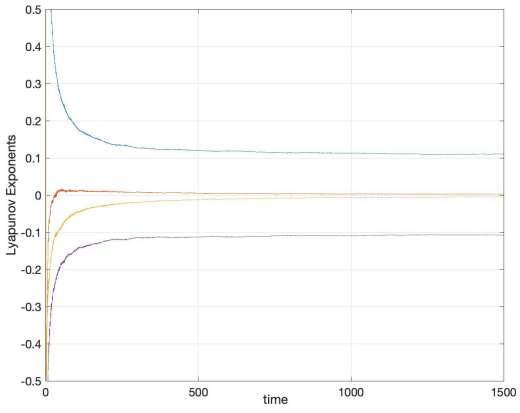

(a) $n = 2$ and $E = 50$

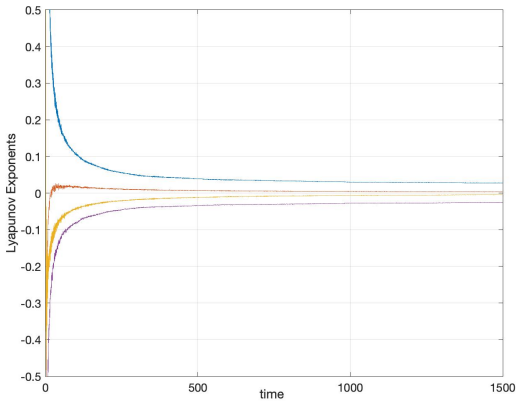

(b) $n = 2$ and $E = 500$

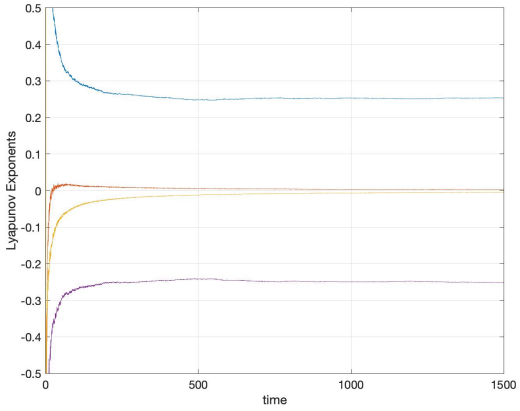

(c) $n = 3$ and $E = 100$

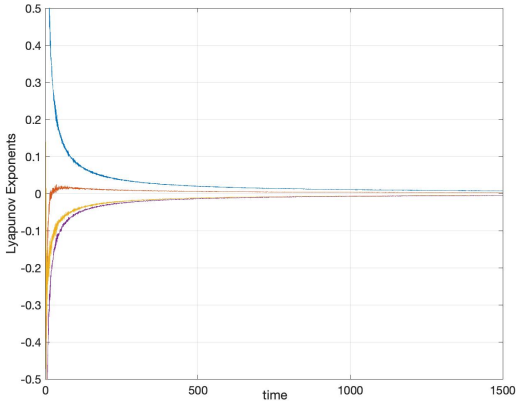

(d) $n = 3$ and $E = 500$

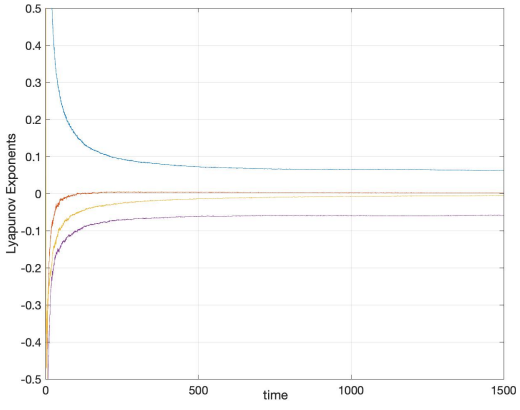

(e) $n = 5$ and $E = 180$

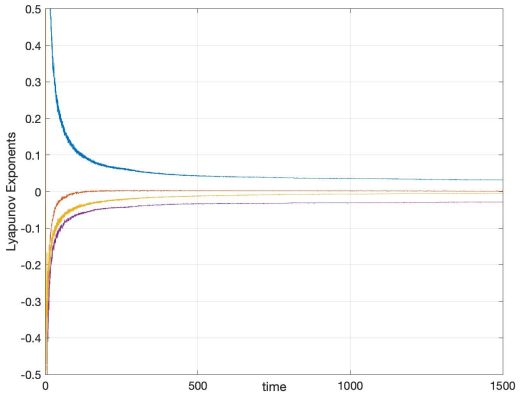

(f) $n = 5$ and $E = 1000$

Figure 4.8: Lyapunov exponents vs. time for Ansatz 2

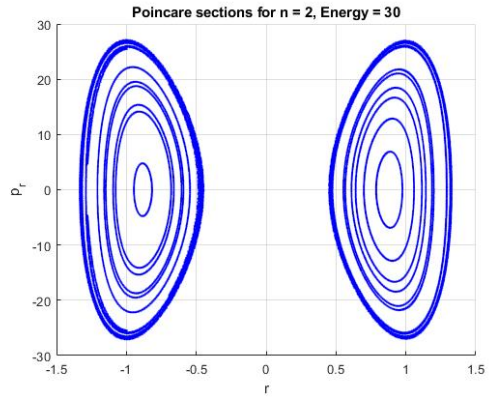

(a) $n = 2$ and $E = 30$

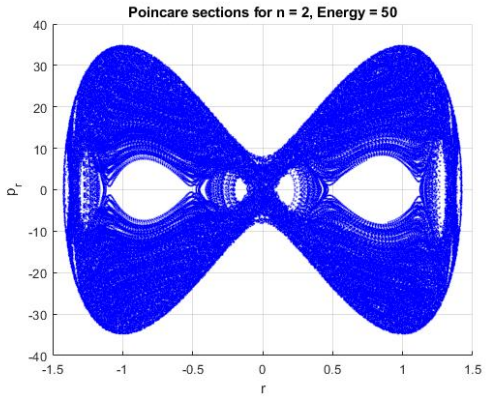

(b) $n = 2$ and $E = 50$

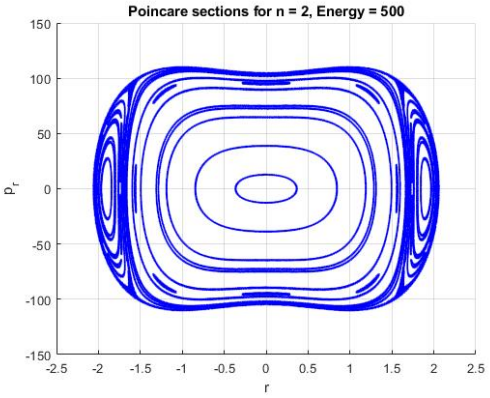

(c) $n = 2$ and $E = 500$

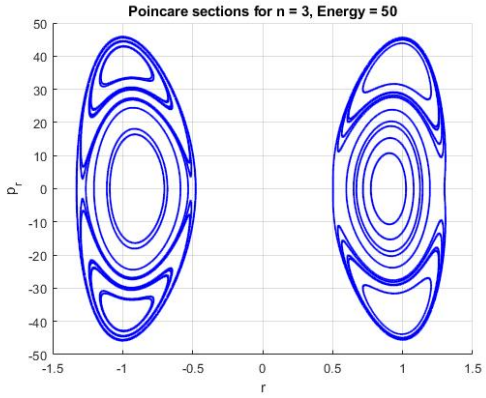

(d) $n = 3$ and $E = 50$

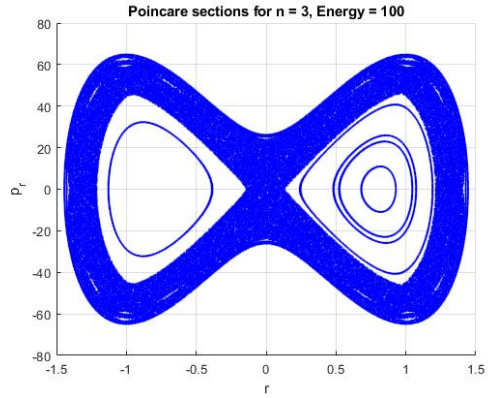

(e) $n = 3$ and $E = 100$

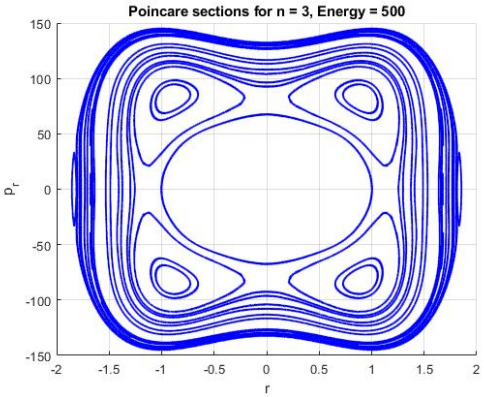

(f) $n = 3$ and $E = 500$

Figure 4.9: Poincarè sections for Ansatz 2

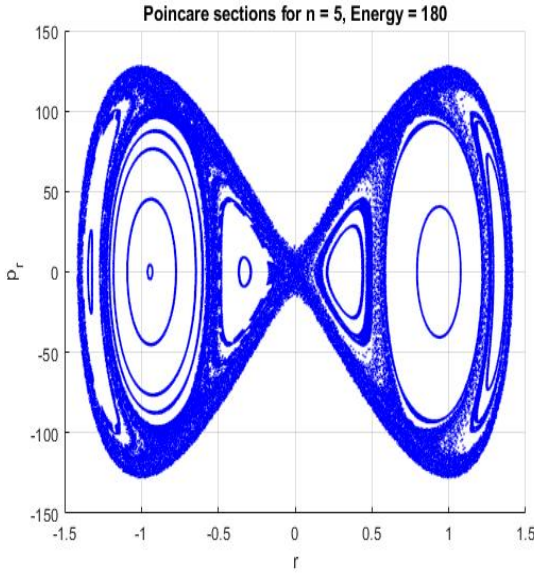

(g) $n = 5$ and $E = 180$

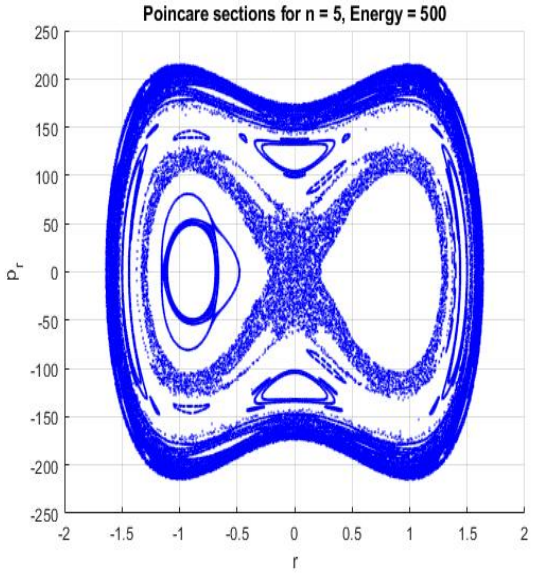

(h) $n = 5$ and $E = 500$

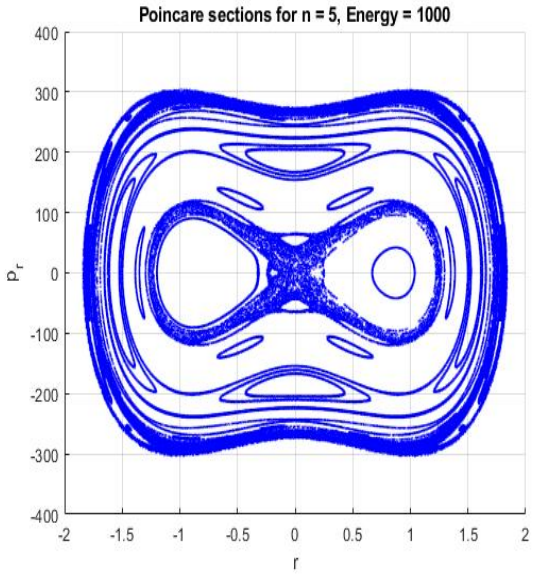

(i) $n = 5$ and $E = 1000$

Figure 4.9: Poincarè sections for Ansatz 2

CHAPTER 5

CONCLUSIONS

This thesis has focused on two research projects investigating the applications of fuzzy spaces to Yang-Mills matrix models. In the second chapter, we started out with reviewing the constructions of fuzzy two- and four-spheres from both geometric and algebraic viewpoints in order to provide necessary background for the discussion of YM matrix models presented in the ensuing chapters. This review was followed by the introduction of the bosonic part of the BFSS matrix model including its derivation from the Yang-Mills theory in $9 + 1$ dimensions by dimensional reduction. In this chapter, we have also demonstrated how fuzzy spheres arise as vacuum solutions to YM matrix models related to massive deformations of the BFSS model.

In chapter 3, we have concentrated on the YM 5-matrix model which can be contemplated as a sector of the bosonic part of the BFSS with only five Hermitian matrices and the same type of massive deformation term, which was introduced in section 2.5. Our primary aim was to obtain new static solutions or vacuum configurations in this model. For this purpose, we have considered matrix configurations involving bilinears of a set of fermionic oscillators spanning a reducible representation of $SO(5)$, which is subsequently decomposed into direct sums of irreducible representations of the latter. Taking tensor products of these IRRs of $SO(5)$ with the $(0, n)$ IRR of $SO(5)$ carried by the standard fuzzy four-sphere, new solutions were formed. Since the direct sum decompositions of this tensor product representation of SO(5) also contains IRRs of SO(5) that does not appear to be related to basic fuzzy four-sphere matrices, it was not possible to express the newly obtained vacuum configurations as the direct sums of S_F^4 matrices only. However, we have noticed that some of these new configurations can be realized as the generalized fuzzy four-sphere configurations,

which were recently encountered in [1]. In order to understand the connection of our results with the generalized fuzzy four-spheres, the quantization of coadjoint orbits method was used. To be more specific, a certain 10-dimensional coadjoint orbit, O_2 of $SO(6) \approx SU(4)$ was quantized to observe the detailed structure of the generalized fuzzy four-spheres. As a by product of this approach, we have also formulated the Landau problem on the coset space O_2. Determining the ground state energy levels in the Landau problem is shown to be equivalent to the quantization of the coadjoint orbit O_2. We have demonstrated that as a result of the quantization procedure of O_2, the generalized fuzzy four-sphere IRRs are obtained. In the last two sections of this chapter, generalized coherent states associated to $SO(6) \approx SU(4)$ were employed to discuss some aspects of both the basic and generalized fuzzy four-spheres.

Chapter 4 was devoted to the examination of a YM matrix model with two distinct mass deformation terms which may be contemplated as a double mass deformation of the bosonic part of the BFSS model. Using an ansatz configuration involving fuzzy two- and four-spheres as backgrounds and assuming collective time dependence of the matrices, we were able to obtain a family of effective models descending from tracing over the fuzzy spheres at matrix levels $N = \frac{1}{6}(n+1)(n+2)(n+3)$, for $n = 1\,, \cdots, 7$. We have performed a detailed numerical analysis and demonstrated the development of chaotic dynamics in these reduced models by obtaining their Lyapunov spectrum and Poincaré sections. From our results, we were able to see that the onset of chaotic motion is at the energies which are at or around the lowest of that of the unstable fixed points and modeled, by fitting curves to the data, how the largest Lyapunov exponents change as a function of the energy for two different set of the mass values. The similarities and differences in these two cases are also discussed. Let us recapitulate some of the key results that we have obtained from these analyses. In section 4.2 we have constructed Ansatz I by introducing two separate collective time-dependent functions, $r(t)$ and $y(t)$, multiplying the fuzzy four- and two-sphere matrices. For this ansatz, we have considered a single spin-$j = \frac{N-1}{2}$ IRR of $SU(2)$ as the fuzzy S^2 configuration and investigated the detailed dynamics for the mass parameters $\mu_1^2 = -16$ and $\mu_2^2 = -2$. A noteworthy observation was the convergence of the mean largest Lyapunov exponents to non-zero values with increasing energy. On that note, we were able to demonstrate through an appropriate fitting function

that mean largest Lyapunov exponents (MLLE)s approximately vary as $1/\sqrt{E}$ with increasing energy. From the value of the derivative of the latter at the fixed point energies, we concluded that the models at low values of n become chaotic more rapidly. In order to observe the impact of mass parameters on the dynamics of our models, we considered assigning different values to the mass parameters and took $\mu_1^2 = -8$ and $\mu_2^2 = 1$. Upon performing a detailed numerical analysis on the new reduced models we demonstrated that MLLEs vary logarithmically with the energies of the reduced actions. In section 4.3, we have focused on another ansatz, whose fuzzy two-sphere configurations consist of a direct sum of spin-$1/2$ fuzzy spheres. These configurations lead to chaos only within a narrow interval of energies in each model. Lastly, in section 4.4 we have examined the dynamics of the quasi-periodic motion induced when $r(t)$ is taken to be equal to $y(t)$. By using explicit derivations and numerical calculations, we have shown that choosing the product of a single time-dependent function, $r(t)$, with S_F^2 and S_F^4 matrices as a solution of S_{MD} results in a periodic motion whose variation in time can be completely described by the Jacobi elliptic function sn.

APPENDIX A

IDENTITIES AND DERIVATIONS RELATED TO S_F^4

A.1 Gamma Matrices, SO(6) Spinor Generators and Fermionic Basis

Gamma matrices in five dimensions are 4x4 matrices satisfying the Clifford algebra $\{\gamma_a, \gamma_b\} = 2\delta_{ab}\mathbb{1}_4$. A possible representation of these matrices is given by

$$\gamma_1 = \sigma_1 \otimes \sigma_1 = \begin{pmatrix} 0 & \sigma_1 \\ \sigma_1 & 0 \end{pmatrix}, \qquad \gamma_2 = \sigma_1 \otimes \sigma_2 = \begin{pmatrix} 0 & \sigma_2 \\ \sigma_2 & 0 \end{pmatrix},$$
$$\gamma_3 = -\sigma_1 \otimes \sigma_3 = -\begin{pmatrix} 0 & \sigma_3 \\ \sigma_3 & 0 \end{pmatrix}, \quad \gamma_4 = -\sigma_2 \otimes \mathbb{1}_2 = i\begin{pmatrix} 0 & \mathbb{1}_2 \\ -\mathbb{1}_2 & 0 \end{pmatrix}, \tag{A.1.1}$$
$$\gamma_5 = \gamma_1\gamma_2\gamma_3\gamma_4 = -\sigma_3 \otimes \mathbb{1}_2 = \begin{pmatrix} -\mathbb{1}_2 & 0 \\ 0 & \mathbb{1}_2 \end{pmatrix}.$$

In terms of the γ-matrices in five dimensions, 4-dimensional $SO(6)$ spinor representations $(1,0,0)$ and $(0,0,1)$ are given as

$$F_{ij} = \frac{1}{4i}[\gamma_i, \gamma_j], \qquad F_{i6} = \mp\frac{1}{2}\gamma_i, \qquad i,j = 1,2,3,4,5. \tag{A.1.2}$$

These fifteen F_{gh} $(g,h = 1,..,6)$ generators satisfy the usual $SO(6)$ commutation relations

$$[F_{gh}, F_{mn}] = i(\delta_{gm}F_{hn} + \delta_{hn}F_{gm} - \delta_{gn}F_{hm} - \delta_{hm}F_{gn}). \tag{A.1.3}$$

The representations of the quadratic Casimir operators are found in the basis given below. There are 16 states here and we label them as follows

$$|B_\pm\rangle = \frac{1}{\sqrt{2}}(|0011\rangle \pm |1100\rangle), \tag{A.1.4}$$

$$
\begin{aligned}
&(1) \Longrightarrow |0000\rangle\,, \quad (2) \Longrightarrow |1000\rangle\,, \quad (3) \Longrightarrow |0100\rangle\,, \qquad \text{(A.1.5)}\\
&(4) \Longrightarrow |0010\rangle\,, \quad (5) \Longrightarrow |0001\rangle\,, \quad (6) \Longrightarrow |B_+\rangle\,, \quad (7) \Longrightarrow |1010\rangle\,,\\
&(8) \Longrightarrow |0110\rangle\,, \quad (9) \Longrightarrow |0101\rangle\,, \quad (10) \Longrightarrow |B_-\rangle\,, \quad (11) \Longrightarrow |1001\rangle\,,\\
&(12) \Longrightarrow |1110\rangle\,, \quad (13) \Longrightarrow |0111\rangle\,, \quad (14) \Longrightarrow |1011\rangle\,,\\
&(15) \Longrightarrow |1101\rangle\,, \quad (16) \Longrightarrow |1111\rangle\,.
\end{aligned}
$$

A.2 Evaluation of $(Y_a)^2$

We use the definitions given in (3.2.13) and (3.2.22) for the operators b_i, $b_i^\dagger$ and the number operators.

$$
\begin{aligned}
Y_1 &= \frac{1}{2}\Psi^\dagger\gamma_1\Psi = \frac{1}{2}\begin{pmatrix} b_1^\dagger & b_2^\dagger & b_3^\dagger & b_4^\dagger \end{pmatrix}\begin{pmatrix} 0 & 0 & 0 & 1\\ 0 & 0 & 1 & 0\\ 0 & 1 & 0 & 0\\ 1 & 0 & 0 & 0 \end{pmatrix}\begin{pmatrix} b_1\\ b_2\\ b_3\\ b_4 \end{pmatrix}\\
&= \frac{1}{2}(b_1^\dagger b_4 + b_2^\dagger b_3 + b_3^\dagger b_2 + b_4^\dagger b_1)\,, \qquad \text{(A.2.1a)}\\
Y_2 &= -\frac{i}{2}(b_1^\dagger b_4 - b_2^\dagger b_3 + b_3^\dagger b_2 - b_4^\dagger b_1)\,, \qquad \text{(A.2.1b)}\\
Y_3 &= -\frac{1}{2}(b_1^\dagger b_3 - b_2^\dagger b_4 + b_3^\dagger b_1 - b_4^\dagger b_2)\,, \qquad \text{(A.2.1c)}\\
Y_4 &= \frac{i}{2}(b_1^\dagger b_3 + b_2^\dagger b_4 - b_3^\dagger b_1 - b_4^\dagger b_2)\,, \qquad \text{(A.2.1d)}\\
Y_5 &= -\frac{1}{2}(b_1^\dagger b_1 + b_2^\dagger b_2 - b_3^\dagger b_3 - b_4^\dagger b_4)\,. \qquad \text{(A.2.1e)}
\end{aligned}
$$

Squaring these expression we find

$$
\begin{aligned}
(Y_1)^2 &= (1/4)(b_1^\dagger b_4 + b_2^\dagger b_3 + b_3^\dagger b_2 + b_4^\dagger b_1)(b_1^\dagger b_4 + b_2^\dagger b_3 + b_3^\dagger b_2 + b_4^\dagger b_1)\\
&= \frac{1}{4}[b_1^\dagger(I - b_4^\dagger b_4)b_1 + b_2^\dagger(I - b_3^\dagger b_3)b_2 + b_3^\dagger(I - b_2^\dagger b_2)b_3 + b_4^\dagger(I - b_1^\dagger b_1)b_4\\
&+ 2(b_1^\dagger b_2^\dagger b_3 b_4 - b_1^\dagger b_2 b_3^\dagger b_4 - b_1 b_2^\dagger b_3 b_4^\dagger + b_1 b_2 b_3^\dagger b_4^\dagger)]\\
&= \frac{1}{4}[(b_1^\dagger b_1 + b_2^\dagger b_2 + b_3^\dagger b_3 + b_4^\dagger b_4) - b_1^\dagger b_4^\dagger b_4 b_1 - b_2^\dagger b_3^\dagger b_3 b_2 - b_3^\dagger b_2^\dagger b_2 b_3 \qquad \text{(A.2.2a)}\\
&- b_4^\dagger b_1^\dagger b_1 b_4 + 2(b_1^\dagger b_2^\dagger b_3 b_4 - b_1^\dagger b_2 b_3^\dagger b_4 - b_1 b_2^\dagger b_3 b_4^\dagger + b_1 b_2 b_3^\dagger b_4^\dagger)]\\
&= \frac{1}{4}[N - 2(N_1 N_4 + N_2 N_3) + 2(b_1^\dagger b_2^\dagger b_3 b_4 - b_1^\dagger b_2 b_3^\dagger b_4 - b_1 b_2^\dagger b_3 b_4^\dagger + b_1 b_2 b_3^\dagger b_4^\dagger)]\,,
\end{aligned}
$$

$$(Y_2)^2 = \frac{1}{4}[N - 2(N_1N_4 + N_2N_3) + 2(b_1^\dagger b_2^\dagger b_3 b_4 + b_1^\dagger b_2 b_3^\dagger b_4 + b_1 b_2^\dagger b_3 b_4^\dagger \quad \text{(A.2.2b)}$$
$$+ b_1 b_2 b_3^\dagger b_4^\dagger)],$$
$$(Y_3)^2 = \frac{1}{4}[N - 2(N_1N_3 + N_2N_4) + 2(b_1^\dagger b_2^\dagger b_3 b_4 - b_1^\dagger b_2 b_3 b_4^\dagger - b_1 b_2^\dagger b_3^\dagger b_4 \quad \text{(A.2.2c)}$$
$$+ b_1 b_2 b_3^\dagger b_4^\dagger)],$$
$$(Y_4)^2 = \frac{1}{4}[N - 2(N_1N_3 + N_2N_4) + 2(b_1^\dagger b_2^\dagger b_3 b_4 + b_1^\dagger b_2 b_3 b_4^\dagger + b_1 b_2^\dagger b_3^\dagger b_4 \quad \text{(A.2.2d)}$$
$$+ b_1 b_2 b_3^\dagger b_4^\dagger)],$$
$$(Y_5)^2 = \frac{1}{4}\{N + 2[N_1N_2 + N_3N_4 - (N_1 + N_2)(N_3 + N_4)]\}. \quad \text{(A.2.2e)}$$

Finally, this gives

$$\begin{aligned}(Y_a)^2 &= \sum_{a=1}^{5} Y_a Y_a \\ &= \frac{1}{4}\{N - 2(N_1N_4 + N_2N_3) + 2(b_1^\dagger b_2^\dagger b_3 b_4 - b_1^\dagger b_2 b_3^\dagger b_4 - b_1 b_2^\dagger b_3 b_4^\dagger + b_1 b_2 b_3^\dagger b_4^\dagger) \\ &+ N - 2(N_1N_4 + N_2N_3) + 2(b_1^\dagger b_2^\dagger b_3 b_4 + b_1^\dagger b_2 b_3^\dagger b_4 + b_1 b_2^\dagger b_3 b_4^\dagger + b_1 b_2 b_3^\dagger b_4^\dagger) + N \\ &- 2(N_1N_3 + N_2N_4) + 2(b_1^\dagger b_2^\dagger b_3 b_4 - b_1^\dagger b_2 b_3 b_4^\dagger - b_1 b_2^\dagger b_3^\dagger b_4 + b_1 b_2 b_3^\dagger b_4^\dagger) + N \\ &- 2(N_1N_3 + N_2N_4) + 2(b_1^\dagger b_2^\dagger b_3 b_4 + b_1^\dagger b_2 b_3 b_4^\dagger + b_1 b_2^\dagger b_3^\dagger b_4 + b_1 b_2 b_3^\dagger b_4^\dagger) + N \\ &+ 2[N_1N_2 + N_3N_4 - (N_1 + N_2)(N_3 + N_4)]\} \\ &= \frac{5}{4}N - \frac{3}{2}(N_1 + N_2)(N_3 + N_4) + \frac{1}{2}(N_1N_2 + N_3N_4) \\ &\qquad + 2(b_1^\dagger b_2^\dagger b_3 b_4 + b_1 b_2 b_3^\dagger b_4^\dagger). \end{aligned} \quad \text{(A.2.3)}$$

(A.2.3) expresses Y_a^2 in terms of the number operators and two terms which cannot be cast in terms of the number operators.

A.3 Evaluation of $(Z_{ab})^2$

Using the same technology, we evaluate the Casimir operator of $SO(5)$ using the generator Z_{ab} given in equation (3.2.18)

$$\begin{aligned}(Z_{ab})^2 &= -\frac{1}{4}(\Psi^\dagger \gamma_k \gamma_l \Psi)^2 \\ &= -\frac{1}{4}[(\Psi^\dagger \gamma_1 \gamma_2 \Psi)^2 + (\Psi^\dagger \gamma_1 \gamma_3 \Psi)^2 + (\Psi^\dagger \gamma_1 \gamma_4 \Psi)^2 + (\Psi^\dagger \gamma_1 \gamma_5 \Psi)^2 \\ &+ (\Psi^\dagger \gamma_2 \gamma_3 \Psi)^2 + (\Psi^\dagger \gamma_2 \gamma_4 \Psi)^2 + (\Psi^\dagger \gamma_2 \gamma_5 \Psi)^2 + (\Psi^\dagger \gamma_3 \gamma_4 \Psi)^2 \\ &+ (\Psi^\dagger \gamma_3 \gamma_5 \Psi)^2 + (\Psi^\dagger \gamma_4 \gamma_5 \Psi)^2]. \end{aligned} \quad \text{(A.3.1)}$$

In expression (A.3.1), we need to evaluate each term explicitly. We have

$$\begin{aligned}\Psi^\dagger\gamma_1\gamma_2\Psi &= \begin{pmatrix} b_1^\dagger & b_2^\dagger & b_3^\dagger & b_4^\dagger \end{pmatrix} \begin{pmatrix} i & 0 & 0 & 0 \\ 0 & -i & 0 & 0 \\ 0 & 0 & i & 0 \\ 0 & 0 & 0 & -i \end{pmatrix} \begin{pmatrix} b_1 \\ b_2 \\ b_3 \\ b_4 \end{pmatrix} \\ &= i(N_1 - N_2 + N_3 - N_4)\,,\end{aligned}$$

$$\begin{aligned}(\Psi^\dagger\gamma_1\gamma_2\Psi)^2 &= -(N_1 - N_2 + N_3 - N_4)(N_1 - N_2 + N_3 - N_4) \\ &= -[(N_1^2 + N_2^2 + N_3^2 + N_4^2) - 2N_1N_2 + 2N_1N_3 - 2N_1N_4 \\ &- 2N_2N_3 + 2N_2N_4 - 2N_3N_4] \\ &= -N + 2(N_1N_2 - N_1N_3 + N_1N_4 + N_2N_3 - N_2N_4 + N_3N_4)\,.\end{aligned} \tag{A.3.2}$$

Similarly, we find

$$\begin{aligned}(\Psi^\dagger\gamma_1\gamma_3\Psi)^2 &= -N + 2(N_1N_2 + N_3N_4) + 2(b_1^\dagger b_2 b_3^\dagger b_4 + b_1^\dagger b_2 b_3 b_4^\dagger \\ &+ b_1 b_2^\dagger b_3^\dagger b_4 + b_1 b_2^\dagger b_3 b_4^\dagger)\,,\end{aligned} \tag{A.3.3}$$

$$\begin{aligned}(\Psi^\dagger\gamma_1\gamma_4\Psi)^2 &= 2(b_1^\dagger b_2 b_3^\dagger b_4 - b_1^\dagger b_2 b_3 b_4^\dagger + b_1 b_2^\dagger b_3 b_4^\dagger - b_1 b_2^\dagger b_3^\dagger b_4) - N \\ &+ 2(N_1N_2 + N_3N_4)\,,\end{aligned} \tag{A.3.4}$$

$$\begin{aligned}(\Psi^\dagger\gamma_1\gamma_5\Psi)^2 &= 2(b_1^\dagger b_2^\dagger b_3 b_4 + b_1 b_2^\dagger b_3 b_4^\dagger + b_1^\dagger b_2 b_3^\dagger b_4 + b_1 b_2 b_3^\dagger b_4^\dagger) - N \\ &+ 2(N_1N_4 + N_2N_3)\,,\end{aligned} \tag{A.3.5}$$

$$\begin{aligned}(\Psi^\dagger\gamma_2\gamma_3\Psi)^2 &= 2(b_1^\dagger b_2 b_3 b_4^\dagger + b_1 b_2^\dagger b_3^\dagger b_4 - b_1^\dagger b_2 b_3^\dagger b_4 - b_1 b_2^\dagger b_3 b_4^\dagger) - N \\ &+ 2(N_1N_2 + N_3N_4)\,,\end{aligned} \tag{A.3.6}$$

$$\begin{aligned}(\Psi^\dagger\gamma_2\gamma_4\Psi)^2 &= -2(b_1^\dagger b_2 b_3^\dagger b_4 + b_1^\dagger b_2 b_3 b_4^\dagger + b_1 b_2^\dagger b_3^\dagger b_4 + b_1 b_2^\dagger b_3 b_4^\dagger) - N \\ &+ 2(N_1N_2 + N_3N_4)\,,\end{aligned} \tag{A.3.7}$$

$$\begin{aligned}(\Psi^\dagger\gamma_2\gamma_5\Psi)^2 &= 2(b_1^\dagger b_2^\dagger b_3 b_4 - b_1 b_2^\dagger b_3 b_4^\dagger + b_1 b_2 b_3^\dagger b_4^\dagger - b_1^\dagger b_2 b_3^\dagger b_4) - N \\ &+ 2(N_1N_4 + N_2N_3)\,,\end{aligned} \tag{A.3.8}$$

$$(\Psi^\dagger\gamma_3\gamma_4\Psi)^2 = -N + 2(N_1N_2 + N_1N_3 - N_1N_4 + N_3N_4 + N_2N_4 - N_2N_3)\,, \quad \text{(A.3.9)}$$

$$\begin{aligned}(\Psi^\dagger\gamma_3\gamma_5\Psi)^2 &= 2(b_1b_2^\dagger b_3^\dagger b_4 + b_1^\dagger b_2^\dagger b_3 b_4 + b_1^\dagger b_2 b_3 b_4^\dagger + b_1 b_2 b_3^\dagger b_4^\dagger) - N \\ &\quad + 2(N_2N_4 + N_1N_3)\,,\end{aligned} \quad \text{(A.3.10)}$$

$$\begin{aligned}(\Psi^\dagger\gamma_4\gamma_5\Psi)^2 &= 2(b_1^\dagger b_2^\dagger b_3 b_4 - b_1^\dagger b_2 b_3 b_4^\dagger - b_1 b_2^\dagger b_3^\dagger b_4 + b_1 b_2 b_3^\dagger b_4^\dagger) - N \\ &\quad + 2(N_1N_3 + N_2N_4)\,.\end{aligned} \quad \text{(A.3.11)}$$

Combining (A.3.2)- (A.3.11) in (A.3.1) we find

$$\begin{aligned}(Z_{ab})^2 = -\frac{1}{4}\{&[2(N_1N_2 - N_1N_3 + N_1N_4 + N_2N_3 - N_2N_4 + N_3N_4) - N] + [2(N_1N_2 \\ &+ N_3N_4) + 2(b_1^\dagger b_2 b_3^\dagger b_4 + b_1^\dagger b_2 b_3 b_4^\dagger + b_1 b_2^\dagger b_3^\dagger b_4 + b_1 b_2^\dagger b_3 b_4^\dagger) - N] + [2(b_1^\dagger b_2 b_3^\dagger b_4 \\ &- b_1^\dagger b_2 b_3 b_4^\dagger + b_1 b_2^\dagger b_3 b_4^\dagger - b_1 b_2^\dagger b_3^\dagger b_4) - N + 2(N_1N_2 + N_3N_4)] + [2(b_1^\dagger b_2^\dagger b_3 b_4 \\ &+ b_1 b_2^\dagger b_3 b_4^\dagger + b_1^\dagger b_2 b_3^\dagger b_4 + b_1 b_2 b_3^\dagger b_4^\dagger) - N + 2(N_1N_4 + N_2N_3)] + [2(b_1^\dagger b_2 b_3 b_4^\dagger \\ &+ b_1 b_2^\dagger b_3^\dagger b_4 - b_1^\dagger b_2 b_3^\dagger b_4 - b_1 b_2^\dagger b_3 b_4^\dagger) - N + 2(N_1N_2 + N_3N_4)] + [2(N_1N_2 \\ &+ N_3N_4) - 2(b_1^\dagger b_2 b_3^\dagger b_4 + b_1^\dagger b_2 b_3 b_4^\dagger + b_1 b_2^\dagger b_3^\dagger b_4 + b_1 b_2^\dagger b_3 b_4^\dagger) - N] + [2(b_1^\dagger b_2^\dagger b_3 b_4 \\ &- b_1 b_2^\dagger b_3 b_4^\dagger + b_1 b_2 b_3^\dagger b_4^\dagger - b_1^\dagger b_2 b_3^\dagger b_4) - N + 2(N_1N_4 + N_2N_3)] + [2(N_1N_2 \\ &+ N_1N_3 - N_1N_4 + N_3N_4 + N_2N_4 - N_2N_3) - N] + [2(b_1 b_2^\dagger b_3^\dagger b_4 + b_1^\dagger b_2^\dagger b_3 b_4 \\ &+ b_1^\dagger b_2 b_3 b_4^\dagger + b_1 b_2 b_3^\dagger b_4^\dagger) - N + 2(N_2N_4 + N_1N_3)] + [2(b_1^\dagger b_2^\dagger b_3 b_4 - b_1^\dagger b_2 b_3 b_4^\dagger \\ &- b_1 b_2^\dagger b_3^\dagger b_4 + b_1 b_2 b_3^\dagger b_4^\dagger) - N + 2(N_1N_3 + N_2N_4)]\}\,,\end{aligned} \quad \text{(A.3.12)}$$

which upon simplification reduces to

$$\begin{aligned}(Z_{ab})^2 &= \frac{5}{2}N - 2(b_1^\dagger b_2^\dagger b_3 b_4 + b_1 b_2 b_3^\dagger b_4^\dagger) - (N_1 + N_2)(N_3 + N_4) \\ &\quad - 3(N_1N_2 + N_3N_4)\,.\end{aligned} \quad \text{(A.3.13)}$$

A.4 Evaluation of $(Z_{gh})^2$

The completeness relation for the generators T_f $(f = 1, .., N^2 - 1)$ of SU(N) in an IRR is given generically in the form [79]

$$\frac{1}{C}(T_f)_{sv}(T_f)_{wy} + \frac{1}{N}\delta_{sv}\delta_{wy} = \delta_{sy}\delta_{wv}\,. \quad \text{(A.4.1)}$$

where C is a constant depending on the IRR. Since $SU(4)$ and $SO(6)$ have isomorphic Lie algebras, for the fundamental spinor representation $(1,0,0)$ of $SO(6)$ we may write the identity with $C=1$ and $N=4$

$$(G_{gh})_{sv}(G_{gh})_{wy} = \delta_{sy}\delta_{wv} - \frac{1}{4}\delta_{sv}\delta_{wy}, \tag{A.4.2}$$

where G_{gh} (g,h= 1,..,6) generators generate the SO(6).

We evaluate the Casimir operator of $SO(6)$ generators Z_{gh} given in (3.2.30)

$$\begin{aligned}
(Z_{gh})^2 &= \Psi^\dagger G_{gh}\Psi\Psi^\dagger G_{gh}\Psi \\
&= (\Psi^\dagger)_i(G_{gh})_{ij}\Psi_j(\Psi^\dagger)_k(G_{gh})_{kl}\Psi_l \\
&= b_i^\dagger(G_{gh})_{ij}b_j b_k^\dagger(G_{gh})_{kl}b_l \\
&= (G_{gh})_{ij}(G_{gh})_{kl}b_i^\dagger b_j b_k^\dagger b_l \\
&= (\delta_{il}\delta_{kj} - \frac{1}{4}\delta_{ij}\delta_{kl})b_i^\dagger b_j b_k^\dagger b_l \\
&= b_i^\dagger b_k b_k^\dagger b_i - \frac{1}{4}b_i^\dagger b_i b_k^\dagger b_k.
\end{aligned} \tag{A.4.3}$$

Since we have

$$\begin{aligned}
b_i^\dagger b_k b_k^\dagger b_i &= b_i^\dagger(4I - b_k^\dagger b_k)b_i = 4b_i^\dagger b_i - b_i^\dagger b_k^\dagger b_k b_i = 4N + b_i^\dagger b_k^\dagger b_i b_k \\
&= 4N + b_i^\dagger(\delta_{ki}I - b_i b_k^\dagger)b_k = 4N + b_i^\dagger b_i - b_i^\dagger b_i b_k^\dagger b_k \\
&= 4N + N - (N)(N) \\
&= 5N - N^2\,,
\end{aligned} \tag{A.4.4}$$

and

$$\begin{aligned}
N^2 &= (N_1+N_2+N_3+N_4)(N_1+N_2+N_3+N_4) = N_1^2+N_2^2+N_3^2+N_4^2 \\
&+ 2(N_1N_2+N_1N_3+N_2N_3+N_1N_4+N_3N_4+N_2N_4) \\
&= N + 2[N_1N_2+N_3N_4+(N_1+N_2)(N_3+N_4)]\,,
\end{aligned} \tag{A.4.5}$$

the calculation yields

$$\begin{aligned}
(Z_{gh})^2 &= 5N - N^2 - \frac{N^2}{4} = 5\left(N - \frac{N^2}{4}\right) \\
&= 5\{N - (1/4)\{2[N_1N_2+N_3N_4+(N_1+N_2)(N_3+N_4)]+N\}\}.
\end{aligned} \tag{A.4.6}$$

$$(Z_{gh})^2 = \frac{15}{4}N - \frac{5}{2}(N_1N_2 + N_3N_4) - \frac{5}{2}(N_1 + N_2)(N_3 + N_4)\,. \tag{A.4.7}$$

Using $(Z_{gh})^2$, $(Z_{ab})^2$ on the basis (A.1.5) yields the results found in chapter 3 in equations (3.2.34), (3.2.38) and (3.2.42).

APPENDIX B

COADJOINT ORBITS OF SU(3)

In order to construct the coadjoint orbits of $SU(3)$, we may start with the group elements

$$g_s = \begin{pmatrix} m_{11} & m_{12} & m_{13} \\ m_{21} & m_{22} & m_{23} \\ m_{31} & m_{32} & m_{33} \end{pmatrix}, \qquad g_s \in SU(3). \tag{B.1}$$

where m_{ij} are complex numbers and $g_s^\dagger g_s = 1$. Consider also the diagonal matrix

$$J_{dg} = diag(ic_1, ic_2, ic_3)\,, \qquad c_1, c_2, c_3 \in \mathbb{R}. \tag{B.2}$$

For the possible coadjoint orbits the requirement is that

$$J_{dg} = g_s J_{dg} {g_s}^\dagger, \tag{B.3}$$

written out explicitly this yields

$$diag(ic_1, ic_2, ic_3) = i g_s diag(c_1, c_2, c_3) {g_s}^\dagger = i \begin{pmatrix} M_{11} & M_{12} & M_{13} \\ M_{21} & M_{22} & M_{23} \\ M_{31} & M_{32} & M_{33} \end{pmatrix}, \tag{B.4}$$

where $M_{\mu\nu}$ (μ, ν=1,2,3) are given as

$$M_{11} = c_1|m_{11}|^2 + c_2|m_{12}|^2 + c_3|m_{13}|^2, \tag{B.5a}$$

$$M_{12} = c_1 m_{11} {m_{21}}^* + c_2 m_{12} {m_{22}}^* + c_3 m_{13} {m_{23}}^*, \tag{B.5b}$$

$$M_{13} = c_1 m_{11} {m_{31}}^* + c_2 m_{12} {m_{32}}^* + c_3 m_{13} {m_{33}}^*, \tag{B.5c}$$

$$M_{21} = c_1 m_{21} {m_{11}}^* + c_2 m_{22} {m_{12}}^* + c_3 m_{23} {m_{13}}^*, \tag{B.5d}$$

$$M_{22} = c_1|m_{21}|^2 + c_2|m_{22}|^2 + c_3|m_{23}|^2, \tag{B.5e}$$

$$M_{23} = c_1 m_{21} {m_{31}}^* + c_2 m_{22} {m_{32}}^* + c_3 m_{23} {m_{33}}^*, \tag{B.5f}$$

$$M_{31} = c_1 m_{31} {m_{11}}^* + c_2 m_{32} {m_{12}}^* + c_3 m_{33} {m_{13}}^*, \tag{B.5g}$$

$$M_{32} = c_1 m_{31} {m_{21}}^* + c_2 m_{32} {m_{22}}^* + c_3 m_{33} {m_{23}}^*, \tag{B.5h}$$

$$M_{33} = c_1 |m_{31}|^2 + c_2 |m_{32}|^2 + c_3 |m_{33}|^2. \tag{B.5i}$$

There are three distinct cases of interest.

Case 1: $c_1 = c_2 = c_3 = c$. This is the trivial case.

$$g_s J_{dg} {g_s}^\dagger = g_s (ic\mathbb{1}_3) {g_s}^\dagger = ic g_s {g_s}^{-1} = ic\mathbb{1}_3 = J_{dg}. \tag{B.6}$$

The stabilizer is $SU(3)$ and the orbit is just a point.

Case 2: $c_1 \neq c_2 \neq c_3$. In this case, (B.5a) requires

$$c_1 |m_{11}|^2 + c_2 |m_{12}|^2 + c_3 |m_{13}|^2 = c_1, \tag{B.7}$$

and it is solved by

$$m_{12} = m_{13} = 0\,, \quad |m_{11}| = 1 \rightarrow m_{11} = e^{i\theta_{11}}. \tag{B.8}$$

Similarly, we have

$$c_1 |m_{21}|^2 + c_2 |m_{22}|^2 + c_3 |m_{23}|^2 = c_2, \tag{B.9}$$

from (B.5e) and the solution is

$$m_{21} = m_{23} = 0\,, \quad m_{22} = e^{i\theta_{22}}\,. \tag{B.10}$$

Finally from (B.5i), we have

$$c_1 |m_{31}|^2 + c_2 |m_{32}|^2 + c_3 |m_{33}|^2 = c_3, \tag{B.11}$$

$$m_{31} = m_{32} = 0\,, \quad m_{33} = e^{i\theta_{33}}. \tag{B.12}$$

Remaining equations in (B.5) are automatically satisfied by these solutions. We may write

$$1 = \det(g_s) = e^{i\theta_{11}} e^{i\theta_{22}} e^{i\theta_{33}} \rightarrow e^{i\theta_{33}} = e^{-i(\theta_{11}+\theta_{22})}. \tag{B.13}$$

$$g_s = \begin{pmatrix} e^{i\theta_{11}} & 0 & 0 \\ 0 & e^{i\theta_{22}} & 0 \\ 0 & 0 & e^{-i(\theta_{11}+\theta_{22})} \end{pmatrix}. \tag{B.14}$$

Since there are two independent phases, we see that the orbit is $SU(3)/(U(1)\times U(1))$.

Case 3: $c_1 = c_2 \neq c_3$ From (B.5a) we have

$$c_1|m_{11}|^2 + c_1|m_{12}|^2 + c_3|m_{13}|^2 = c_1\,, \tag{B.15}$$

but this time we have

$$m_{13} = 0\,, \quad |m_{11}|^2 + |m_{12}|^2 = 1\,, \tag{B.16}$$

contrary to (B.8). Proceeding with (B.5e) and (B.5i) we have

$$c_1|m_{21}|^2 + c_1|m_{22}|^2 + c_3|m_{23}|^2 = c_1, \tag{B.17}$$

$$m_{23} = 0\,, \quad |m_{21}|^2 + |m_{22}|^2 = 1. \tag{B.18}$$

$$c_1|m_{31}|^2 + c_1|m_{32}|^2 + c_3|m_{33}|^2 = c_3, \tag{B.19}$$

$$m_{31} = m_{32} = 0\,, \quad m_{33} = e^{i\theta_{33}}. \tag{B.20}$$

Putting these together we have

$$g_s = \begin{pmatrix} m_{11} & m_{12} & 0 \\ m_{21} & m_{22} & 0 \\ 0 & 0 & e^{i\theta_{33}} \end{pmatrix} \equiv \begin{pmatrix} G_m & 0 \\ 0 & e^{i\theta_{33}} \end{pmatrix}. \tag{B.21}$$

Since $\det(g_s) = 1$ we have $\det(G_m) = e^{-i\theta_{33}}$, therefore the corresponding orbit is $SU(3)/S[U(2)\times U(1)]$. This is a 4-dimensional manifold and it is isomorphic to the complex projective space $\mathbb{CP}^2$.

APPENDIX C

THE WESS-ZUMINO TERM AND COADJOINT ORBITS

In order to understand some features of coadjoint orbits of compact Lie groups, we follow the method given in [80] and discuss the quantization of the Wess-Zumino Lagrangian. A common property of this kind of systems is that elements S of the group G are treated as dynamical variables. The action S_{wz} is given by

$$S_{wz} = -i \int \mathrm{tr}\Big(\Lambda S^{-1}\dot{S}\Big)\,\mathrm{d}t, \tag{C.1}$$

where $\dot{S} = \frac{dS}{dt}$. The group element S can be parametrized in terms of real variables $(\xi_1, \xi_2, ..., \xi_d)$ and expressed as

$$S(\xi) = e^{i\sum_k T_k \xi_k}, \tag{C.2}$$

where d is the dimension of the Lie algebra of G and $\xi_i \equiv \xi_i(t)$. T_k's form a basis for this Lie algebra and satisfy

$$[T_k, T_l] = i f_{kls} T_s, \tag{C.3}$$

where f_{kls} are the corresponding structure constants. Now let us define a set of functions

$$f(\mathscr{E}) \equiv (f_1(\mathscr{E}), f_2(\mathscr{E}), ..., f_d(\mathscr{E})), \tag{C.4}$$

where $\mathscr{E} = (\mathscr{E}_1, \mathscr{E}_2, ..., \mathscr{E}_d)$ and $f(0) = \xi$. A change in the local coordinates $\xi \to f(\mathscr{E})$ leads to

$$S[f(\mathscr{E})] = e^{i\sum_k T_k \mathscr{E}_k} S(\xi), \tag{C.5}$$

and

$$\frac{\partial S}{\partial \mathscr{E}_l} = \sum_s \frac{\partial S}{\partial f_s}\frac{\partial f_s}{\partial \mathscr{E}_l} = i T_k \delta_{kl} e^{i\sum_k T_k \mathscr{E}_k} S(\xi)\,. \tag{C.6}$$

At $\mathscr{E} = 0$, we have

$$i T_l S(\xi) = \sum_s \frac{\partial S}{\partial f_s}\bigg|_{\mathscr{E}=0} \frac{\partial f_s}{\partial \mathscr{E}_l}\bigg|_{\mathscr{E}=0} = \sum_s \frac{\partial S(\xi)}{\partial \xi_s} N_{sl}\,, \quad (N(\xi))_{sl} = \frac{\partial f_s}{\partial \mathscr{E}_l}\bigg|_{\mathscr{E}=0} \tag{C.7}$$

Note that, for the total variation of S we may write

$$dS = \sum_l \frac{\partial S}{\partial \xi_l} d\xi_l \,, \quad \dot{S} = \frac{dS}{dt} = \sum_l \frac{\partial S}{\partial \xi_l} \dot{\xi}_l \,, \tag{C.8}$$

from which it follows that

$$\frac{\partial \dot{S}}{\partial \dot{\xi}_k} = \sum_l \frac{\partial S}{\partial \xi_l} \delta_{kl} = \frac{\partial S}{\partial \xi_k} . \tag{C.9}$$

Using (C.9) conjugate momenta is derived from (C.1)

$$\begin{aligned}
\pi_k &= \frac{\partial L}{\partial \dot{\xi}_k} \\
&= -i \frac{\partial}{\partial \dot{\xi}_k} \sum_{a_1} ((\Lambda)_{a_1 b_1} (S^{-1})_{b_1 c_1} (\dot{S})_{c_1 a_1}) \\
&= -i \sum_{a_1} ((\Lambda)_{a_1 b_1} (S^{-1})_{b_1 c_1} \frac{\partial}{\partial \dot{\xi}_k} (\dot{S})_{c_1 a_1}) \\
&= -i \ \mathrm{tr} \left(\Lambda S^{-1} \frac{\partial \dot{S}}{\partial \dot{\xi}_k} \right) \\
&= -i \ \mathrm{tr} \left(\Lambda S^{-1} \frac{\partial S}{\partial \xi_k} \right) .
\end{aligned} \tag{C.10}$$

Local coordinates and conjugate momenta satisfy the canonical Poisson brackets

$$\{\xi_k, \pi_l\} = \delta_{kl} \,, \quad \{\xi_k, \xi_l\} = \{\pi_k, \pi_l\} = 0 \,. \tag{C.11}$$

Since $N(\xi)$ in (C.7) is an invertible matrix, conjugate momenta, t_i, associated to variables ξ can be written as

$$t_k = -\sum_l \pi_l N_{lk} \,. \tag{C.12}$$

They satisfy the following Poisson brackets

$$\{t_k, S\} = i T_k S \,, \tag{C.13a}$$

$$\left\{t_k, S^{-1}\right\} = -i S^{-1} T_k \,, \tag{C.13b}$$

$$\{t_k, t_l\} = f_{kls} t_s \,. \tag{C.13c}$$

These relations make it obvious that t_i are the generators of the left action of G.

It is also possible to define a right action of the generators

$$\Lambda_k = {t_k}^R = -\sum_l t_l R_{lk}, \tag{C.14}$$

where $R_{lk} = R_{lk}(S)$ denote the adjoint representation of G, which has the property

$$\sum_l R_{lk} T_l = S T_k S^{-1} . \tag{C.15}$$

The right generators satisfy the following Poisson brackets

$$\{\Lambda_k, S\} = -i S T_k , \tag{C.16a}$$

$$\left\{\Lambda_k, S^{-1}\right\} = i T_k S^{-1} , \tag{C.16b}$$

$$\{\Lambda_k, \Lambda_l\} = f_{kls} \Lambda_s . \tag{C.16c}$$

Comparison with (C.7) shows that Λ_k are indeed the generators of the right action of G

$$\sum_l i T_l S (N^{-1})_{lp} = \sum_l \sum_s \frac{\partial S}{\partial \xi_s} N_{sl} (N^{-1})_{lp} = \sum_s \frac{\partial S}{\partial \xi_s} \delta_{sp} = \frac{\partial S}{\partial \xi_p}, \tag{C.17}$$

$$\frac{\partial S}{\partial \xi_p} = i \sum_l T_l S (N^{-1})_{lp} . \tag{C.18}$$

By combining equations (C.10),(C.12),(C.14) and (C.18) the right generators can be rewritten as

$$\begin{aligned}
\Lambda_k = t_k{}^R &= -\sum_u t_u R_{uk} = \sum_{u,l} \pi_l N_{lu} R_{uk} \\
&= \sum_{u,l} -i \operatorname{tr}\left(\Lambda S^{-1} \frac{\partial S}{\partial \xi_l} \right) N_{lu} R_{uk} \\
&= -i \sum_{u,l,s} \operatorname{tr}\big(\Lambda S^{-1} i T_s S (N^{-1})_{sl} \big) N_{lu} R_{uk} \\
&= \sum_{u,s} \operatorname{tr}\big(\Lambda S^{-1} T_s S \big) \delta_{su} R_{uk} \\
&= \sum_s \operatorname{tr}\big(\Lambda S^{-1} T_s S \big) R_{sk} \\
&= \sum_s \operatorname{tr}\big(\Lambda S^{-1} (R_{sk} T_s) S \big) \\
&= \operatorname{tr}\big(\Lambda S^{-1} (S T_k S^{-1}) S \big) \\
&= \operatorname{tr}(\Lambda T_k) .
\end{aligned} \tag{C.19}$$

APPENDIX D

QUANTIZATION OF O_4

For the quantization of the coadjoint orbit $O_4 \cong \mathbb{CP}^3$, we should concentrate on the Lie algebra of $SU(4)$ and the L_{wz} in (C.1) written for $S \in SU(4)$. The latter has 15 generators, T_k, $(k = 1, ..., 15)$ that satisfy the trace condition

$$\mathrm{tr}(T_k T_l) = \frac{1}{2}\delta_{kl}\,. \tag{D.1}$$

We take $\Lambda = \frac{\sqrt{6}}{2} n_0 T_{15}$ where n_0 is the $U(1)$ charge. The right generators are

$$\Lambda_k = \frac{\sqrt{6}}{2}\,\mathrm{tr}(n_0 T_{15} T_k) = \frac{\sqrt{6}}{4}\, n_0 \delta_{k,15}\,. \tag{D.2}$$

Since we will apply Dirac constraint formalism for quantization, the last equation should be reexpressed more precisely as

$$C_k = \Lambda_k - \frac{\sqrt{6}}{4}\, n_0 \delta_{k,15} \approx 0, \tag{D.3}$$

where " $\approx$ " denotes a weak equality and C_k is a primary constraint. As it is emphasized in [63], the constraint equations $\Lambda_k = \frac{\sqrt{6}}{4} n_0 \delta_{k,15}$ must not be used before working out all the Poisson brackets. To remind us of this rule, constraint equations are written as $C_k \approx 0$ and said to be "weakly equal" to zero.

According to Dirac formalism, constraint equations can be classified as first-class constraints and second-class constraints. If a constraint has vanishing Poisson brackets with all other constraints, it is called first-class constraint. Otherwise, it is called a second-class constraint [81].

The non-vanishing structure constants f_{kls} of the Lie algebra of $SU(4)$ can be found in several sources, for instance in [67] and [82]. Now let us start with the Poisson brackets of Λ_1. For instance, we have

$$\{\Lambda_1, \Lambda_2\} = f_{123}\Lambda_3 = \Lambda_3 \approx \frac{\sqrt{6}}{4}\, n_0 \delta_{3,15} = 0, \tag{D.4}$$

$$\{\Lambda_1, \Lambda_4\} = f_{147}\Lambda_7 = \frac{1}{2}\Lambda_7 \approx \frac{\sqrt{6}}{8} n_0 \delta_{7,15} = 0\,. \tag{D.5}$$

The remaining Poisson brackets also vanish. Therefore, we deduce that Λ_1 is a first-class constraint. In fact, we have all $\Lambda_{a'}$ with $a' = 1, \ldots, 8$ are primary first-class constraints and they constitute an $SU(3)$ subalgebra of $SU(4)$. We have

$$\{\Lambda_{a'}, \Lambda_{b'}\} = f_{a'b'c'}\Lambda_{c'} \approx 0\,. \tag{D.6}$$

Λ_{15} has also zero Poisson brackets with all other constraints due to (D.3). Thus, we conclude that Λ_k ($k = 1, 2, \ldots, 8, 15$) are all first-class constraints.

For Λ_9, we have

$$\{\Lambda_9, \Lambda_{10}\} = f_{9,10,15}\Lambda_{15} = \sqrt{\frac{2}{3}}\Lambda_{15} \approx \sqrt{\frac{2}{3}}\left(\frac{\sqrt{6}}{4} n_0\right) = \frac{n_0}{2}, \tag{D.7}$$

$\{\Lambda_9, \Lambda_{10}\} \approx \frac{n_0}{2}$, so Λ_9 is a second class constraint. In fact, all of the remaining six constraints Λ_l ($l = 9, ..., 14$) are second-class constraints. However, they can be rearranged to form a complete set of first-class constraints. Consider the combinations

$$\Phi_{n'}{}^{\pm} = \Lambda_{n'} \pm i\Lambda_{n'+1}, \tag{D.8}$$

where $n' = 9, 11, 13$. If $n' = 9$, we have

$$\left\{\Lambda_{10}, \Phi_9{}^{\pm}\right\} = \{\Lambda_{10}, \Lambda_9\} \tag{D.9}$$

$$= f_{10,9,3}\Lambda_3 \tag{D.10}$$

$$= -\frac{1}{2}\Lambda_3 \approx 0\,. \tag{D.11}$$

Proceeding similarly, it is easy to see that either the $\Phi_{n'}{}^{+}$ or $\Phi_{n'}{}^{-}$ can be shown to constitute first-class constraints for $n_0 > 0$ and $n_0 < 0$ respectively. Furthermore, their Poisson brackets with Λ_3 reveal another important identity; for instance we have

$$\begin{aligned}\left\{\Lambda_3, \Phi_9{}^{\pm}\right\} &= \{\Lambda_3, \Lambda_9\} \pm i\,\{\Lambda_3, \Lambda_{10}\} \\ &= -\frac{i}{2}(i\Lambda_{10} \pm \Lambda_9) \\ &= \mp\frac{i}{2}\Phi_9{}^{\pm}\,.\end{aligned} \tag{D.12}$$

Similar relations for $\Phi_{11}{}^{\pm}$ and $\Phi_{13}{}^{\pm}$ are

$$\left\{\Lambda_3, \Phi_{11}{}^{\pm}\right\} = \pm\frac{i}{2}\Phi_{11}{}^{\pm}, \quad \left\{\Lambda_3, \Phi_{13}{}^{\pm}\right\} = 0, \tag{D.13}$$

so Poisson brackets of the form $\left\{\Lambda_3, {\Phi_{n'}}^{\pm}\right\}$ vanish on the surface defined by equation (D.3) for $n_0 > 0$ & $n_0 < 0$, respectively. In addition, Λ_8 and Λ_{15} satisfy

$$\left\{\Lambda_8, {\Phi_9}^{\pm}\right\} = \mp\frac{i}{2\sqrt{3}}{\Phi_9}^{\pm}, \quad \left\{\Lambda_8, {\Phi_{11}}^{\pm}\right\} = \mp\frac{i}{2\sqrt{3}}{\Phi_{11}}^{\pm}, \tag{D.14}$$

$$\left\{\Lambda_8, {\Phi_{13}}^{\pm}\right\} = \pm\frac{i}{\sqrt{3}}{\Phi_{13}}^{\pm}, \quad \left\{\Lambda_{15}, {\Phi_{n'}}^{\pm}\right\} = \mp i\sqrt{\frac{2}{3}}{\Phi_{n'}}^{\pm}. \tag{D.15}$$

Then, Poisson brackets $\left\{\Lambda_8, {\Phi_{n'}}^{\pm}\right\}$ and $\left\{\Lambda_{15}, {\Phi_{n'}}^{\pm}\right\}$ also weakly equal to zero for $n_0 > 0$ & $n_0 < 0$, corresponding to $\pm$ superscripts. We also infer from last four equations that ${\Phi_{n'}}^{\pm}$ have the structure of ladder operators of $SU(4)$.

Summarizing we have

$$\Phi_k \coloneqq \Lambda_k \approx 0\,, \quad \Phi_{15} \coloneqq \Lambda_{15} - \frac{\sqrt{6}}{4}n_0 \approx 0\,, \qquad k = 1, 2, \ldots, 8\,, \tag{D.16}$$

$${\Phi_{n'}}^{+} \approx 0 \;\text{ for }\; n_0 > 0\,, \quad {\Phi_{n'}}^{-} \approx 0 \;\text{ for }\; n_0 < 0\,. \tag{D.17}$$

The states satisfying these constraints have the non-vanishing eigenvalue $\frac{\sqrt{6}}{4}n_0$ of Λ_{15}

$$\Lambda_{15}\left|\Lambda_3, \Lambda_8, \Lambda_{15}\right\rangle = \frac{\sqrt{6}}{4}n_0\left|\Lambda_3, \Lambda_8, \Lambda_{15}\right\rangle\,. \tag{D.18}$$

Together with equations (D.16), the set of constraints ${\Phi_{n'}}^{\pm}$ map to different irreducible representations of SU(4). For $n_0 < 0$, they select $(0, 0, |n_0|)$ irreps and for $n_0 > 0$ they select $(n_0, 0, 0)$ irreps. These irreducible representations are IRR of $SU(4)$ which may be obtained from the $|n_0|$ fold symmetric tensor product of $(0, 0, 1)$ and $(1, 0, 0)$ respectively. Their dimensions are equal to

$$\frac{1}{6}(|n_0| + 1)(|n_0| + 2)(|n_0| + 3)\,. \tag{D.19}$$

In this way, we complete the quantization procedure of $\mathbb{CP}^3$. In agreement with [51], representations obtained are totally symmetric representations of $SU(4)$.

APPENDIX E

CANONICAL COHERENT STATES

Our discussion of canonical coherent states begins with a consideration of the simple harmonic oscillator Hamiltonian given by [83]

$$H_{sh} = \frac{1}{2m}\hat{p}^2 + \frac{1}{2}m\omega^2\hat{x}^2 = \hbar\omega\left(\hat{a}^\dagger\hat{a} + \frac{1}{2}\right), \tag{E.1}$$

where $\hat{a}$ and $\hat{a}^\dagger$

$$\hat{a} = \sqrt{\frac{m\omega}{2\hbar}}\left(\hat{x} + \frac{i}{m\omega}\hat{p}\right), \quad \hat{a}^\dagger = \sqrt{\frac{m\omega}{2\hbar}}\left(\hat{x} - \frac{i}{m\omega}\hat{p}\right), \tag{E.2}$$

are the canonical annihilation and creation operators, respectively. It is obvious that both $\hat{a}$ and $\hat{a}^\dagger$ are non-Hermitian, dimensionless and they satisfy the basic commutation relation

$$\left[\hat{a}, \hat{a}^\dagger\right] = 1. \tag{E.3}$$

The occupation number operator is defined as

$$\widehat{M} \equiv \hat{a}^\dagger\hat{a}\,, \tag{E.4}$$

and satisfies

$$\left[\widehat{M}, \hat{a}\right] = -\hat{a}, \quad \left[\widehat{M}, \hat{a}^\dagger\right] = \hat{a}^\dagger. \tag{E.5}$$

Simultaneous eigenkets of H_{sh} and $\widehat{M}$ are denoted by its eigenvalue m, and span the infinite dimensional Fock space, spanned by $|m\rangle$. We have

$$\widehat{M}\,|m\rangle = m\,|m\rangle\,. \tag{E.6}$$

The actions of annihilation and creation operators on $|m\rangle$ are listed by

$$\hat{a}\,|m\rangle = \sqrt{m}\,|m-1\rangle\,, \quad \hat{a}^\dagger\,|m\rangle = \sqrt{m+1}\,|m+1\rangle\,. \tag{E.7}$$

The fact that any energy eigenket can be obtained by the successive application of $\hat{a}^\dagger$ on the ground state is manifestly evident from the relation

$$|m\rangle = \frac{1}{\sqrt{m!}}\left(\hat{a}^\dagger\right)^m |0\rangle \,. \tag{E.8}$$

It is straightforward to determine the uncertainty product for the eigenstates $|m\rangle$:

$$\begin{aligned}\left\langle \left(\Delta\hat{x}\right)^2 \right\rangle_m \left\langle \left(\Delta\hat{p}\right)^2 \right\rangle_m &= \left(\left\langle \hat{x}^2 \right\rangle_m - \langle\hat{x}\rangle_m^2\right)\left(\left\langle \hat{p}^2 \right\rangle_m - \langle\hat{p}\rangle_m^2\right) \\ &= \frac{\hbar}{m\omega}\left(n+\frac{1}{2}\right) m\hbar\omega\left(n+\frac{1}{2}\right) \\ &= \frac{\hbar^2}{4}(2n+1)^2.\end{aligned} \tag{E.9}$$

Therefore, only the ground state $|0\rangle$ saturates the Heisenberg's uncertainty bound.

A coherent state $|\eta\rangle$ is an eigenstate of the non-Hermitian operator $\hat{a}$ [84]

$$\hat{a}\,|\eta\rangle = \eta\,|\eta\rangle \,, \tag{E.10}$$

where η is a complex number. From this definition and equation (E.8), we have

$$\begin{aligned}|\eta\rangle &= \sum_m |m\rangle\langle m|\eta\rangle \\ &= \sum_m \frac{1}{\sqrt{m!}}\,|m\rangle\langle 0|\hat{a}^m|\eta\rangle \\ &= \langle 0|\eta\rangle \sum_m \frac{\eta^m}{\sqrt{m!}}\,|m\rangle \,.\end{aligned} \tag{E.11}$$

Normalization of $|\eta\rangle$ can be fixed by the condition

$$\begin{aligned}1 = \langle\eta|\eta\rangle &= |\langle 0|\eta\rangle|^2 \sum_{k,m} \frac{(\eta^*)^k \eta^m}{\sqrt{k!m!}}\,\langle k|m\rangle \\ &= |\langle 0|\eta\rangle|^2 \sum_k \frac{1}{k!}\left(|\eta|^2\right)^k \\ &= |\langle 0|\eta\rangle|^2 e^{|\eta|^2},\end{aligned} \tag{E.12}$$

upon choosing $\langle 0|\eta\rangle$ to be real and positive yields

$$|\eta\rangle = e^{-\frac{1}{2}|\eta|^2} \sum_m \frac{\eta^m}{\sqrt{m!}}\,|m\rangle \,. \tag{E.13}$$

Combining (E.8) and (E.13), one can obtain

$$|\eta\rangle = e^{-\frac{1}{2}|\eta|^2} \sum_m \frac{\eta^m}{\sqrt{m!}} \frac{1}{\sqrt{m!}}\left(\hat{a}^\dagger\right)^m |0\rangle$$

$$
\begin{aligned}
&= e^{-\frac{1}{2}|\eta|^2} \sum_m \frac{\left(\eta \hat{a}^\dagger\right)^m}{m!} |0\rangle \\
&= e^{-\frac{1}{2}|\eta|^2} e^{\eta \hat{a}^\dagger} |0\rangle \\
&= e^{-\frac{1}{2}|\eta|^2} e^{\eta \hat{a}^\dagger} e^{-\eta^* \hat{a}} |0\rangle . \qquad \text{(E.14)}
\end{aligned}
$$

Here to derive the last line, we employed equation (E.10) and the requirements that the state remains normalized and the corresponding dual element is $\langle \eta |$.

Recalling the Baker-Campbell-Hausdorff formula gives [85]

$$
e^{M_1} e^{M_2} = e^{M_1 + M_2 + \frac{1}{2}[M_1, M_2]}, \qquad \text{(E.15)}
$$

for $[M_1, [M_1, M_2]] = [M_2, [M_1, M_2]] = 0$, using (E.15) equation (E.14) assumes the form

$$
\begin{aligned}
|\eta\rangle &= e^{-\frac{1}{2}|\eta|^2} e^{\eta \hat{a}^\dagger - \eta^* \hat{a} - \frac{|\eta|^2}{2}\left[\hat{a}^\dagger, \hat{a}\right]} |0\rangle \\
&= e^{-\frac{1}{2}|\eta|^2} e^{\eta \hat{a}^\dagger - \eta^* \hat{a}} e^{\frac{1}{2}|\eta|^2} |0\rangle \\
&= e^{\eta \hat{a}^\dagger - \eta^* \hat{a}} |0\rangle . \qquad \text{(E.16)}
\end{aligned}
$$

Let us define the displacement operator as

$$
D(\eta) = e^{\eta \hat{a}^\dagger - \eta^* \hat{a}}, \qquad \text{(E.17)}
$$

then, (E.16) can be simply expressed as

$$
|\eta\rangle = D(\eta) |0\rangle , \qquad \text{(E.18)}
$$

which offers another way of understanding the notion of coherent state $|\eta\rangle$ as a displaced ground state by the magnitude $|\eta|$ of η. Alternatively, (E.18) can be taken as the definition of η and the property (E.10) can be derived from this.

The uncertainty products for coherent states $|\eta\rangle$ are

$$
\begin{aligned}
\left\langle \left(\Delta \hat{x}\right)^2 \right\rangle_\eta \left\langle \left(\Delta \hat{p}\right)^2 \right\rangle_\eta &= \left(\langle \eta | \hat{x}^2 | \eta \rangle - \langle \eta | \hat{x} | \eta \rangle^2 \right) \left(\langle \eta | \hat{p}^2 | \eta \rangle - \langle \eta | \hat{p} | \eta \rangle^2 \right) \\
&= \frac{\hbar}{2m\omega} \left(\eta^2 + 1 + 2\eta^* \eta + (\eta^*)^2 - (\eta + \eta^*)^2 \right) \qquad \text{(E.19)} \\
&\left(\frac{-m\hbar\omega}{2} \right) \left((\eta^*)^2 - 1 - 2\eta^* \eta + \eta^2 - (\eta^* - \eta)^2 \right) \\
&= \frac{\hbar^2}{4},
\end{aligned}
$$

demonstrating that the canonical coherent states are minimum uncertainty states.

The overlap of two coherent states reads

$$\begin{aligned}\langle\eta_1|\eta_2\rangle &= \left(e^{-\frac{1}{2}|\eta_1|^2}\sum_m \langle m|\,\frac{\left(\eta_1{}^*\right)^m}{\sqrt{m!}}\right)\left(e^{-\frac{1}{2}|\eta_2|^2}\sum_k \frac{\eta_2{}^k}{\sqrt{k!}}\,|k\rangle\right)\\ &= e^{-\frac{1}{2}\left(|\eta_1|^2+|\eta_2|^2\right)}\sum_k \frac{\left(\eta_1{}^*\eta_2\right)^k}{k!}\\ &= e^{\eta_1{}^*\eta_2-\frac{1}{2}\left(|\eta_1|^2+|\eta_2|^2\right)}.\end{aligned} \tag{E.20}$$

Therefore, we have

$$|\langle\eta_1|\eta_2\rangle|^2 = \langle\eta_2|\eta_1\rangle\langle\eta_1|\eta_2\rangle = e^{-|\eta_1-\eta_2|^2}, \tag{E.21}$$

indicating that the coherent states form an overcomplete basis as $|\langle\eta_1|\eta_2\rangle|^2$ attains a nonzero value if η_1 is not equal to η_2. It can be shown that the closure relation can be defined as follows [84]

$$\frac{1}{\pi}\int_{\mathbb{C}} \mathrm{d}^2\eta|\eta\rangle\langle\eta| = \mathbb{1}. \tag{E.22}$$

A detailed discussion and further details may be found in [84, 86, 87].

APPENDIX F

DERIVATION OF CP^3 EMBEDDING FUNCTIONS

In chapter 3, we have written equation (3.5.6) as follows

$$
\begin{aligned}
y_k &= \langle M| T_k |M\rangle && \text{(F.1)}\\
&= \langle v| e^{iH} T_k e^{-iH} |v\rangle = \sum_{l=1}^{15} \langle v| p_{k,l} T_l |v\rangle \\
&= \langle v| p_{k,15} T_{15} |v\rangle = \langle v| p_{k,15} t_{15} |v\rangle && \text{(F.2)}\\
&= \frac{1}{2\sqrt{6}} \langle v| p_{k,15} |v\rangle && \text{(F.3)}\\
&= \frac{1}{2\sqrt{6}} p_{k,15}\,,
\end{aligned}
$$

where, we have used the notation

$$
H = -(aT^9 + bT^{10} + cT^{11} + dT^{12} + eT^{13} + fT^{14}). \qquad \text{(F.4)}
$$

In order to compute the embedding functions we may make use of the B.C.H. formula, which is given as [70]

$$
e^{iH} T_k e^{-iH} = T_k + i[H, T_k] + \frac{i^2}{2!}[H,[H,T_k]] + \frac{i^3}{3!}[H,[H,[H,T_k]]] + ... \qquad \text{(F.5)}
$$

As a concrete example we work out $p_{k,15}$ for $k = 1$, the remaining functions y_k can also be determined by the application of the same method. We have,

$$
\begin{aligned}
\sum_{l=1}^{15} p_{1,l} T_l &= e^{iH} T_1 e^{-iH} \\
&= T_1 + i[H, T_1] - \frac{1}{2}[H,[H,T_1]] - \frac{i}{6}[H,[H,[H,T_1]]] + ... \\
&= \left(\frac{a^4}{24} + \frac{a^2 b^2}{12} + \frac{7a^2 c^2}{12} + \frac{a^2 d^2}{12} + ... \right) T_1 && \text{(F.6)}
\end{aligned}
$$

$$
\begin{aligned}
&+\left(\frac{db^2c}{2}+\frac{abc^2}{2}-\frac{ad^2b}{2}-\frac{a^2dc}{2}+...\right)T_2\\
&+\left(\frac{a^3c}{4}-\frac{ac^3}{4}-\frac{bd^3}{4}+\frac{b^3d}{4}+...\right)T_3\\
&+\dots\\
&-2\sqrt{6}\left(-\frac{a^3c}{9}-\frac{a^2bd}{9}-\frac{ab^2c}{9}-\frac{ac^3}{9}+...\right)T_{15}\,.
\end{aligned}
$$

By rearranging the coefficient of the fifteenth generator, we obtain

$$
\begin{aligned}
p_{1,15} &= -2\sqrt{6}\,\frac{(ac+bd)}{135}\Big(2a^4+4a^2b^2+4a^2c^2+4a^2d^2+4a^2e^2+4a^2f^2-15a^2\\
&\quad+2b^4+4b^2c^2+4b^2d^2+4b^2e^2+4b^2f^2-15b^2+2c^4+4c^2d^2+4c^2e^2+4c^2f^2\\
&\quad-15c^2+2d^4+4d^2e^2+4d^2f^2-15d^2+2e^4+4e^2f^2-15e^2+2f^4-15f^2\\
&\quad+45+...\Big)=-\frac{2\sqrt{6}}{135}(ac+bd)\Big[45-15\Big(a^2+b^2+c^2+d^2+e^2+f^2\Big)\\
&\quad+2\Big(a^2+b^2+c^2+d^2+e^2+f^2\Big)^2+...\Big] \qquad \text{(F.7)}\\
&=-\frac{2\sqrt{6}}{135}(ac+bd)\Big(45-15r^2+2r^4+...\Big)\\
&=-\frac{2\sqrt{6}}{135}45(ac+bd)\Big(1-\frac{r^2}{3}+\frac{2}{45}r^4+...\Big)=-\frac{2\sqrt{6}}{3}(ac+bd)\frac{\sin^2(r)}{r^2}\,,
\end{aligned}
$$

and this finally gives

$$
y_1=\frac{1}{2\sqrt{6}}\,p_{1,15}=-\frac{1}{3}(ac+bd)\frac{\sin^2(r)}{r^2}. \qquad \text{(F.8)}
$$

APPENDIX G

MATLAB CODES

The MATLAB programming language is a powerful and versatile tool to perform calculations on large collections of data. In this regard, it was chosen as the platform of implementation for the task of determination of S_n^4 matrices. In this appendix, the original MATLAB functions and script developed to calculate $X_a^{(n)}$ of (2.3.55) are presented.

```
clc; clear all; close all

N = 2;
mtxNo = 5;
Nstart = N;
Nend = N;
matSr = mtxNo;
matEd = mtxNo;

for NN = Nstart:Nend
for matNo = matSr:matEd
M = genFzzN(NN,matNo);
txtStr = strcat('N',num2str(NN),'X',num2str(matNo),'.mat');
save(txtStr,'M')
```

```
end
end
```

```
function fzM = genFzzN(fzOrd,mtrNo)

algbScL = 1/2;
sigma0 = eye(2);

sigma1 = [0 1; 1 0];
sigma2 = [0 -i;i 0];
sigma3 = [1 0; 0 -1];
Gamma1 = kron(sigma2,sigma1);
Gamma2 = kron(sigma2,sigma2);
Gamma3 = kron(sigma2,sigma3);
Gamma4 = kron(sigma1,sigma0);
Gamma5 = kron(sigma3,sigma0);
gmmLst = {Gamma1 Gamma2 Gamma3 Gamma4 Gamma5};
mtrxLst = cell(fzOrd,1);

if fzOrd == 1
fzM = gmmLst{mtrNo};
else
mtrxLst{1} = gmmLst{mtrNo};
for f = 2:fzOrd
mtrxLst{f} = eye(4);
end
fzM = fzOrd*symKron(mtrxLst);
end

fzM = algbScL*fzM;
```

```
function symMat = symKron(matLst)

set = [1 2 3 4];
k = length(matLst);
l=length(set);
shp=zeros(l^k,k);

for j = 1:k
shp(:,j)=reshape(reshape(repmat((1:l),1,l^(k-1)),l^j...
,l^(k-j))',l^k,1);
end

res=set(shp);
res = sort(res,2);
[u1, i1] = unique(res,'rows','first');
iDpRw = setdiff(1:size(res,1), i1);

res(iDpRw,:) = [];
[rN cN] = size(res);
for i = 1:rN
permV = perms(res(i,:));
[u2,i2] = unique(permV,'rows','first');
iDpRw1 = setdiff(1:size(permV,1), i2);
permV(iDpRw1,:) = [];
symLst{i} = permV;
end

symMat = zeros(rN);
for ii = 1:rN
for jj = 1:rN
symMat(ii,jj) = fndMtE(symLst{ii},symLst{jj},matLst);
```

```
end
end
```

```
function outE = fndMtE(M1,M2,mtLst)

[r1 cL1] = size(M1);
[r2 cL2] = size(M2);
sum = 0;
for a1 = 1:r1
v1 = M1(a1,:);
for b1 = 1:r2
v2 = M2(b1,:);
prd = 1;
for a2 = 1:cL1
mtNw = mtLst{a2};
prd = prd*mtNw(v1(a2),v2(a2));
end
sum = sum + prd;
end
end

outE = sum/(sqrt(r1)*sqrt(r2));
```

APPENDIX H

JACOBI ELLIPTIC FUNCTIONS

The Jacobi elliptic functions are a set of elliptic functions which appear in a variety of problems in physics such as the motion of a simple pendulum and the motion of a force-free asymmetric top [78, 88, 89]. For the derivation of Jacobi elliptic function sn, one may consider the problem of planar pendulum. The planar pendulum is assumed to consist of a small-diameter bob of mass m attached to one end of a massless rod of length l. The other end of the rod is attached to a pivot point. The energy of the system is given by

$$E = \frac{1}{2}ml^2\dot{\vartheta}^2 + mgl(1 - cos\vartheta), \tag{H.1}$$

where ϑ is the angular displacement measured from the position of equlibrium. It is possible to express this energy equation in dimensionless form as

$$\frac{E}{mgl} = \frac{1}{2\omega_0^2}\dot{\vartheta}^2 + 1 - cos\vartheta, \tag{H.2}$$

where $\omega_0^2 = \dfrac{g}{l}$. Since the kinetic energy of the pendulum vanishes at the point of maximum angular displacement, ϑ_m, (H.1) may also be rewritten as

$$E = mgl(1 - cos\vartheta_m), \tag{H.3}$$

where $0 < \vartheta_m < \pi$. From (H.2) and (H.3) , we have

$$\begin{aligned} 1 - cos\vartheta_m &= \frac{1}{2\omega_0^2}\dot{\vartheta}^2 + 1 - cos\vartheta \\ 2sin^2(\vartheta_m/2) &= \frac{1}{2\omega_0^2}\dot{\vartheta}^2 + 2sin^2(\vartheta/2) \\ \left(\frac{\mathrm{d}\vartheta}{\mathrm{d}t}\right)^2 &= 4\omega_0^2\big\{sin^2(\vartheta_m/2) - sin^2(\vartheta/2)\big\} \\ \left(\frac{\mathrm{d}\vartheta}{\mathrm{d}y}\right)^2 &= 4\big\{sin^2(\vartheta_m/2) - sin^2(\vartheta/2)\big\}, \end{aligned} \tag{H.4}$$

where the dimensionless variable y is given as

$$y = \sqrt{\frac{g}{l}}t = \omega_0 t. \tag{H.5}$$

Let us introduce the variable s as

$$s = \sin\left(\frac{\vartheta_m}{2}\right), \qquad 0 < s < 1. \tag{H.6}$$

Applying Euler's substitution [78]

$$\sin\varphi = \frac{1}{s}\sin\left(\frac{\vartheta}{2}\right), \tag{H.7}$$

on equation (H.4) yields

$$\left(\frac{\mathrm{d}\vartheta}{\mathrm{d}y}\right)^2 = 4\Big(s^2 - s^2 sin^2(\varphi)\Big). \tag{H.8}$$

Differentiating both sides of (H.7) with respect to φ, one can obtain the useful identity

$$cos\varphi = \frac{1}{2s}\cos\left(\frac{\vartheta}{2}\right)\frac{\mathrm{d}\vartheta}{\mathrm{d}\varphi}\,, \quad \frac{\mathrm{d}\vartheta}{\mathrm{d}\varphi} = \frac{2s\cos\varphi}{\cos(\vartheta/2)}\,. \tag{H.9}$$

Combining equations (H.8) and (H.9) gives

$$\begin{aligned}
\left(\frac{\mathrm{d}\vartheta}{\mathrm{d}y}\right)^2 &= \left(\frac{\mathrm{d}\vartheta}{\mathrm{d}\varphi}\right)^2\left(\frac{\mathrm{d}\varphi}{\mathrm{d}y}\right)^2 \\
4s^2\Big(1 - sin^2(\varphi)\Big) &= \frac{4s^2 cos^2(\varphi)}{\cos^2(\vartheta/2)}\left(\frac{\mathrm{d}\varphi}{\mathrm{d}y}\right)^2 \\
\left(\frac{\mathrm{d}\varphi}{\mathrm{d}y}\right)^2 &= \cos^2\left(\frac{\vartheta}{2}\right) = 1 - s^2 sin^2(\varphi),
\end{aligned} \tag{H.10}$$

then by taking the positive root, we arrive at the crucial relation

$$\frac{\mathrm{d}y}{\mathrm{d}\varphi} = \frac{1}{\sqrt{1 - s^2 sin^2(\varphi)}}, \tag{H.11}$$

which may be integrated under the given initial conditions to obtain

$$y(\varphi, s) = \int_0^{\varphi}\Big(1 - s^2 sin^2(\varphi')\Big)^{-\frac{1}{2}}\mathrm{d}\varphi'. \tag{H.12}$$

Since the pendulum is assumed to be swinging between ϑ_m and $-\vartheta_m$, equation (H.12) should be valid within the range $K(s) \geq y \geq -K(s)$ where K is the complete elliptic integral of the first kind defined as [90]

$$K(k) = \int_0^{\frac{\pi}{2}}\Big(1 - k^2 sin^2(\vartheta)\Big)^{-\frac{1}{2}}\mathrm{d}\vartheta, \tag{H.13}$$

with $0 \leq k^2 < 1$.

The Jacobi elliptic function $sn(y)$ is defined by [89]

$$sn(y) \equiv sn(y|k) = sin\varphi, \tag{H.14}$$

where y can be given in terms of the inverse-functional relationship

$$\begin{aligned} y(\varphi, k) &= sn^{-1}(sin\varphi|k) \\ &= \int_0^{sin\varphi} \Big(\Big(1-\alpha^2\Big)\Big(1-k^2\alpha^2\Big)\Big)^{-\frac{1}{2}} \mathrm{d}\alpha \\ &= \int_0^{\varphi} \Big(1-k^2 sin^2(\varphi')\Big)^{-\frac{1}{2}} \mathrm{d}\varphi'. \end{aligned} \tag{H.15}$$

Aside from the elliptic sine, sn, there are two other Jacobi elliptic functions: elliptic cosine cn and delta amplitude dn. By performing substitutions similar to (H.7), these functions can be defined as follows

$$cn(y) \equiv cn(y|k) = cos\varphi, \tag{H.16}$$

$$dn(y) \equiv dn(y|k) = \sqrt{1-k^2 sin^2(\varphi)}. \tag{H.17}$$

When the elliptic modulus is equal to zero i.e. $k = 0$, the functions satisfy the limiting definitions

$$sn(y|0) = siny, \quad cn(y|0) = cosy, \quad dn(y|0) = 1. \tag{H.18}$$

The Jacobi elliptic functions sn, cn, dn are doubly periodic with periods $\big(4K, 2iK'\big)$, $\big(4K, 4iK'\big)$ and $\big(2K, 4iK'\big)$ respectively:

$$sn(y+4K) = sn\big(y+2iK'\big) = sn(y), \tag{H.19}$$

$$cn(y+4K) = cn\big(y+4iK'\big) = cn(y), \tag{H.20}$$

$$dn(y+2K) = dn\big(y+4iK'\big) = dn(y). \tag{H.21}$$

where $K' = K(k_c)$ and the complementary elliptic modulus is given by the relation $k_c = (1-k^2)^{\frac{1}{2}}$.

APPENDIX I

POINCARÉ SECTIONS

In dynamical systems theory, a Poincaré section (or surface of section) plot is a way of representing phase space trajectories by a sequence of points that are obtained from the reduction of a continuous time flow to a discrete time chart [75, 91, 92, 93]. Consider an M-dimensional phase space. Let S_{pn} be an $(M-1)$-dimensional hyperplane which is preferably transverse to the continuous flow. The Poincaré section plot is generated by recording the points formed by the intersections of the phase path with S_{pn}. Each time the trajectory comes back around to pierce S_{pn}, it leaves a point on the Poincaré section. Thus, the Poincaré section plot consists of a pattern of points that can be utilized to study the dynamics of the system. In periodic motion, depending on the number of oscillation frequencies, the Poincaré section plot consists of a single fixed point or several discrete points whose locations can vary for distinct initial conditions. Instead of discrete points, a quasi-periodic trajectory would draw a closed contour in the surface of section and chaotic motion appears in plots as a collection of randomly scattered points.

As an example to illustrate the usage of Poincaré sections to probe chaotic behavior, we may consider the Hénon-Heiles model whose Hamiltonian is given by [94, 22]

$$H = \frac{1}{2}\left(p_x^2 + p_y^2\right) + \frac{1}{2}\left(x^2 + y^2\right) + x^2 y - \frac{1}{3}y^3. \tag{I.1}$$

The Hamilton's equations read

$$\dot{x} = p_x\,, \tag{I.2a}$$

$$\dot{y} = p_y\,, \tag{I.2b}$$

$$\dot{p_x} = -x(2y+1)\,, \tag{I.2c}$$

$$\dot{p_y} = y(y-1) - x^2\,. \tag{I.2d}$$

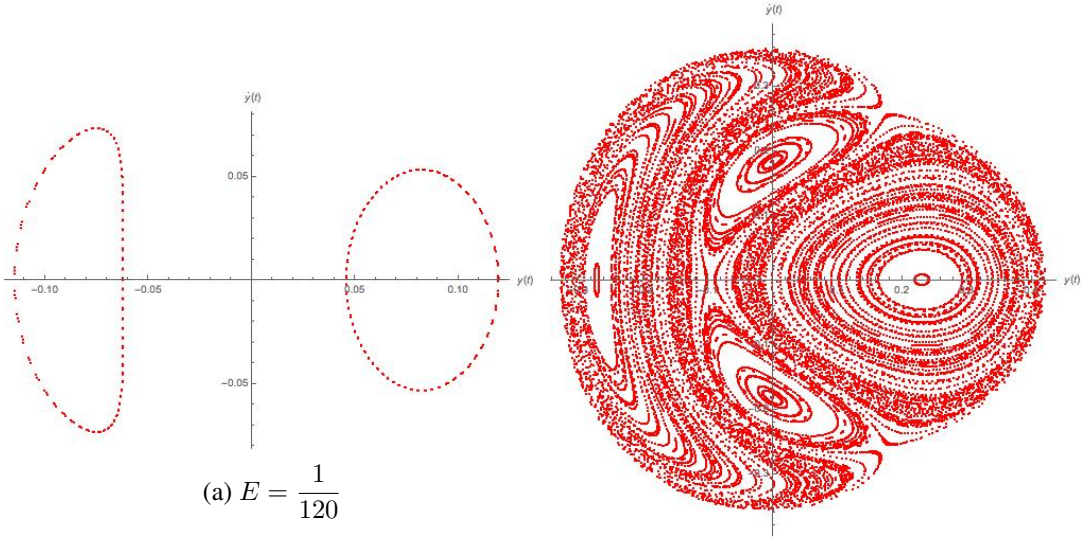

(a) $E = \dfrac{1}{120}$

(b) $E = \dfrac{1}{15}$

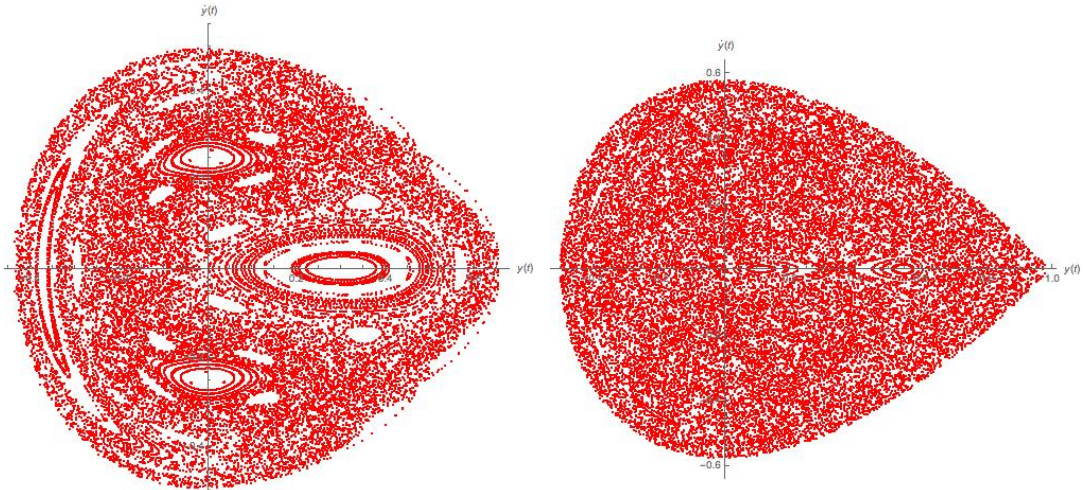

(c) $E = \dfrac{1}{8}$

(d) $E = \dfrac{1}{6}$

Figure I.1: Poincarè sections for E = $\dfrac{1}{120}, \dfrac{1}{15}, \dfrac{1}{8}, \dfrac{1}{6}$

The surface of section graphs of figure I.1 are plotted for the Hénon-Heiles model with four distinct energy values. The plots depict the variation of $\dot{y}(t)$ with $y(t)$ at values where $x(t) = 0$. It should be noted that to fill out a surface of section a variety of initial conditions consistent with the same energy value are picked. The Poincarè section of figure I.1a fall on two ellipses that correspond to periodic or quasi-periodic

orbits. Although the majority of solutions shown in figure I.1b correspond to quasi-periodic orbits, it is seen that these orbits coexist with the chaotic ones. The physical implication of this observation is that while some initial conditions lead to quasi-periodic trajectories, others lead to chaotic ones. One may easily deduce from an examination of I.1c that chaotic trajectories occupy a considerably larger region of phase space if the energy is increased further. Finally, nearly all of the Poincarè section plot of I.1d is filled with densely distributed scattered dots which suggest that a chaotic trajectory covers almost the entire phase space.

APPENDIX J

LYAPUNOV EXPONENTS

The notion of exponential separation of neighboring trajectories can be made formal and precise with a study of the Lyapunov exponents of a dynamical system [95, 96, 97, 22]. They provide a way to explore what chaotic behavior means quantitatively by measuring the average exponential rate of divergence of nearby initial conditions. In order to compute the Lyapunov exponents of a multidimensional chaotic system, we consider the system of first order differential equations in $M-$dimensional phase space described by

$$\dot{\boldsymbol{y}}(t) = \boldsymbol{G}(\boldsymbol{y}(t)), \tag{J.1}$$

where $\boldsymbol{y}(t) = (y_1(t), ..., y_M(t))^T$. Concentrating only on linear deviations about an arbitrary element of $\boldsymbol{y}(t)$ yields the equation of motion for the variation as

$$\delta\dot{y}_\varepsilon(t) = G_\varepsilon(y_{\tilde{\varepsilon}}(t) + \delta y_{\tilde{\varepsilon}}(t)) - G_\varepsilon(y_{\tilde{\varepsilon}}(t)) \approx \frac{\partial G_\varepsilon}{\partial y_{\tilde{\varepsilon}}}\delta y_{\tilde{\varepsilon}}. \tag{J.2}$$

where $\varepsilon, \tilde{\varepsilon} = 1, ..., M$. With the help of the time evolution operator, T_t, the deviation vector can be related to its initial value:

$$\delta\boldsymbol{y}(t) = T_t\delta\boldsymbol{y}(0). \tag{J.3}$$

Besides, from the linearity of T_t we have

$$\delta\boldsymbol{y}(t_a + t_b) = T_{t_a}T_{t_b}\delta\boldsymbol{y}(0). \tag{J.4}$$

Suppose that the final evaluation time, t_e, of the system is divided into m steps of size Δt. Then, employing the linearity property, the Lyapunov exponent for the deviation vector can be defined by

$$\lambda \equiv \lim_{t_e\to\infty} \frac{1}{t_e} \log\left(\frac{|\delta\boldsymbol{y}(t_e)|}{|\delta\boldsymbol{y}(0)|}\right)$$

$$\equiv \lim_{m\to\infty} \frac{1}{m\Delta t} \log\left(\frac{|\delta \boldsymbol{y}(m\Delta t)|}{|\delta \boldsymbol{y}(0)|}\right) \tag{J.5}$$
$$\equiv \lim_{m\to\infty} \frac{1}{m\Delta t} \log\left(\frac{|T_{\Delta t}...T_{\Delta t}\delta \boldsymbol{y}(0)|}{|\delta \boldsymbol{y}(0)|}\right).$$

The procedure detailed above can be generalized to determine all M exponents by first forming an orthonormal basis set that spans the tangential component of the trajectory vector and then observing its evolution in time. Let $\left\{\boldsymbol{b}_0^1, ..., \boldsymbol{b}_0^{\tilde{\varepsilon}}, ..., \boldsymbol{b}_0^M\right\}$ denote such a set where $\boldsymbol{b}_0^{\tilde{\varepsilon}}$ corresponds to the basis constructed with $\tilde{\varepsilon}^{th}$ initial condition at time t = 0. Evolving each basis by $T_{\Delta t}$ yields the new set

$$\left\{\boldsymbol{c}_1^1, ..., \boldsymbol{c}_1^{\tilde{\varepsilon}}, ..., \boldsymbol{c}_1^M\right\} = \left\{T_{\Delta t}\boldsymbol{b}_0^1, ..., T_{\Delta t}\boldsymbol{b}_0^{\tilde{\varepsilon}}, ..., T_{\Delta t}\boldsymbol{b}_0^M\right\}, \tag{J.6}$$

which is not necessarily orthonormal. Let $\left\{\bar{\boldsymbol{b}}_1^1, ..., \bar{\boldsymbol{b}}_1^M\right\}$ denote the orthogonal set that is produced from $\left\{\boldsymbol{c}_1^1, ..., \boldsymbol{c}_1^M\right\}$ by applying the Gram-Schmidt orthogonalization process. This set can be normalized in the usual way:

$$\boldsymbol{b}_1^{\tilde{\varepsilon}} = \frac{\bar{\boldsymbol{b}}_1^{\tilde{\varepsilon}}}{e_1^{\tilde{\varepsilon}}}, \tag{J.7}$$

where $e_1^{\tilde{\varepsilon}}$ is the expansion rate defined by

$$e_1^{\tilde{\varepsilon}} \equiv \frac{\left|\bar{\boldsymbol{b}}_1^{\tilde{\varepsilon}}\right|}{\left|\boldsymbol{b}_0^{\tilde{\varepsilon}}\right|} = \left|\bar{\boldsymbol{b}}_1^{\tilde{\varepsilon}}\right|. \tag{J.8}$$

As a result of the orthonormalization process, the basis set $\left\{\boldsymbol{b}_1^1, ..., \boldsymbol{b}_1^M\right\}$, which constitutes the initial conditions for the next cycle, is obtained. Upon completing the remaining $m-1$ cycles, one determines the whole set of Lyapunov exponents whose ε^{th} member can be defined in terms expansion rates as

$$\lambda_\varepsilon \equiv \lim_{m\to\infty} \frac{1}{m\Delta t} \sum_{j=1}^{m} \log\left(e_j^\varepsilon\right). \tag{J.9}$$

REFERENCES

[1] H. C. Steinacker, "Emergent gravity on covariant quantum spaces in the ikkt model," *Journal of High Energy Physics*, vol. 2016, no. 12, p. 156, 2016.

[2] T. Banks, W. Fischler, S. H. Shenker, and L. Susskind, "M theory as a matrix model: A Conjecture," *Phys. Rev.*, vol. D55, pp. 5112–5128, 1997.

[3] H. Aoki, N. Ishibashi, S. Iso, H. Kawai, Y. Kitazawa, and T. Tada, "Noncommutative Yang-Mills in IIB matrix model," *Nucl. Phys.*, vol. B565, pp. 176–192, 2000.

[4] R. Dijkgraaf and C. Vafa, "Matrix models, topological strings, and supersymmetric gauge theories," *Nucl. Phys.*, vol. B644, pp. 3–20, 2002.

[5] D. E. Berenstein, J. M. Maldacena, and H. S. Nastase, "Strings in flat space and pp waves from N=4 superYang-Mills," *JHEP*, vol. 04, p. 013, 2002.

[6] H. Steinacker, "Emergent Geometry and Gravity from Matrix Models: an Introduction," *Class. Quant. Grav.*, vol. 27, p. 133001, 2010.

[7] E. Kiritsis, *String theory in a nutshell*, vol. 21. Princeton University Press, 2019.

[8] B. Ydri, *Matrix Models of String Theory*. 2053-2563, IOP Publishing, 2018.

[9] S. Hyun and H. Shin, "Branes from matrix theory in pp-wave background," *Physics Letters B*, vol. 543, no. 1-2, pp. 115–120, 2002.

[10] B. Ydri, "Review of M(atrix)-Theory, Type IIB Matrix Model and Matrix String Theory," 2017.

[11] W. Taylor, "Lectures on D-branes, gauge theory and M(atrices)," in *2nd Trieste Conference on Duality in String Theory Trieste, Italy, June 16-20, 1997*, pp. 192–271, 1997. [,192(1997)].

[12] D. Berenstein and D. Trancanelli, "Dynamical tachyons on fuzzy spheres," *Physical Review D*, vol. 83, no. 10, p. 106001, 2011.

[13] N. Itzhaki, J. M. Maldacena, J. Sonnenschein, and S. Yankielowicz, "Supergravity and the large n limit of theories with sixteen supercharges," *Physical Review D*, vol. 58, no. 4, p. 046004, 1998.

[14] H. Năstase, *Introduction to the AdS/CFT Correspondence*. Cambridge University Press, 2015.

[15] D. Berenstein and D. Kawai, "Smallest matrix black hole model in the classical limit," *Phys. Rev. D*, vol. 95, p. 106004, May 2017.

[16] Y. Sekino and L. Susskind, "Fast Scramblers," *JHEP*, vol. 10, p. 065, 2008.

[17] R. Hübener, Y. Sekino, and J. Eisert, "Equilibration in low-dimensional quantum matrix models," *Journal of High Energy Physics*, vol. 2015, p. 166, Apr 2015.

[18] G. Gur-Ari, M. Hanada, and S. H. Shenker, "Chaos in Classical D0-Brane Mechanics," *JHEP*, vol. 02, p. 091, 2016.

[19] H. C. Steinacker, "One-loop stabilization of the fuzzy four-sphere via softly broken susy," *Journal of High Energy Physics*, vol. 2015, no. 12, p. 115, 2015.

[20] U. Coskun, S. Kurkcuoglu, G. C. Toga, and G. Unal, "Chaos from equivariant fields on fuzzy S^4," *JHEP*, vol. 12, p. 015, 2018.

[21] I. Ya. Aref'eva, P. B. Medvedev, O. A. Rytchkov, and I. V. Volovich, "Chaos in M(atrix) theory," *Chaos Solitons Fractals*, vol. 10, pp. 213–223, 1999.

[22] Y. Asano, D. Kawai, and K. Yoshida, "Chaos in the BMN matrix model," *Journal of High Energy Physics*, vol. 2015, p. 191, Jun 2015.

[23] M. Berkooz and M. R. Douglas, "Five-branes in M(atrix) theory," *Phys. Lett.*, vol. B395, pp. 196–202, 1997.

[24] S. Kurkcuoglu, "New fuzzy extra dimensions from $SU(\mathcal{N})$ gauge theories," *Phys. Rev.*, vol. D92, p. 025022, 2015.

[25] S. Kürkçüoğlu and G. Ünal, "Equivariant Fields in an $SU(\mathcal{N})$ Gauge Theory with new Spontaneously Generated Fuzzy Extra Dimensions," *Phys. Rev.*, vol. D93, no. 10, p. 105019, 2016.

[26] A. P. Balachandran, G. Marmo, B. S. Skagerstam, and A. Stern, "Gauge Theories and Fibre Bundles - Applications to Particle Dynamics," *Lect. Notes Phys.*, vol. 188, pp. 1–140, 1983.

[27] B. A. Bernevig, C.-H. Chern, J.-P. Hu, N. Toumbas, and S.-C. Zhang, "Effective field theory description of the higher dimensional quantum hall liquid," *Annals of Physics*, vol. 300, no. 2, pp. 185–207, 2002.

[28] J. Madore, "The Fuzzy sphere," *Class. Quant. Grav.*, vol. 9, pp. 69–88, 1992.

[29] J. Hoppe, *Quantum theory of a massless relativistic surface and a two-dimensional bound state problem*. PhD thesis, MIT, 1982.

[30] H. Grosse, C. Klimcik, and P. Presnajder, "Topologically nontrivial field configurations in noncommutative geometry," *Commun. Math. Phys.*, vol. 178, pp. 507–526, 1996.

[31] A. P. Balachandran, S. Kurkcuoglu, and S. Vaidya, "Lectures on fuzzy and fuzzy SUSY physics," 2005.

[32] H. Grosse, C. Klimcik, and P. Presnajder, "On finite 4-D quantum field theory in noncommutative geometry," *Commun. Math. Phys.*, vol. 180, pp. 429–438, 1996.

[33] J. Castelino, S. Lee, and W. Taylor, "Longitudinal five-branes as four spheres in matrix theory," *Nucl. Phys.*, vol. B526, pp. 334–350, 1998.

[34] Y. Kimura, "Noncommutative gauge theory on fuzzy four sphere and matrix model," *Nucl. Phys.*, vol. B637, pp. 177–198, 2002.

[35] C. J. Isham, *Modern differential geometry for physicists*, vol. 61. World Scientific, 1999.

[36] J. D. Jackson, "Classical electrodynamics," 1999.

[37] K. Zarembo, "Integrability in Sigma-Models," in *Les Houches Summer School: Integrability: From Statistical Systems to Gauge Theory Les Houches, France, June 6-July 1, 2016*, 2017.

[38] B. Ydri, *Lectures on Matrix Field Theory*. Springer, 2017.

[39] Y. M. Shnir, *Magnetic monopoles*. Springer Science & Business Media, 2006.

[40] A. Zee, *Group theory in a nutshell for physicists*, vol. 17. Princeton University Press, 2016.

[41] R. Mosseri, "Two-qubit and three-qubit geometry and hopf fibrations," in *Topology in Condensed Matter*, pp. 187–203, Springer, 2006.

[42] M. Nakahara, *Geometry, topology and physics*. CRC Press, 2003.

[43] G. Landi, C. Pagani, and C. Reina, "A Hopf bundle over a quantum four-sphere from the symplectic group," *Commun. Math. Phys.*, vol. 263, pp. 65–88, 2006.

[44] H. Nastase and C. Papageorgakis, "Bifundamental fuzzy 2-sphere and fuzzy Killing spinors," *SIGMA*, vol. 6, p. 058, 2010.

[45] N. M. J. Woodhouse, *Geometric quantization*. Oxford University Press, 1997.

[46] Y. Abe, *Construction of Fuzzy Spaces and Their Applications to Matrix Models*. PhD thesis, City U., New York, 2006.

[47] L. C. Biedenharn and J. D. Louck, *Angular momentum in quantum physics: theory and application*. Cambridge University Press, 1984.

[48] J. Schwinger, "Angular momentum," in *Quantum Mechanics*, pp. 149–181, Springer, 2001.

[49] T. Azuma, *Matrix models and the gravitational interaction*. PhD thesis, Kyoto U., 2004.

[50] U. Carow-Watamura, H. Steinacker, and S. Watamura, "Monopole bundles over fuzzy complex projective spaces," *J. Geom. Phys.*, vol. 54, pp. 373–399, 2005.

[51] A. Balachandran, B. P. Dolan, J. Lee, X. Martin, and D. O'Connor, "Fuzzy complex projective spaces and their star-products," *Journal of Geometry and Physics*, vol. 43, no. 2, pp. 184–204, 2002.

[52] M. Kaku, *Quantum field theory: A Modern introduction*. 1993.

[53] S. Murray and C. Saemann, "Quantization of Flag Manifolds and their Supersymmetric Extensions," *Adv. Theor. Math. Phys.*, vol. 12, no. 3, pp. 641–710, 2008.

[54] R. J. Szabo, *An introduction to string theory and D-brane dynamics*. World Scientific, 2004.

[55] D. Karabali, V. P. Nair, and S. Randjbar-Daemi, "Fuzzy spaces, the M(atrix) model and the quantum Hall effect," pp. 831–875, 2004.

[56] F. Balli, A. Behtash, S. Kurkcuoglu, and G. Unal, "Quantum Hall Effect on the Grassmannians $\mathbf{Gr}_2(\mathbb{C}^N)$," *Phys. Rev.*, vol. D89, no. 10, p. 105031, 2014.

[57] W. G. McKay and J. Patera, *Tables of dimensions, indices, and branching rules for representations of simple Lie algebras*. Dekker, 1981.

[58] F. Iachello, *Lie algebras and applications*, vol. 12. Springer, 2006.

[59] W. Fulton and J. Harris, *Representation theory: a first course*. Springer, 1991.

[60] A. A. Kirillov, *Lectures on the orbit method*, vol. 64. American Mathematical Society Providence, RI, 2004.

[61] G. Rudolph and M. Schmidt, *Differential geometry and mathematical physics*. Springer, 2012.

[62] J. Bernatska, P. Holod, *et al.*, "Geometry and topology of coadjoint orbits of semisimple lie groups," in *Proceeding of 9-th International Conference on Geometry Integrability and Quantization Varna*, pp. 1–21, 2007.

[63] A. Paul, "Dirac. lectures on quantum mechanics," *Belfer graduate school of science, Yeshiva University*, 1964.

[64] V. P. Nair and A. P. Polychronakos, "Quantum mechanics on the noncommutative plane and sphere," *Phys. Lett.*, vol. B505, pp. 267–274, 2001.

[65] P. A. Horvathy, "The Noncommutative Landau problem and the Peierls substitution," *Annals Phys.*, vol. 299, pp. 128–140, 2002.

[66] D. Karabali and V. P. Nair, "Quantum Hall effect in higher dimensions," *Nucl. Phys.*, vol. B641, pp. 533–546, 2002.

[67] W. Greiner and B. Müller, *Quantum mechanics: symmetries*. Springer Science & Business Media, 2012.

[68] M. Daoud and A. Jellal, "Quantum Hall effect on the flag manifold F(2)," *Int. J. Mod. Phys.*, vol. A23, pp. 3129–3154, 2008.

[69] B. Stefanski, Jr. and A. A. Tseytlin, "Large spin limits of AdS/CFT and generalized Landau-Lifshitz equations," *JHEP*, vol. 05, p. 042, 2004.

[70] J. J. Sakurai, *Modern quantum mechanics; rev. ed.* Reading, MA: Addison-Wesley, 1994.

[71] I. Bena, M. Graña, S. Kuperstein, P. Ntokos, and M. Petrini, "D 3-brane model building and the supertrace rule," *Physical review letters*, vol. 116, no. 14, p. 141601, 2016.

[72] E. Sokatchev, "Projection Operators and Supplementary Conditions for Superfields with an Arbitrary Spin," *Nucl. Phys.*, vol. B99, pp. 96–108, 1975.

[73] I. C. Percival and D. Richards, *Introduction to dynamics*. Cambridge University Press, 1982.

[74] G. Layek, *An introduction to dynamical systems and chaos*. Springer, 2015.

[75] E. Ott, *Chaos in Dynamical Systems*. Cambridge University Press, 2 ed., 2002.

[76] S. L. Campbell and R. Haberman, *Introduction to differential equations with dynamical systems*. Princeton University Press, 2011.

[77] H. Dankowicz, *Chaotic dynamics in Hamiltonian systems: with applications to celestial mechanics*, vol. 25. World Scientific, 1997.

[78] J. V. Armitage and W. F. Eberlein, *Elliptic functions*, vol. 67. Cambridge University Press, 2006.

[79] C. C. Nishi, "Simple derivation of general Fierz-like identities," *Am. J. Phys.*, vol. 73, pp. 1160–1163, 2005.

[80] A. Balachandran, G. Marmo, B. Skagerstam, and A. Stern, *Classical topology and quantum states*. World Scientific, 1991.

[81] H. J. Müller-Kirsten, *Introduction to quantum mechanics: Schrödinger equation and path integral*. World Scientific, 2012.

[82] W. Pfeifer, *The Lie algebras su(N): an introduction*. Springer Science & Business Media, 2003.

[83] J. J. Sakurai, J. Napolitano, *et al.*, *Modern quantum mechanics*, vol. 185. Pearson Harlow, 2014.

[84] J. R. Klauder and B.-S. Skagerstam, *Coherent states: applications in physics and mathematical physics*. World scientific, 1985.

[85] W. Greiner and J. Reinhardt, *Field quantization*. Springer Science & Business Media, 2013.

[86] A. M. Perelomov, "Coherent states for arbitrary lie group," *Communications in Mathematical Physics*, vol. 26, no. 3, pp. 222–236, 1972.

[87] W.-M. Zhang, R. Gilmore, *et al.*, "Coherent states: theory and some applications," *Reviews of Modern Physics*, vol. 62, no. 4, p. 867, 1990.

[88] D. F. Lawden, *Elliptic functions and applications*, vol. 80. Springer Science & Business Media, 2013.

[89] A. J. Brizard, "A primer on elliptic functions with applications in classical mechanics," *European Journal of Physics*, vol. 30, no. 4, p. 729, 2009.

[90] H. J. Weber and G. B. Arfken, *Essential mathematical methods for physicists, ISE*. Elsevier, 2003.

[91] R. Hilborn, *Chaos and Nonlinear Dynamics: An Introduction for Scientists and Engineers*. Oxford University Press, 1994.

[92] T. Tél and M. Gruiz, *Chaotic dynamics: an introduction based on classical mechanics*. Cambridge University Press, 2006.

[93] S. Thornton and J. Marion, *Classical Dynamics of Particles and Systems*. Brooks/Cole, 2004.

[94] M. Hénon and C. Heiles, "The applicability of the third integral of motion: some numerical experiments," *The Astronomical Journal*, vol. 69, p. 73, 1964.

[95] S. H. Strogatz, *Nonlinear dynamics and chaos: with applications to physics, biology, chemistry, and engineering*. CRC Press, 2018.

[96] J. R. Dorfman, *An introduction to chaos in nonequilibrium statistical mechanics*. No. 14, Cambridge University Press, 1999.

[97] A. Wolf, J. B. Swift, H. Swinney, and J. A. Vastano, "Determining lyapunov exponents from a time series," *Physica D: Nonlinear Phenomena*, vol. 16, pp. 285–317, 07 1985.

CURRICULUM VITAE

PERSONAL INFORMATION

Surname, Name: Oktay, Onur
Nationality: Turkish (TC)
Contact: onur.oktay@metu.edu.tr

EDUCATION

Degree	Institution	Year of Graduation
M.S.	Physics, Middle East Technical University	2012
B.S.	Electrical and Electronics Engineering, Bilkent University	2008

PROFESSIONAL EXPERIENCE

Year	Place	Enrollment
2006	Turkish Radio and Television Corporation	Intern

PUBLICATIONS

Preprints

- "Chaos from Massive Deformations of Yang-Mills Matrix Models". arXiv:1912.00932, (2019). K. Baskan, S. Kurkcuoglu, O. Oktay and C. Tasci.

HOBBIES AND INTERESTS

Antique firearms, playing harmonica.